AD-A076 219 CALSPAN CORP BUFFALO N Y F/G 19/6
SHOCK TUBE GUN MELTING EROSION STUDY.(U)
AUG 79 F A VASSALLO , W R BROWN DAAK11-77-C-0018
UNCLASSIFIED CALSPAN-VQ-6123-D-1 ARBRL-CR-00406 NL

1 OF 2
AD-
A076219

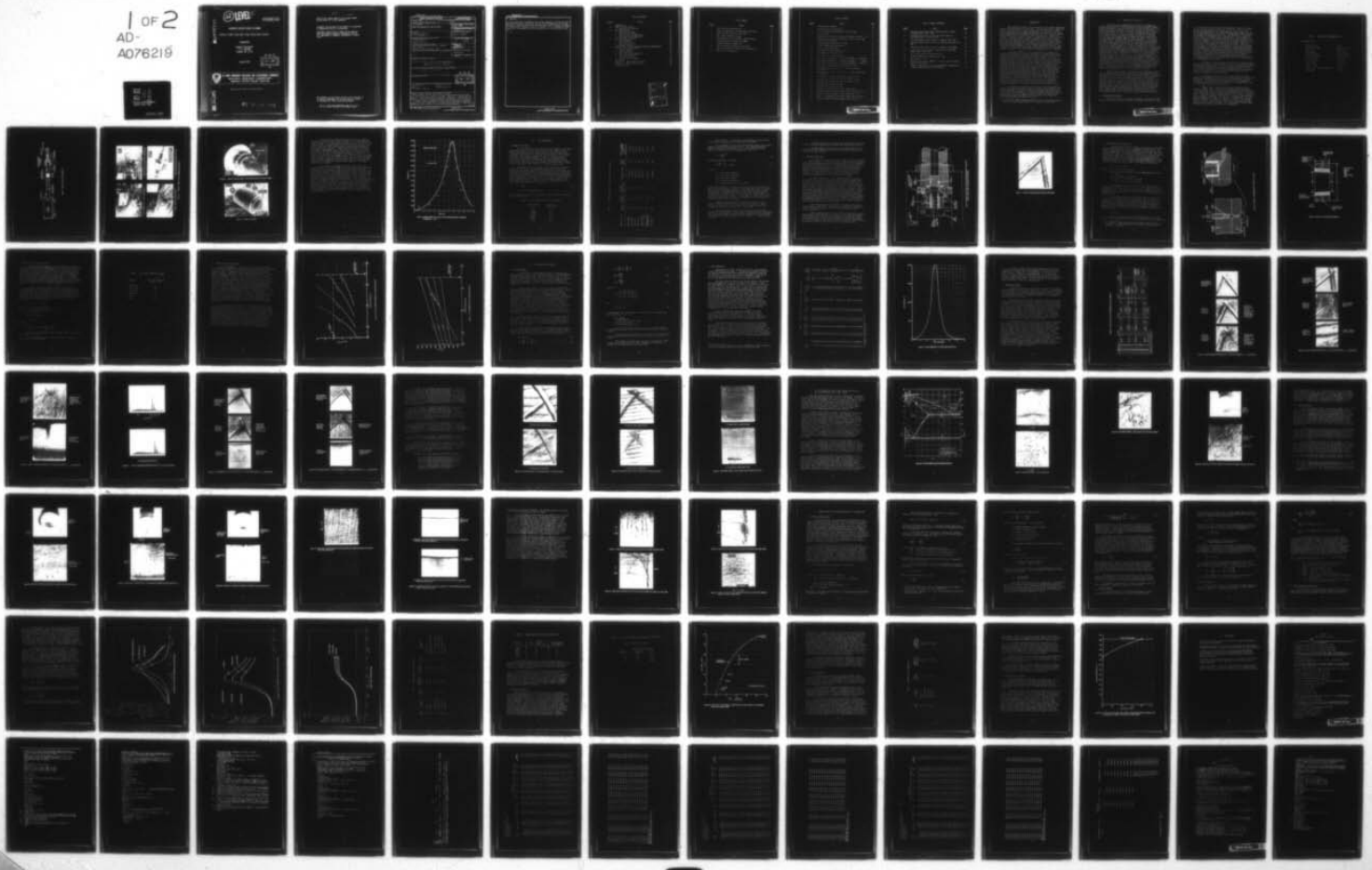

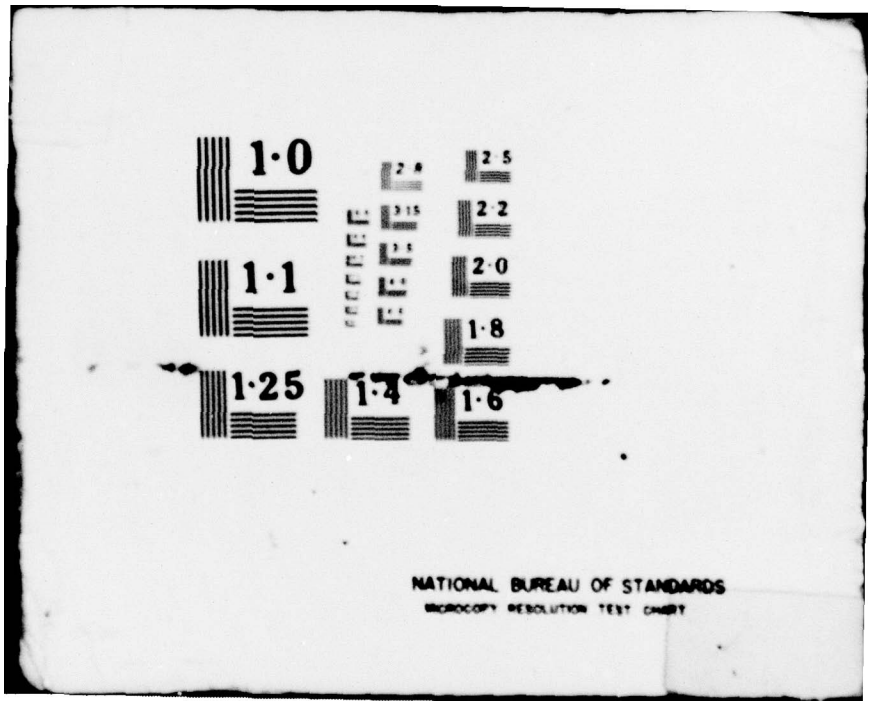
1·0
1·1
1·25
1·4
1·6
2·5
2·2
2·0
1·8
NATIONAL BUREAU OF STANDARDS
MICROCOPY RESOLUTION TEST CHART

(12) LEVEL III

AD-E430 312

AD A076219

CONTRACT REPORT ARBRL-CR-00406

SHOCK TUBE GUN MELTING EROSION STUDY

Prepared by

Calspan Corporation
P. O. Box 400
Buffalo, NY 14225

August 1979

US ARMY ARMAMENT RESEARCH AND DEVELOPMENT COMMAND
BALLISTIC RESEARCH LABORATORY
ABERDEEN PROVING GROUND, MARYLAND

Destroy this report when it is no longer needed.
Do not return it to the originator.

Secondary distribution of this report by originating or sponsoring activity is prohibited.

Additional copies of this report may be obtained from the National Technical Information Service, U.S. Department of Commerce, Springfield, Virginia 22161.

The findings in this report are not to be construed as an official Department of the Army position, unless so designated by other authorized documents.

The use of trade names or manufacturers' names in this report does not constitute indorsement of any commercial product.

UNCLASSIFIED

SECURITY CLASSIFICATION OF THIS PAGE (When Data Entered)

REPORT DOCUMENTATION PAGE

READ INSTRUCTIONS BEFORE COMPLETING FORM

1. REPORT NUMBER: CONTRACT REPORT ARBRL-CR-00406
2. GOVT ACCESSION NO.
3. RECIPIENT'S CATALOG NUMBER

4. TITLE (and Subtitle): SHOCK TUBE GUN MELTING EROSION STUDY.
5. TYPE OF REPORT & PERIOD COVERED: Final Report. 13 May 1977 — 29 Dec 1978
6. PERFORMING ORG. REPORT NUMBER: VQ-6123-D-1

7. AUTHOR(s): Franklin A. Vassallo, W. Richard Brown
8. CONTRACT OR GRANT NUMBER(s): DAAK11-77-C-0018

9. PERFORMING ORGANIZATION NAME AND ADDRESS: Calspan Corporation, P. O. Box 400, Buffalo, NY 14225
10. PROGRAM ELEMENT, PROJECT, TASK AREA & WORK UNIT NUMBERS: 1L1

11. CONTROLLING OFFICE NAME AND ADDRESS: USA Ballistic Research Laboratory, ARRADCOM, ATTN: DRDAR-BLP, Aberdeen Proving Ground, MD 21005
12. REPORT DATE: AUGUST 1979
13. NUMBER OF PAGES: 120

14. MONITORING AGENCY NAME & ADDRESS (if different from Controlling Office): CALSPAN-VQ-6123-D-1
15. SECURITY CLASS. (of this report): UNCLASSIFIED
15a. DECLASSIFICATION/DOWNGRADING SCHEDULE

16. DISTRIBUTION STATEMENT (of this Report)

Approved for public release; distribution unlimited.

ARBRL, SBIE

17. DISTRIBUTION STATEMENT (of the abstract entered in Block 20, if different from Report)

CR-0406, AD-E430 312

18. SUPPLEMENTARY NOTES

DDC RECEIVED NOV 6 1979 B

19. KEY WORDS (Continue on reverse side if necessary and identify by block number)

Heat Transfer
Melting
Bore Surface Cracking
Erosion
Interior Ballistics

20. ABSTRACT (Continue on reverse side if necessary and identify by block number)

Heat transfer, melting, and erosion tests were conducted using a unique Shock Tube Gun Facility available at Calspan. Materials of interest were subjected to intense heating using non-reactive gas mixtures. Pure melting of materials was obtained at heating conditions representing those of actual guns.

A computer code was formulated, written, tested, and shown to adequately normalize the gross thermal data, thus permitting determination of expected bore temperatures and/or material loss for given heating conditions. (cont'd)

DD FORM 1 JAN 73 1473 EDITION OF 1 NOV 65 IS OBSOLETE

UNCLASSIFIED

SECURITY CLASSIFICATION OF THIS PAGE (When Data Entered)

407 727

JOB

20. (cont'd)

It was found that, although the bore surface temperature of steels tested in the non-reactive gases of the Shock Tube Gun achieved temperatures of the same magnitude as those in large caliber guns where bore surface cracking is produced, no similar surface cracking of steels was observed. It is concluded that chemical activity of gun gases is partially responsible for crack initiation in gun tubes.

TABLE OF CONTENTS

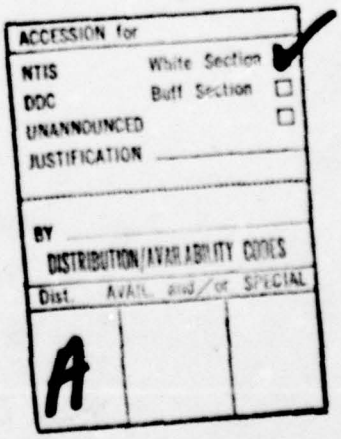

LIST OF TABLES

LIST OF FIGURES

LIST OF FIGURES (CONTINUED)

I. INTRODUCTION

Bore heating at high flux rate can result in bore surface temperatures exceeding the melting point of some steels. This melting region is emphasized in more recent high kinetic energy weapons where very high charge-to-mass ratio is generally used to produce required projectile velocity, with attendant increased pressure and propellant gas flow. For this situation, general surface melting has been suspected to have occurred even in single-shot firings.[1] There was, however, evidence to suggest that the melting exhibited by steels in question arises in part by chemical activity at the surface which lowers the melting range of the steel (such as by addition of carbon) and/or provides additional local heating due to exothermic surface reactions. Bore heat input measurements in such firings and estimated heat flux histories allow direct computation of bore surface temperature histories which, in general, are found to be much below the melting point of the steel where melting is observed. Thus, the presence of chemical activity is indicated.

In testing heretofore, it has been difficult to evaluate the mechanism of melting erosion and its predictability through computer analysis because of inability to separate the effects of pure forced convection heating of the bore from combined thermochemical effects. Use of propellants containing carbon and oxygen as a means of providing bore surface heating and erosion is clearly in conflict with the desire for separation of effects but has until now been the only means by which heating conditions of sufficient magnitude could be produced. With the introduction of its Shock Tube Gun (STG), described later in this report, Calspan has now provided a tool which overcomes the limitations of the combustion approach to erosion testing and can now permit examination of the thermochemical nature of erosion in the near-melting range. This report describes the results of an exploratory study of melting erosion using the Calspan STG. The primary objective of this baseline study was to investigate the melting erosion of various metals in a gun-like environment using non-reactive gases. Steels with different carbon content and other materials with known melting points were used as test subjects. The amount of material loss for given gas test conditions was a primary measurement along with measurement of bore heating through the use of specially designed calorimeters. This primary objective has been largely achieved.

A secondary but important objective was to develop a predictive capability for melting erosion in terms of measurable test quantities such as bulk heat input. A predictive computer code was developed which presently yields bore temperatures in essential agreement with those indicated by inspection of the test sample, but does not yet fully agree with the amount of melting erosion experienced by the sample. This remains an area requiring further refinement of the code.

---

1. F.A. Vassallo, "Heat Transfer and Erosion in the Ares 75mm High Velocity Cannon," Calspan Technical Report No. VL-5645-D-1, October 1975.

II. SHOCK TUBE GUN FACILITY

Full scale tube instrumentation and field test evaluations, although of great value in final performance testing of improved charges, should be preceded by a more efficient and cost effective approach to optimization of propelling charges. Calspan has recently tested a unique variable gun system, the operation of which is based upon shock tube principles (Shock Tube Gun). Thus, in contrast to measuring erosion that results from firing a vast number of rounds, the facility is designed to be used as a developmental tool for ammunition design changes and to assure an approach to optimal ammunition-tube interfaces. In achieving this goal, tests in the Shock Tube Gun are supported by special erosion and thermal sensors, metallurgical analyses, and ballistic measurements. Briefly, the STG generates a high pressure, high-temperature test gas by a polytropic compression process. As shown in Figure 1, the facility consists of a driver chamber, driven tube, a flying piston, a gas collection chamber and an instrumented gun tube containing a projectile. Compression of the test gas (the counterpart to the propellant gas in an actual gun) within the driven tube is accomplished by motion of the flying piston contained within this tube. Motion of the piston is the result of force applied by the pressure of the driver gas. As the piston approaches the collection chamber, the test gas pressure and temperature rapidly increase in a time history representative of actual gun firings. A projectile contained at the start of the gun tube is acted upon by this collected gas. Suitable means are provided in the facility to allow regulation of shot start pressure on the projectile. Once released, the projectile is accelerated along the tube in a ballistic cycle dependent upon selected input factors. Data regarding pressure, velocity, heating, and erosion are collected through measurements in the instrumented test barrel.

With suitable variation in parameters, factors affecting erosion such as pressure history, propellant gas velocity, gas temperature, gas composition, tube composition, and propellant additives may be investigated. The compression ratio, driven gas composition and its initial conditions essentially govern the peak temperature and pressure; piston motion, influenced by its mass, and projectile movement effectively govern the pressure pulse duration. Variation of piston mass, initial conditions, and compression ratio then permit independent change in peak temperature and pressure as well as time. Obviously, the effect of change of driven gas composition may be tested under controlled interior ballistic conditions. This is a most powerful experimental mode of operation of the facility. Other variable items can also be explored in specific tests, such as rotating band design and the relationship between obturation and erosion.

1. Design and Construction

The Shock Tube Gun is designed to adequately represent predicted ballistic conditions within guns as large as the eight-inch howitzer. Thus,

it is designed to permit testing at peak chamber pressures up to 40,000 psi and at projectile velocities up to 2500 ft/sec. Table 1 lists the present structural makeup of the Shock Tube Gun. These values were established through the use of a preliminary mathematical model of piston action based upon adiabatic compression. Through exercise of the model, approximate size requirements were established with final selection of sizes dictated by available engineering materials. The photographs of Figure 2 illustrate the resulting Shock Tube Gun assembly as well as its individual components. As shown, the projectile launch components consist of the driven tube, chamber and 30mm smooth bore barrel. These are supported on a carriage which is free to move on tracks in the direction of piston motion. The tracks allow movement of the carriage during the extreme impulse loads imposed by the unbalanced chamber pressure during test gas compression, thus maintaining integrity of the supporting base structure. In early firings conducted without installation of the tracks, splitting tensile failure of the supporting concrete structure was evidenced, thus suggesting the need for a mount having less rigidity. Following installation of the floating mount system, which requires use of a pneumatic brake on the driven tube for safety, test firings produced no further damage to the concrete.

The projectile capture components consist of a telescoping tube coupled to the barrel, a blast chamber, and a sand filled tube to decelerate the projectile (impact zone). The blast chamber, the purpose of which is to reduce the noise and pressure levels at projectile exit of the tube, also contains an internal provision for measurement of projectile velocity using velocity screens. The telescoping tube allows motion of the carriage independent of the blast chamber.

Also shown in Figure 2 are views of the chamber and toggle restraint system needed to contain the high chamber pressures and associated axial loads. Chamber pressures are sensed using piezoelectric pressure transducers. The entrance region of the launch tube can accommodate pressure, heat flux, and erosion sensing devices. The launch tube itself is a 30mm smooth bore barrel, 15 feet long.

Figures 3 and 4 illustrate two essential components of the facility. Figure 3 shows a view of the brake area at the upstream end of the driven tube. This brake limits the maximum permissible axial load on the driven tube during the rapid piston deceleration period. Without it, loads could exceed the axial strength capability of the tube. In essence, load is limited by slippage in the brake at a preselected load below the failure strength of the tube. The brake is a[illegible]ctuated and, thus may be adjusted according to the amount of slippage desired up to the strength limit of the tube. The brake is presently used at only about one-half capacity without excessive slippage. Hence, much greater maximum chamber pressures than presently produced can be accommodated.

TABLE 1. SHOCK TUBE GUN CHARACTERISTICS

Configuration Data:

Driven Tube I.D.	7.5 in.
Driven Tube Length	80.81 ft (970 in.)
Piston Area	44.179 sq. in.
Piston Weight	Up to 200 lb.
Projectile Diameter	1.181/30 in./mm
Projectile Area	1.095 sq. in.
Projectile Weight	Up to 2 lb.
Driver Volume	54,000 cu. in.
Chamber Volume	130.8 cu. in.
Pressure - at release of projectile	Variable
Tube Length	180 in.

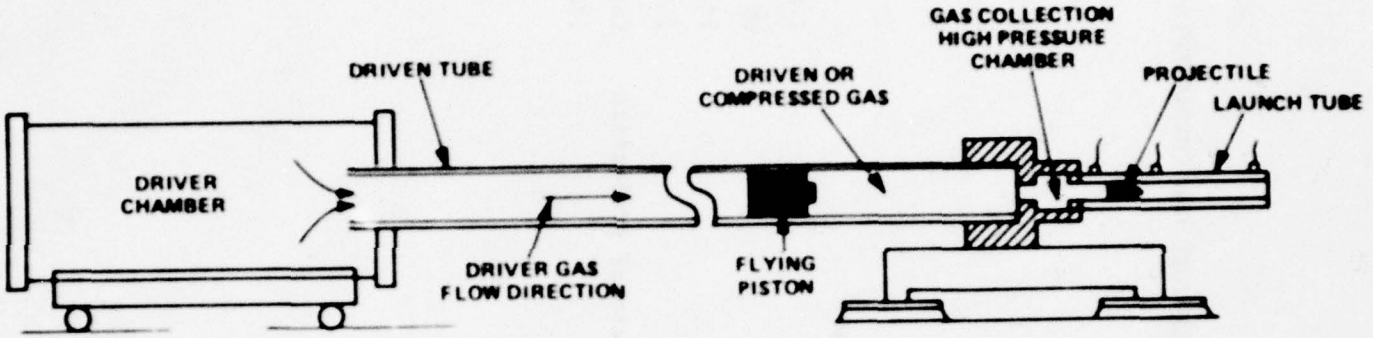

Figure 1 SHOCK TUBE GUN SCHEMATIC

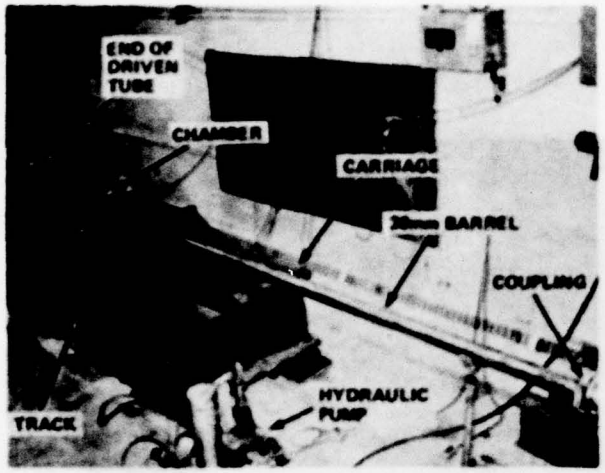

VIEW OF PROJECTILE LAUNCH COMPONENTS

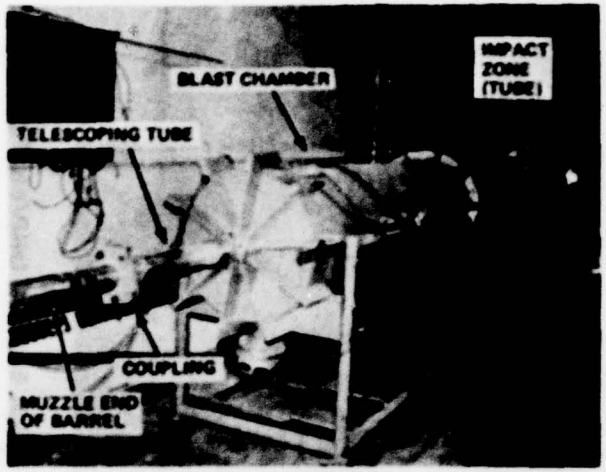

VIEW OF PROJECTILE CAPTURE COMPONENTS

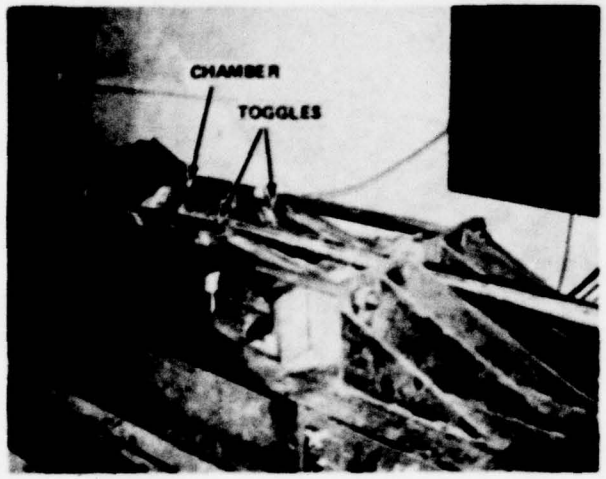

VIEW OF TOGGLE ARRANGEMENT

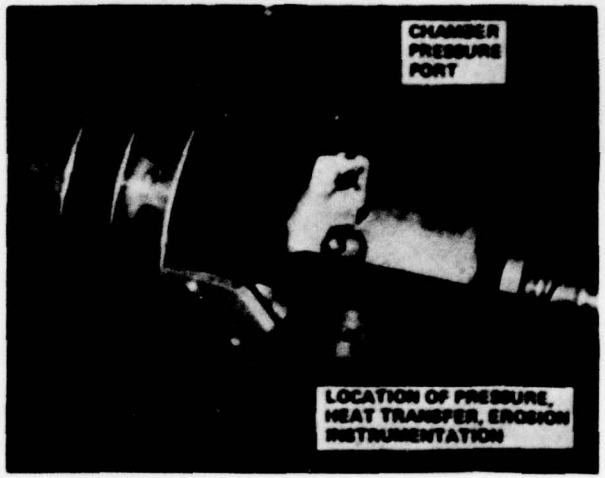

VIEW OF INSTRUMENTED AREA OF TUBE

Figure 2 SHOCK TUBE GUN (DOWNSTREAM END)

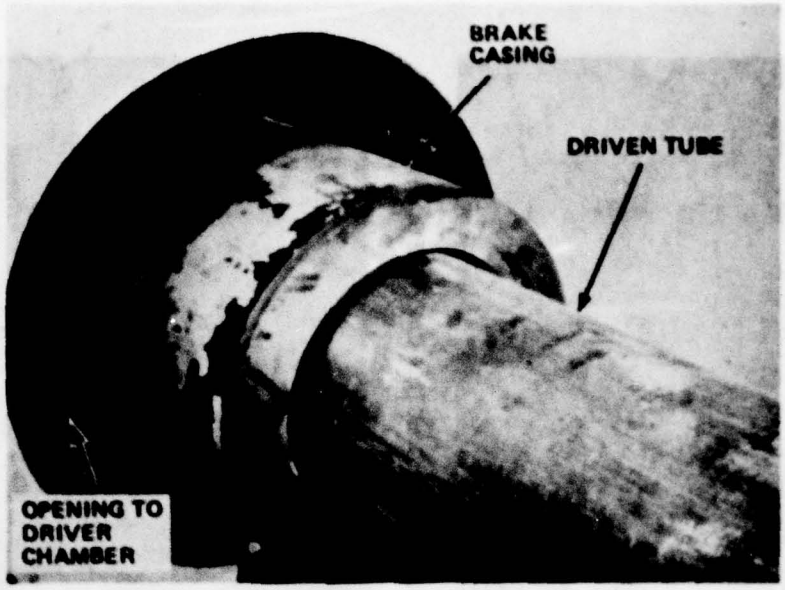

Figure 3 VIEW OF BRAKE AREA (UPSTREAM END OF DRIVEN TUBE)

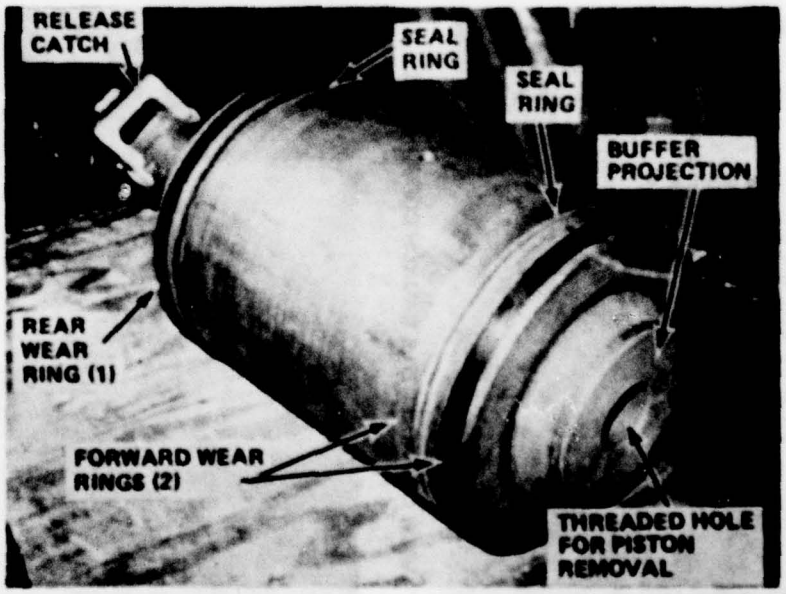

Figure 4 VIEW OF PISTON

A view of one of several pistons which are used to compress test gas in the driven tube is shown in Figure 4. It is made from 4340 steel and weighs 150 lb. including the release catch at its rear end. As shown, gas seal is obtained using "T" rings at the front and rear of the piston. Three brass wear rings are used to prevent metal-to-metal contact between piston and tube. A buffer projection on the face of the piston and a complementary close fitting port at the end of the driven tube entering the chamber preclude direct impact of the piston with the end of the driven tube in the event that driven gas is exhausted too rapidly as by a failure in the chamber. The buffer projection is necessitated by the presence of the chamber volume at the end of the driven tube which can permit piston contact at the driven tube end with insufficient chamber pressure development. Metal-to-metal impact if allowed to take place could cause damage to the piston and/or tube face. The buffer prevents this occurrence.

For any particular combination of driven (test) gases and desired ballistic result, Shock Tube Gun settings namely; driver pressure, piston and projectile weights, and driven gas initial pressure are determined using a simplified computer code which models the dynamic conditions within the gun. The computer code was validated in early developmental testing of the STG whereby piston position, chamber pressure, and projectile velocity were measured and compared with those prediced. As an example of the performance of the code Figure 5 shows a comparison of predicted and measured chamber pressure histories at a condition representing Zone 7 in the eight-inch howitzer. It is clear that chamber pressure is more than adequately predicted by the computer code both with regard to magnitudes of pressure and time. Using the computer code, then, STG input factors can be chosen to result in preselected test conditions of pressure, temperature, gas velocity and gas activity at the entrance of the launch tube. These represent parameters which are important in tube heating and erosion.

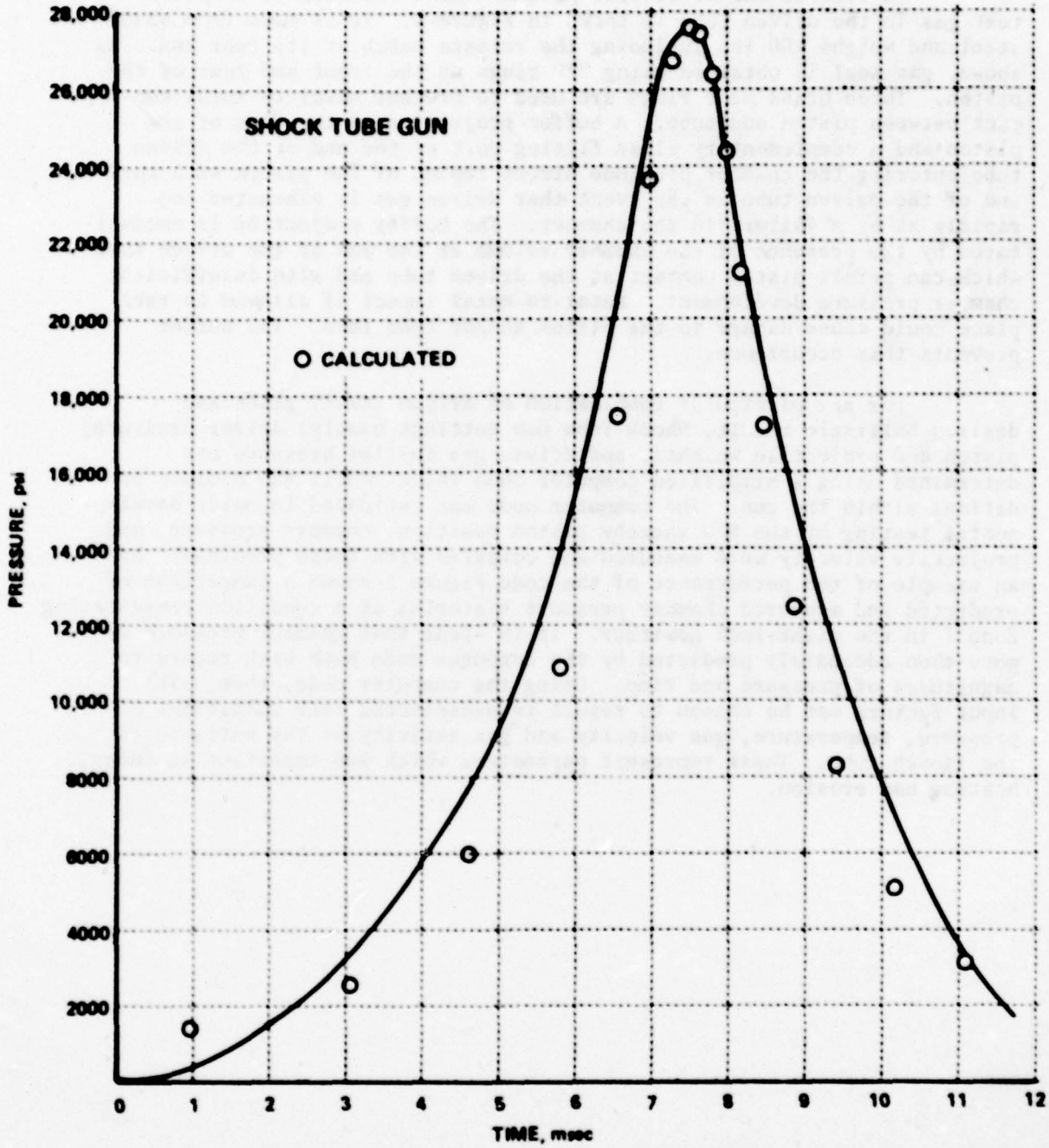

Figure 5 COMPARISON OF CALCULATED AND MEASURED CHAMBER PRESSURES – AIR

III. TEST PREPARATIONS

1. Materials Selection

As noted earlier the chief objective of this work is to determine gun conditions which lead to pure melting at the bore surface and to examine and characterize bore surface condition after test in an effort to establish baseline materials behavior when subjected to severe heating conditions in the absence of significant chemical activity. To do this effectively, test specimens amenable to analysis and representing a sufficiently wide range of thermal properties including melting point were first selected. Table 2 lists the pure metals and alloys tested in this work. These were deemed most appropriate because of their thermal property range and/or their similarity to conventional gun steels.

Pure melting of solids exposed to intense heating is governed primarily by the severity of the thermal gradient with the body away from the surface and the magnitude of its melting point. Because the rate of conduction of heat away from the heated surface is much less than that arriving at the surface from the gas, thermal gradients within the material become steep and the material can absorb only a little heat before melting of the surface begins. The depth of heat penetration in materials and, thus, the amount absorbed is dependent on their thermal diffusivity and the exposure time. For semi-infinite solids, the heated depth at any time is given approximately by the equation

$$\delta = \sqrt{6\alpha t} \qquad (1)$$

α = is the thermal diffusivity

For illustration, the expected heated depth in 4340 steel as a function of time is given in Table 3.

TABLE 3. HEAT PENETRATION DEPTH IN 4340 STEEL

Heated Depth δ, in.	Time, t Milliseconds
0.0026	0.1
0.0036	0.2
0.0058	0.5
0.0082	1.0
0.012	2.0
0.018	5.0
0.026	10.0

TABLE 2. PHYSICAL PROPERTIES OF SELECTED METALS AND ALLOYS

Metal or Alloy	Density lb/ft^3	Specific Heat BTU/lb-°R	Thermal Conductivity BTU/ft-hr-°R	Solidus/Liquidus °F	Latent Heat BTU/lb	Merit Parameter $\Delta T_m \sqrt{kc\rho}$ $BTU/ft^2\text{-}hr^{1/2}$
Pure Copper	510	0.1	220	1981/1981	90	202,315
Naval Brass	512	0.1	84	1630/1650	75	102,960
Pure Iron	476	0.14	23	2780/2780	117	111,110
4340 Steel	490	0.14	19.6	2640/2720	100	93,687
Cupro Nickel (70 cu - 30 ni)	540	0.12	32	2140/2260	100	93,150
Maraging Steel (Vascomax 300)	490	0.14	17	2600/2650	100	86,000
1095 Steel	490	0.12	16	2450/2600	100	73,000

Clearly, Table 3 shows that only small amounts of this material can be heated in time periods of present large caliber guns.

As a consequence of this shallow heated depth and the steep thermal gradients, surface melting can begin quickly, with subsequent material removal. The equation for temperature rise at the surface of a semi-infinite solid when subjected to a constant heat flux, q, is

$$\Delta T = \frac{2q\sqrt{t}}{\sqrt{\pi \rho c k}} \tag{2}$$

which may be rewritten in the form

$$2q\sqrt{\frac{t_m}{\pi}} = (T_m - T_i)\sqrt{\rho c k} \tag{3}$$

in which

T_m is the melting temperature

T_i is the initial temperature

t_m is the time to melting

k is the thermal conductivity

$c\rho$ is the heat capacity per unit volume.

In this form, (Equation 3), the materials properties are collected on the right side of the equation. The value on the right then serves as a useful figure of merit for comparing materials. The larger the figure of merit, the larger the time required to attain melting at any constant heat flux. Those materials selected for this baseline study are listed in Table 2 in order of their figures of merit. It will later be of interest to observe whether the figure of merit depicts the performance of these materials in non-constant gun heating environments.

Among the pure metals melting between say 1500°F and 2500°F figures of merit are high and melting is difficult to achieve. Copper provides one example of this. Much lower figures of merit are available in common alloys. Those listed in Table 2 serve well.

Naval brass begins to melt at 1630°F, has an average thermal conductivity of 84 Btu/hr-ft-°F and a figure of merit of 102,960. Cupronickel alloy of 70 Cu-30Ni composition has a solidus temperature of 2140°F and less than one-half the thermal conductivity of naval brass. Its figure of merit is 93,150.

The alloy steels 4340 and Vascomax represent materials of current interest in weapons manufacture, and possess mid-range figures of merit.

The high carbon steel and the pure iron permit examination of the effect of carbon addition on materials melting behavior and fill out the range of figures of merit.

2. Specimen Installation

The erosion test section within the chamber of the Shock Tube Gun is as shown in Figure 6. Each test specimen is fabricated in the form of a ring and placed downstream from the entrance throat. The bore diameter of the ring specimens was selected to be 20mm and each was 0.5 inches long. Rings of this size fit easily on the specimen stage of Calspan's Etec Autoscan Scanning Electron Microscope (SEM) such that "before and after" examination of the bore surface can be conducted without recourse to replicas. Of course, several other factors entered into selection of specimen size, especially the need to maximize heat transfer so that relatively high melting alloys such as steel could be melted.

As shown in Figure 6, several specimens placed in series may be installed in each test. Because the heating conditions should change but little over the short axial distance of the samples, a number of materials can be tested at once under essentially the same test conditions. Early testing in this study reported later (Tests No. 1-7) utilized three samples of nearly identical bore diameter and regular cylindrical shape. Slight tolerance differences between samples, however, resulted in slightly non-concentric alignment of the rings and thus some edge effects on each ring. These edge effects tended to produce some flow separation at downstream areas with resulting questionable gas flow-surface interactions. Later tests used stacked 5° conical cylinders which maintained a favorable pressure gradient in the gas flow and little separation. The downstream bore diameter change due to the internal conical shape was very minor over the total axial length of the specimens and, in fact, tended to maintain a more constant heating over all test specimens.

Each test specimen was characterized with regard to weight and surface condition before test. Specimens were weighed using an analytical balance so that weight changes of a fraction of a milligram could be readily determined.

Surface characterization using the SEM was facilitated by placing indexing marks on each specimen, as in Figure 7, which serve to establish unique locations for before and after examination. In addition, Calspan has found that burrs or asperities intentionally left at the sharp edges of the scratch marks are very useful in detecting threshold erosion, because such asperities receive greater heating per unit conductive area.

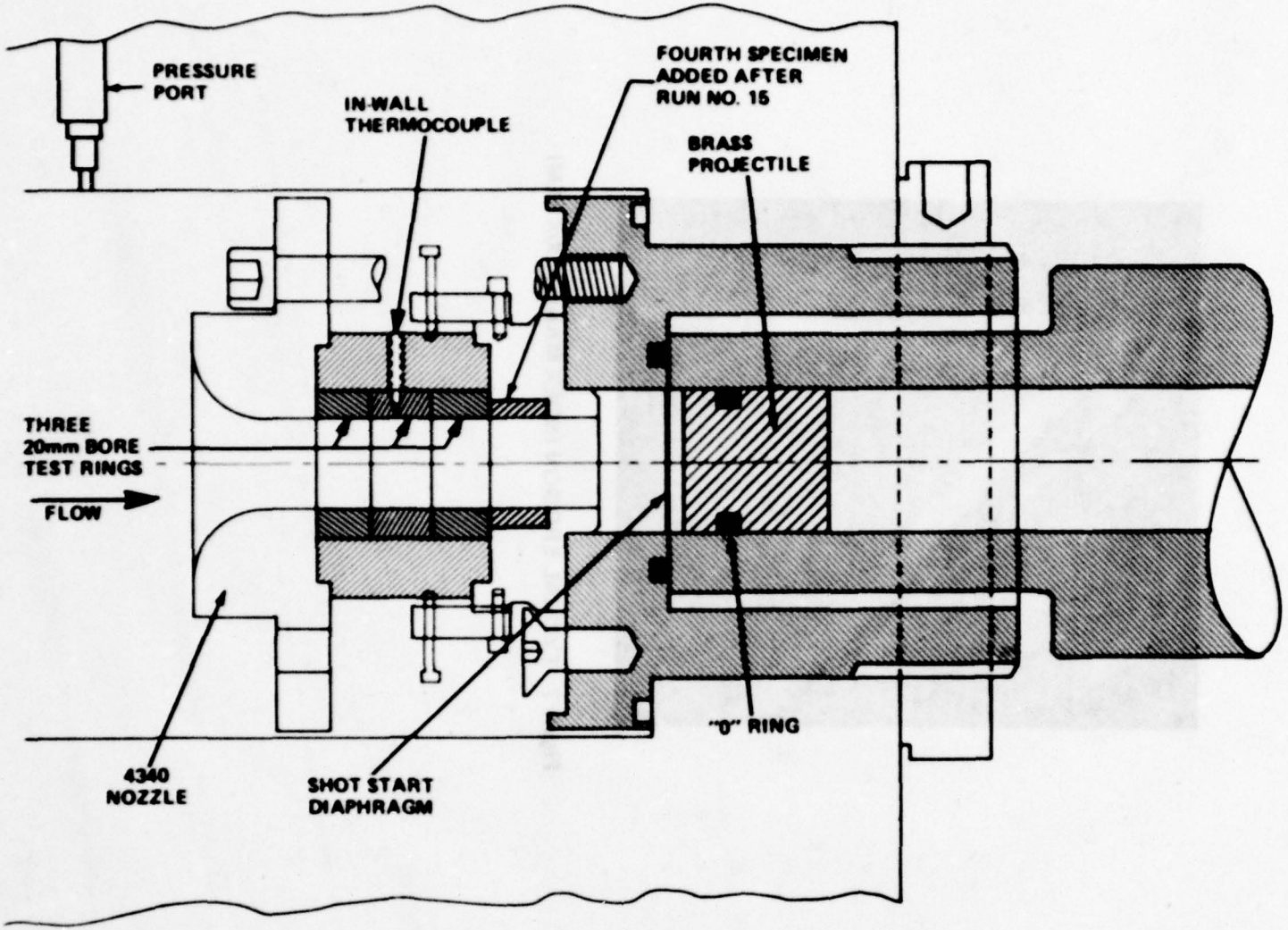

Figure 6 SHOCK TUBE GUN TEST SECTION MODIFIED TO ACCEPT THREE 20mm BORE EROSION TEST RINGS

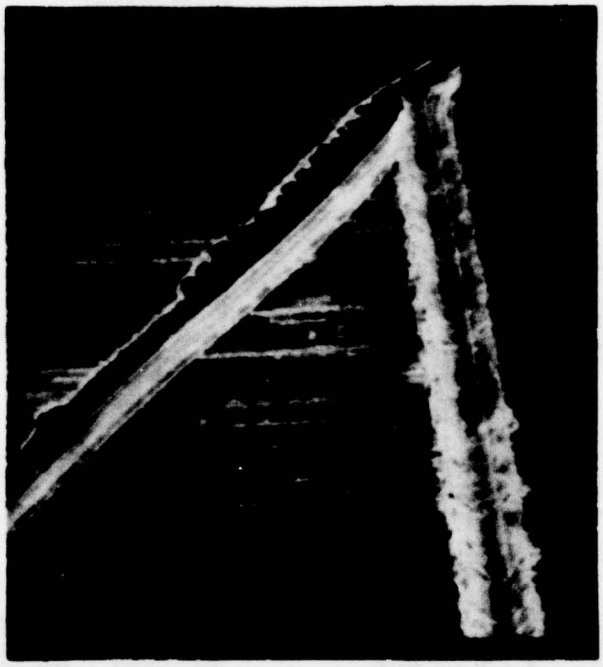

Figure 7 TYPICAL EROSION INDEX MARK (100X SEM)

3. Heat Transfer Instrumentation

A primary measurement of the study is the amount of bore heating associated with each test. For this measurement, two methods were used. First, in-depth thermocouples were installed in selected samples. These in-depth thermocouples were placed at distances of 0.020 and 0.040 inches from the bore surface. The method of installation is as shown in Figure 8. Each of these thermocouples independently may be used to determine net heating to the bore. Total heat input is calculated from the in-wall thermocouples output by use of methods developed and reported by Calspan.[2] Briefly, conversion of in-wall thermocouple outputs (millivolts vs. time) to total net heat input per unit area is made by use of the relation

$$Q(t) = \Delta T(t) \sqrt{\pi k c \rho t} \tag{4}$$

where $Q(t)$ is the net bore heat input

$\Delta T(t)$ is the indicated change in in-wall temperature as a function of time

k_m is the thermal conductivity

$c\rho$ is the heat capacity per unit volume

t is the time after start of heating.

Data reduction procedure is simply to apply Equation (4) at successive time intervals (e.g., 0.05, 0.1, 0.15 sec, etc.) resulting in a plot of $Q(t)$ vs. t. The curve thus produced will be asymptotic to the desired heat input. This method is very insensitive to the actual thermocouple depth and therefore both the 0.020 and 0.040 inch thermocouples yield redundant values.

A second method by which net total heat input was derived was to use the test specimen itself as a calorimeter. For this several ring calorimeter specimens were made according to the sketch of Figure 9. Thermocouples were installed in the calorimeter portion of the specimen as shown and the calorimeter was fabricated of the material under test. Here, the in-depth thermocouple could be used to obtain heat input via Equation 4 while the outermost thermocouple yielded heat input through use of the expression

$$Q = \frac{c\rho m}{A} \Delta T_R \tag{5}$$

Since m is the mass of the sensing ring, Equation 5 is simply a ratio of the change in heat content of the sensing ring over the temperature

---

2. F.A. Vassallo, "Mathematical Models and Computer Routines Used in Evaluation of Caseless Ammunition Heat Transfer," Calspan Report No. QM-2948-Z-1, June 1971.

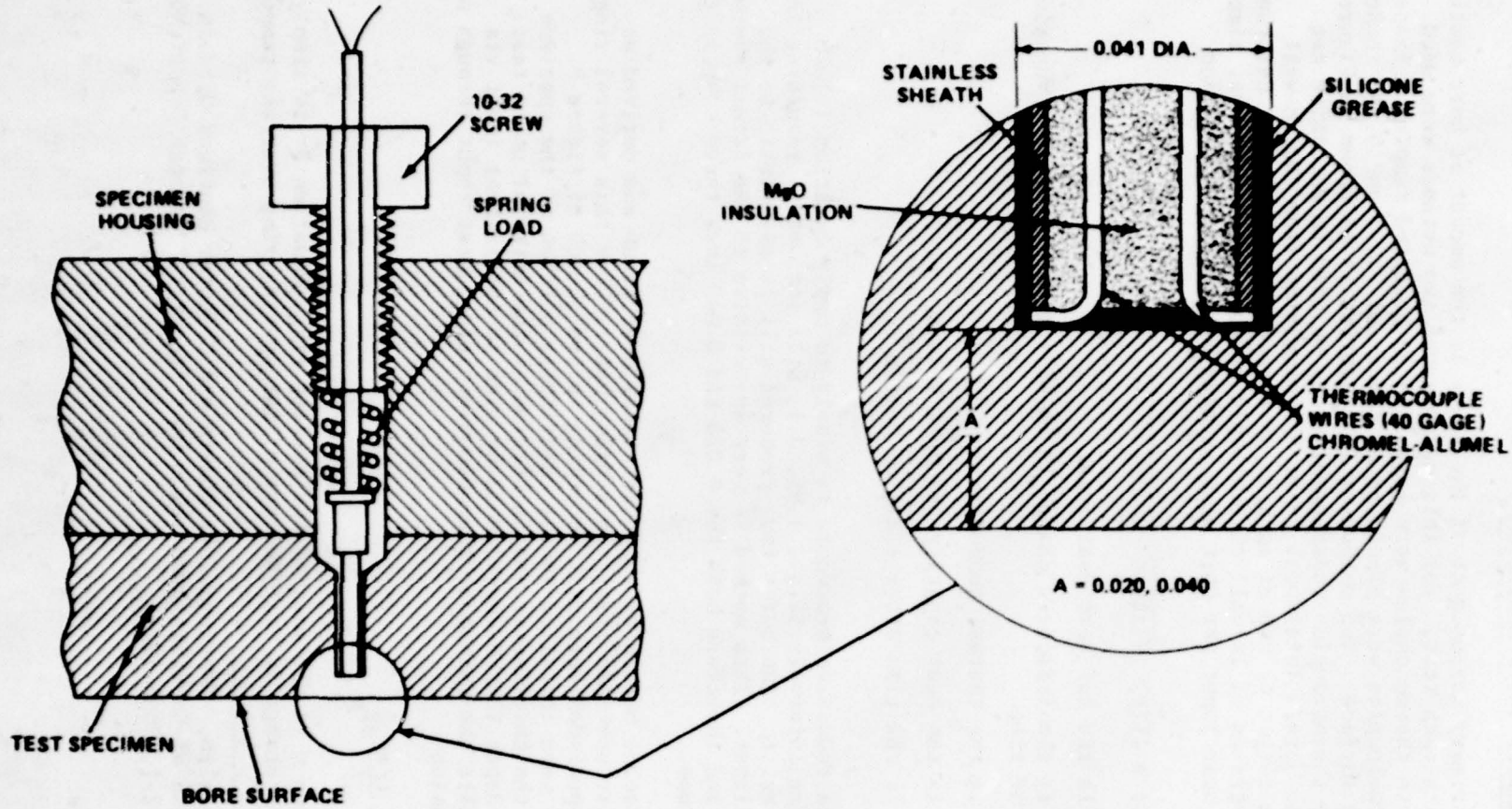

Figure 8 IN-WALL THERMOCOUPLE INSTALLATION

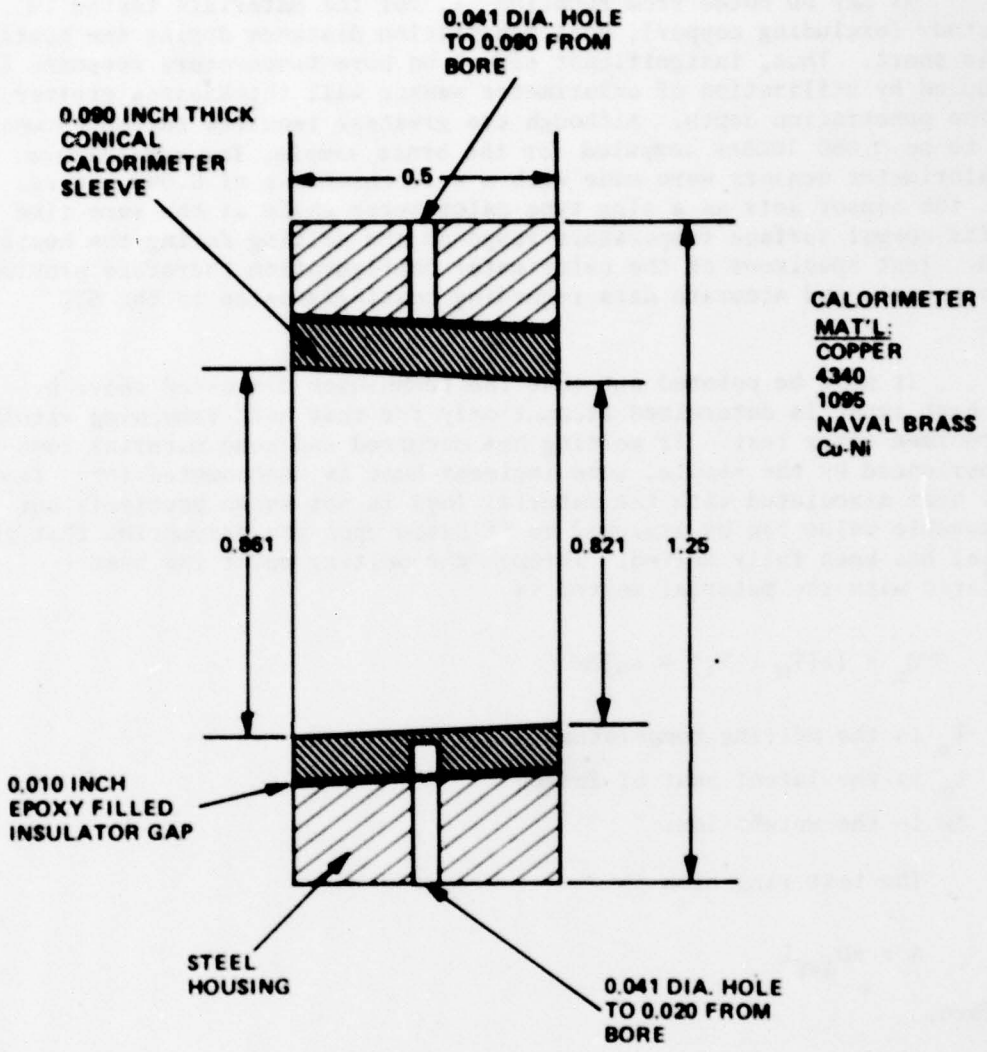

Figure 9 CONICAL CALORIMETER SAMPLE

rise ΔT_R to the bore heat input area.

As may be noted from Equation 1, for the materials tested in this study (excluding copper), heat penetration distance during the heating time is short. Thus, insignificant effect on bore temperature response is introduced by utilization of calorimeter sensor wall thicknesses greater than the penetration depth. Although the greatest required thickness was found to be 0.060 inches computed for the brass sample, for convenience, all calorimeter sensors were made with a wall thickness of 0.090 inches. Hence, the sensor acts as a slug type calorimeter while at the same time exhibits normal surface temperature response and melting during the heating period. Test specimens of the calorimeter configuration therefore provide the most basic and accurate data regarding heating/erosion in the STG tests.

It must be pointed out that the techniques discussed above by which heat input is determined account only for that heat remaining within the specimen after test. If melting has occurred and some material loss is experienced by the sample, some incident heat is unaccounted for. The actual heat associated with the material loss is not known precisely but a reasonable value can be assigned to it based upon the assumption that the material has been fully melted. Through the melting point the heat associated with the material melted is

$$Q_m = [c(T_m - T_i) + L_m]\Delta w \tag{6}$$

where T_m is the melting temperature

and L_m is the latent heat of fusion

Δw is the weight loss

The test ring area is

$$A = \pi D_{AVE} L$$

Therefore,

$$Q_{CORR} = Q_m/A = \frac{[c(T_m - T_i) + L_m]\Delta w}{\pi D_{AVE} L} \tag{7}$$

Table 4 lists an estimated value of Q_{CORR} per gm of loss for each of the material types tested.

Where significant loss was observed, the net heat input was corrected by the indicated amount.

TABLE 4. HEAT INPUT CORRECTIONS, Q_{CORR}

Material Loss	Heat Input Correction Btu/Ft^2 - Gm
Naval Brass	58
Cupronickel	88
1095 Steel	97
4340 Steel	103
Copper	70
Iron	124

4. Selection of Test Conditions

Basic requirements in the selection of test gas and conditions are that bore surface melting be produced with as little chemical interaction with the surface as possible. Therefore, the test gas should contain negligible oxygen. Furthermore, gas pressures and temperatures of the magnitude generally obtained in large caliber weapons were taken as design goals. A fundamental property of the gas which governs the pressure/temperatures produced in the shock tube compression process is its ratio of specific heats, γ_m. Figures 10 and 11 illustrate characteristic performance curves for the present Shock Tube Gun as a function of driver pressure and ratio of specific heats. Figure 10 illustrates the maximum pressures obtainable, whereas Figure 11 shows corresponding maximum temperatures. Although modification of the facility would allow a greater performance range, in its present configuration maximum allowable driver pressure is 650 psia and maximum chamber pressures should be limited to about 40,000 psi. These limits determine the performance envelope as shown in Figure 10. As may be observed, the limiting chamber pressure may be achieved with a wide selection of ratios of specific heat. Reference to Figure 11, however, shows that generation of high pressure for those gas mixtures having low values of γ_m is obtained at sacrifice in maximum gas temperature. The dashed curve in Figure 11 represents the locus of the maximum temperature attainable with a 40,000 psi chamber pressure limit. Thus, for a γ_m of 1.4 $T_{max} = 5100°R$.

In considering the pure monatomic gases Helium and Argon, it is found that their ratio of specific heats ($\gamma = 1.666$) results in too little chamber pressure generation (<25,000 psi) with unrealistically high maximum gas temperatures (>10,000°R). Furthermore, use of Helium results in only a small amount of test gas being compressed due to its low molecular weight. Reference to Figures 10 and 11 reveals that the pressure-temperature conditions are maximized with γ_m set at about 1.53. To promote development of pressures above 40,000 psi taken as a test goal, initial tests were conducted with a Nitrogen-Argon mix having a ratio of specific heats of 1.5 which was obtained by use of a mixture containing 54.5% Argon and 45.5% Nitrogen by weight. Final testing was performed by adjusting γ_m to 1.53 using a 63/37% Argon/Nitrogen mix. Two other specific mixtures were also used for selected tests in an effort to confirm the performance curves.

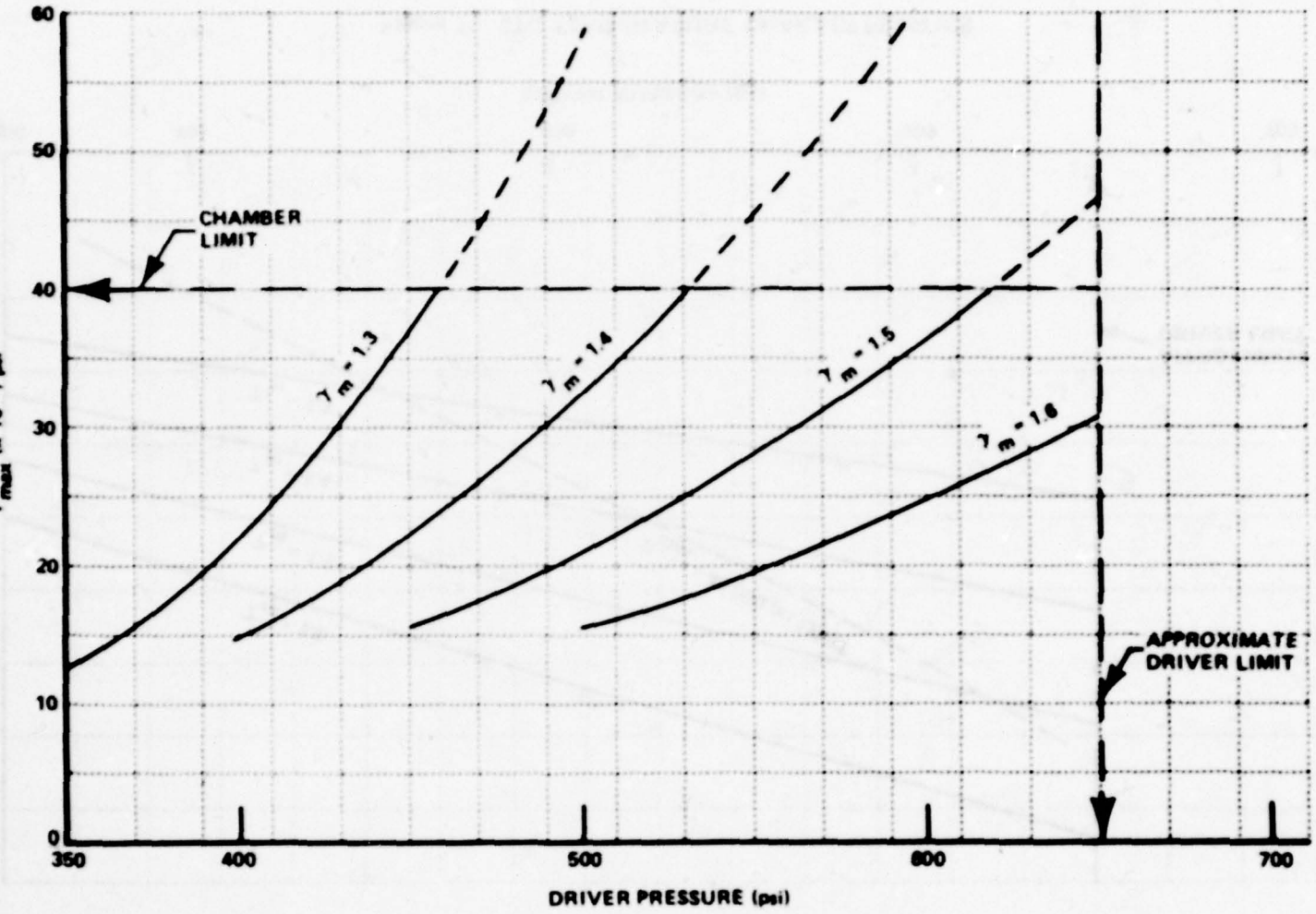

Figure 10 STG CHAMBER PRESSURE CHARACTERISTICS

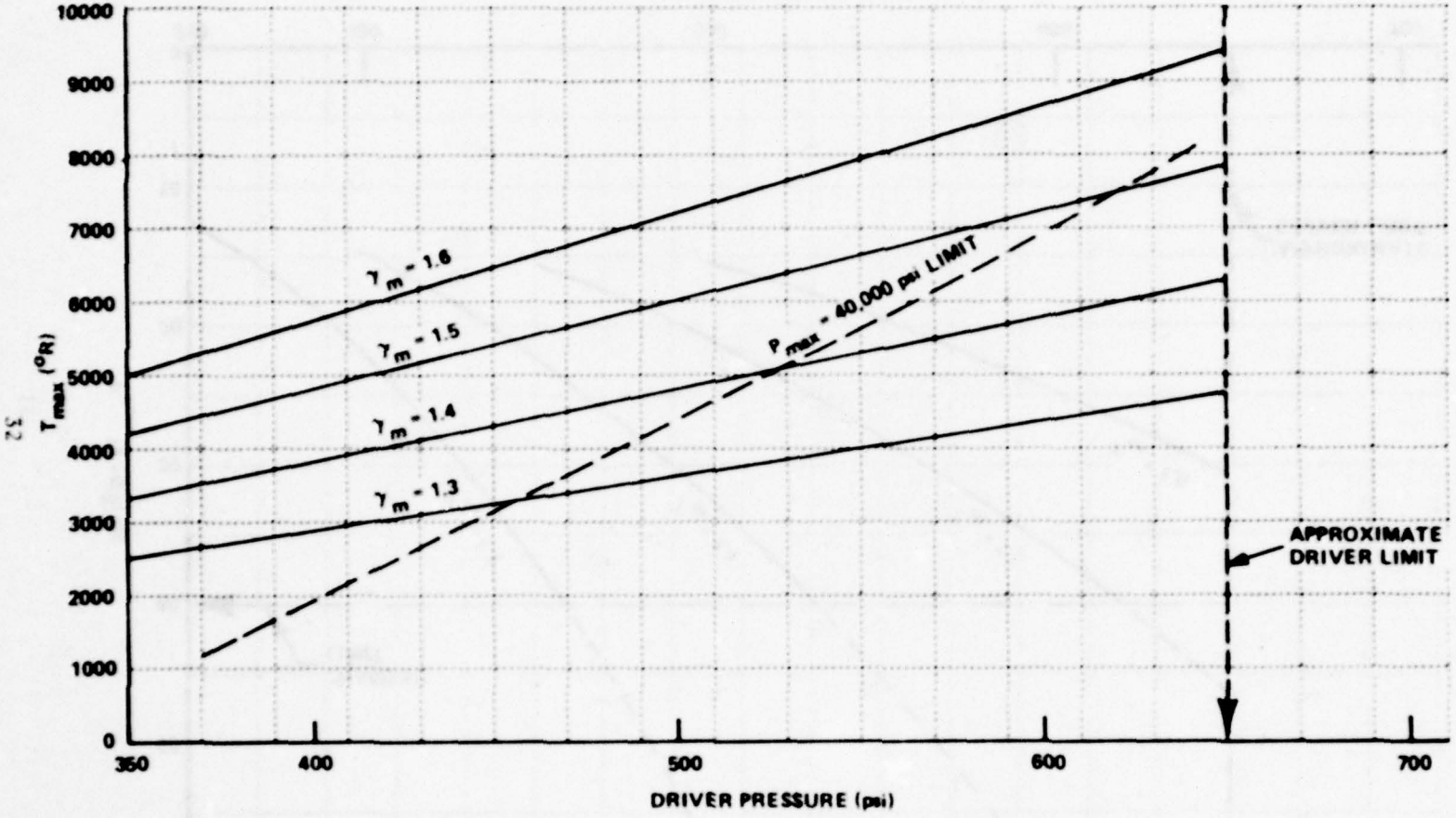

Figure 11 STG TEMPERATURE CHARACTERISTICS

IV. TEST PROCEDURE AND RESULTS

1. Test Procedures

Collection of test data regarding ballistics, heating, and erosion followed a more-or-less standard procedure. First, all important components of the facility were inspected for attrition due to previous firings, expendable items such as "O" rings and other seals were replaced. The driven tube, chamber, and piston were carefully cleaned to avoid presence of contaminants. The piston was then fixed in position at the upstream end of the driven tube. The projectile was inserted into the barrel.

Specimens were characterized prior to test using the SEM for surface appearance and an analytical balance for initial weight. Selected specimens or calorimeters were then installed within the chamber as shown in Figure 6 earlier. In selected tests, M-11 crusher gages were also installed in the chamber for a redundant measure of pressure. All required instrumentation including pressure transducers, thermocouples, and velocity screens were connected to suitable recording devices; the piezoelectric pressure output was recorded on a Bell and Howell tape recorder at a speed of 30 in/sec; thermocouple output was recorded directly on a Consolidated Electrodynamics Corporation oscillograph at a paper speed of 5 inches per second; the projectile transit time between velocity screens was recorded by use of a Tektronix Scope Set for 1 millisecond per division. The Tektronix Scope was also used to record the pressure signal playback from the tape which was performed at a tape speed of 1 7/8 inches/second, or a time expansion of 16:1 over the recording time.

After installation of the projectile and specimens, the entire driver tube including the chamber was evacuated to a pressure level of less than 0.1 inch of Mercury. The chamber was then purged by filling with pure Nitrogen. It was again evacuated and filled to the required partial pressure of Nitrogen. Pure Argon was then added to result in the required mix pressure.

The required partial pressures of Nitrogen and Argon are dependent upon the mix ratio desired and this is determined by the desired ratio of specific heats for the mix. Equations for establishing partial pressure settings were derived from simple mixing laws and are:

$$W_m = W_N + W_A \tag{8}$$

$$\gamma_m = \frac{W_N}{W_m}\,\gamma_N + \frac{W_A}{W_m}\,\gamma_A \tag{9}$$

$$R_m = \frac{W_A}{W_m} R_A + \frac{W_N}{W_m} R_N \tag{10}$$

$$W_m = \frac{P_m V_m}{R_m T_m} \tag{11}$$

$$P_N = \frac{W_N R_N T_m}{V_m} \tag{12}$$

From which,

$$P_N = \frac{\left[1 - \frac{\gamma_N - \gamma_m}{\gamma_N - \gamma_A}\right] R_N P_m}{R_N + (R_A - R_N) \frac{\gamma_N - \gamma_m}{\gamma_N - \gamma_A}} \tag{13}$$

and

$$P_A = P_m - P_N \tag{14}$$

In these expressions, subscripts m, N, and A refer to mix, Nitrogen, and Argon respectively. Also,

W is weight
P is the pressure
γ is the ratio of specific heats
R is the gas constant
V is the driven tube volume

For any selected ratio of specific heats, γ_m, and mix pressure P_m, the partial pressures of Nitrogen and Argon are specified by Equations 13 and 14.

Following these test preparations, the driven tube was pressurized to the desired level, recording devices were activated and the piston was released.

After exhausting residual driver pressure, specimens were removed and hard copy was made of the test data. Specimens were inspected, reweighed and photographed when deemed appropriate.

2. Heat Input Data

Heating/ballistic data collected for all test runs conducted in this study are given in Table 5. The general test approach involved assessment of heating and materials response with gradually increasing test severity. In this way, the action and performance of the facility could be established with minimum chance of irrepairable damage to it while at the same time permitting collection of meaningful data.

The first seven runs were chiefly for the purpose of determining heating and temperature response of the naval brass specimen. Total heat input amounts were gradually increased to 119 Btu/ft^2 with resulting melting of the brass (see Section IV.3). In Runs 8 and 9 a special specimen configuration was used whereby each successive in-line specimen was reduced in diameter, presenting a raised leading edge to the gas stream. The objective was to increase heat transfer to the edge to force local melting of resistant materials. The raised edge on the brass heat input specimen exhibited considerable local melting which apparently induced greater downstream total heat input as indicated by the increase to 135 Btu/ft^2 from 119 Btu/ft^2 recorded in the earlier run at the same test condition. It is believed that the increased heat input arises in part by resolidification of upstream melt at the downstream thermocouple sensing station and in part by overestimation of the heat input associated with material loss via Equation 7 in this totally non-uniform heating situation. For this reason, the "stepped" specimen configuration was not continued beyond Run Number 9.

Runs 10 through 25 were generally attempts to increase the heating conditions through change in driver pressure, piston weight, projectile weight, and gas mixture. It was found, however, that maximum heating conditions obtainable for the conical samples used (about 20mm diameter) were limited to below that needed to melt pure Iron.*

Comparative heating values for the five types of calorimeters were obtained in Runs 26 through 30 at the highest presently obtainable Shock Tube Gun test condition. Total heat input data were obtained for each of these samples as were erosion data to be discussed presently. The chief purpose of Runs 26 through 30 was to evaluate the heating/melting performance of the various materials at essentially the same flow condition. The maximum pressure in these runs was about 40,000 psi with a corresponding gas temperature of about 8250°F. Figure 12 illustrates a pressure history typical of these runs.

---

*For future test work, the facility will be upgraded to increase maximum test conditions through the addition of heaters on the driven tube.

TABLE 5. HEATING/BALLISTIC TEST RESULTS - SHOCK TUBE GUN

Test No.	γ*	Driver Pressure psi	Piston Weight lb.	Chamber Pressure psi	Gas Temperature °R	Projectile Weight lb.	Projectile Velocity Ft/sec	Heat Specimen	Heat Input Btu/Ft^2
1	1.5	350	150	5300	3790	1.0	1100	Brass	64
2	↓	400	↓	11500	4910	↓		↓	87
3		430		(12900)	5100		1610		97
4		460		19500	5860		1720		109
5		500		23000	6190		1850		105
6		550		(31500)	6870		1660		--
7		565		(32700)	6960		2380		119
8		565		31000	6840		1920		135
9		590		34500	7080		2220		128
10		565		31000	6840		1938	Iron	90
11		590		34000	7050		1886	↓	93
13		630		(38000)	7320		2120		93
14		630		(38000)	7320	↓	2127	Iron 4340	90/81
15		600		35500	7150	.5	2702	↓	95/82
16		630		39500	7410	↓	2631		89/81
17		630		43500	7650		2560	Cu. CAL.	143
18		630	↓	40000	7440		2500	4340 CAL.	82
19		575	200	34500	7080	1.0	1960	↓	90
20		630	↓	41000	7500	↓	2170		85
21	↓	600		37000	7250	.5	2170		85
22	1.615	600	150	22000	8630	↓	1960		72
23	1.4	500	↓	28500	4630		--		77
24	↓	550		35500	4930		1670		77
25	1.53	650		39500	8220	.25	2440	↓	85
26	↓	650		39500	8220	↓	2570	Brass CAL.	110
27		650		40000	8250		2800	Cu-Ni CAL.	100
28		650		39500	8220		2222	4340 CAL.	86.5
29		650		40000	8250		2666	1095 CAL.	84.5
30		620		36500	8000		2400	Cu. CAL.	135
31		650		42000	8430		2050	4340 CYL#1	90
32	↓	650	↓	42000	8400	↓	2250	↓	89

() indicates crusher gage pressure result

*γ = Ratio of specific heats

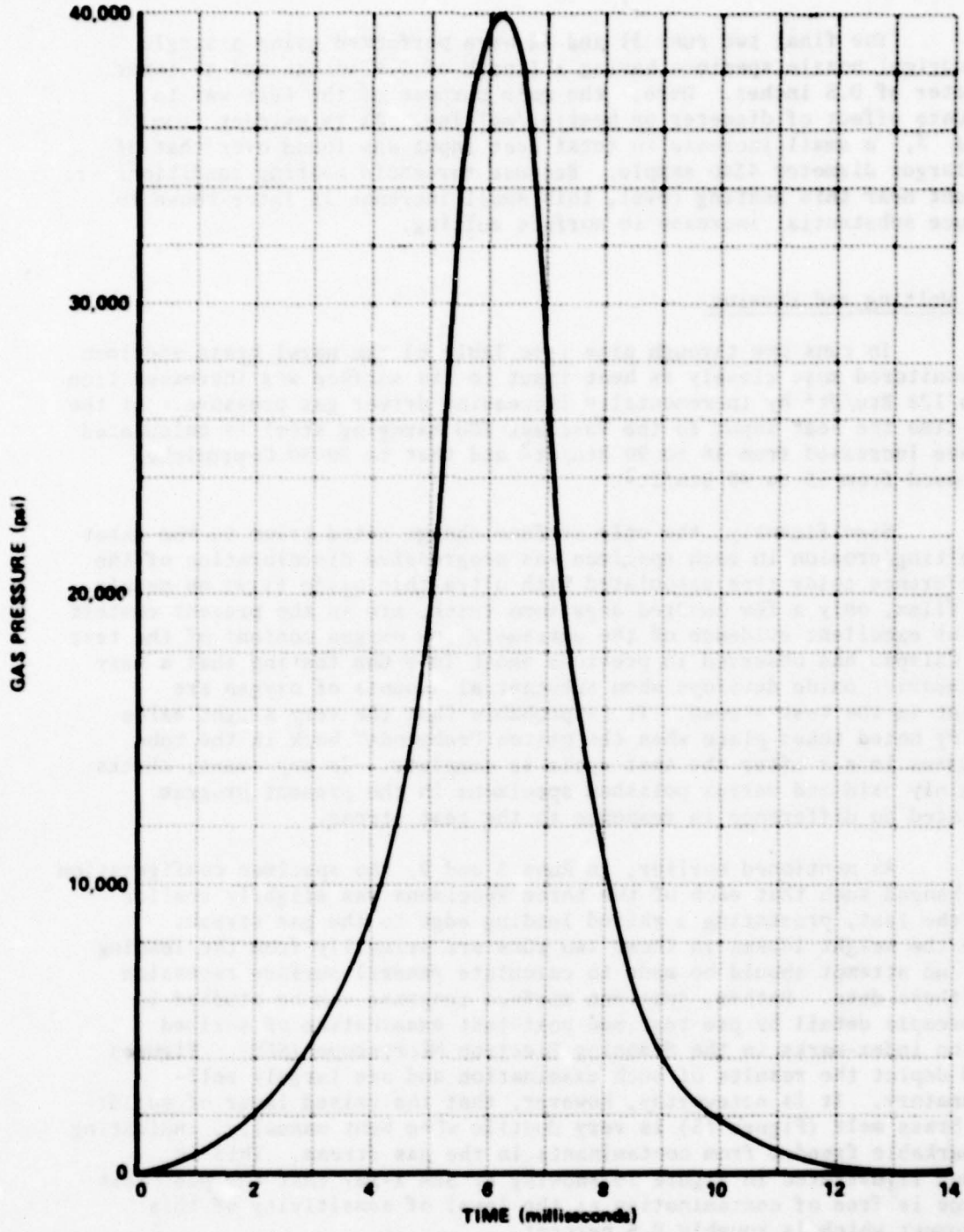

Figure 12 GAS PRESSURE VS. TIME FOR RUN NO. 29

The final two runs 31 and 32 were performed using a single cylindrical nozzle specimen having a length of 1.5 inches and an inner diameter of 0.5 inches. Here, the main purpose of the test was to evaluate effect of diameter on heating/melting. As is evident from Table 5, a small increase in total heat input was found over that of the larger diameter 4340 sample. Because threshold melting conditions are present near this heating level, this small increase is later shown to produce substantial increase in surface melting.

3. Melting and Erosion

In runs one through nine (see Table 6) the naval brass specimen was monitored most closely as heat input to its surface was increased from 64 to 128 Btu/ft^2 by incrementally increasing driver gas pressure. At the same time the heat input to the Vascomax 300 maraging steel is calculated to have increased from 48 to 90 Btu/ft^2 and that to 70-30 Cupronickel increased from 55 to 90 Btu/ft^2.

Significantly, the only surface change noted prior to the onset of melting/erosion in each specimen was progressive discoloration of the interference color type associated with ultra-thin oxide films on metals. Such films, only a few hundred angstroms thick, are in the present context seen as excellent evidence of the extremely low oxygen content of the test gas; Calspan has observed in previous Shock Tube Gun testing that a very much heavier oxide develops when substantial amounts of oxygen are present in the test stream. It is probable that the very slight oxide tinting noted takes place when the piston "rebounds" back in the tube and draws in air after the test cycle is complete. In any event, checks of thinly oxidized versus polished specimens in the present program indicated no difference in response to the test stream.

As mentioned earlier, in Runs 8 and 9, the specimen configuration was changed such that each of the three specimens was slightly smaller than the last, presenting a raised leading edge to the gas stream. Since the weight losses in these two runs are primarily from the leading edge, no attempt should be made to calculate general surface recession from these data. Rather, specimen surface response can be studied in microscopic detail by pre-test and post-test examination of scribed erosion index-marks in the Scanning Electron Microscope (SEM). Figures 13-18 depict the results of such examination and are largely self-explanatory. It is noteworthy, however, that the raised layer of solidified brass melt (Figure 15) is very ductile when bent manually, indicating a remarkable freedom from contaminants in the gas stream. This is further illustrated in Figure 16 showing by SEM x-ray that the post test surface is free of contamination at the level of sensitivity of this instrument which is roughly 0.5 percent.

Table 6 SPECIMEN SURFACE RESPONSE DATA SUMMARY

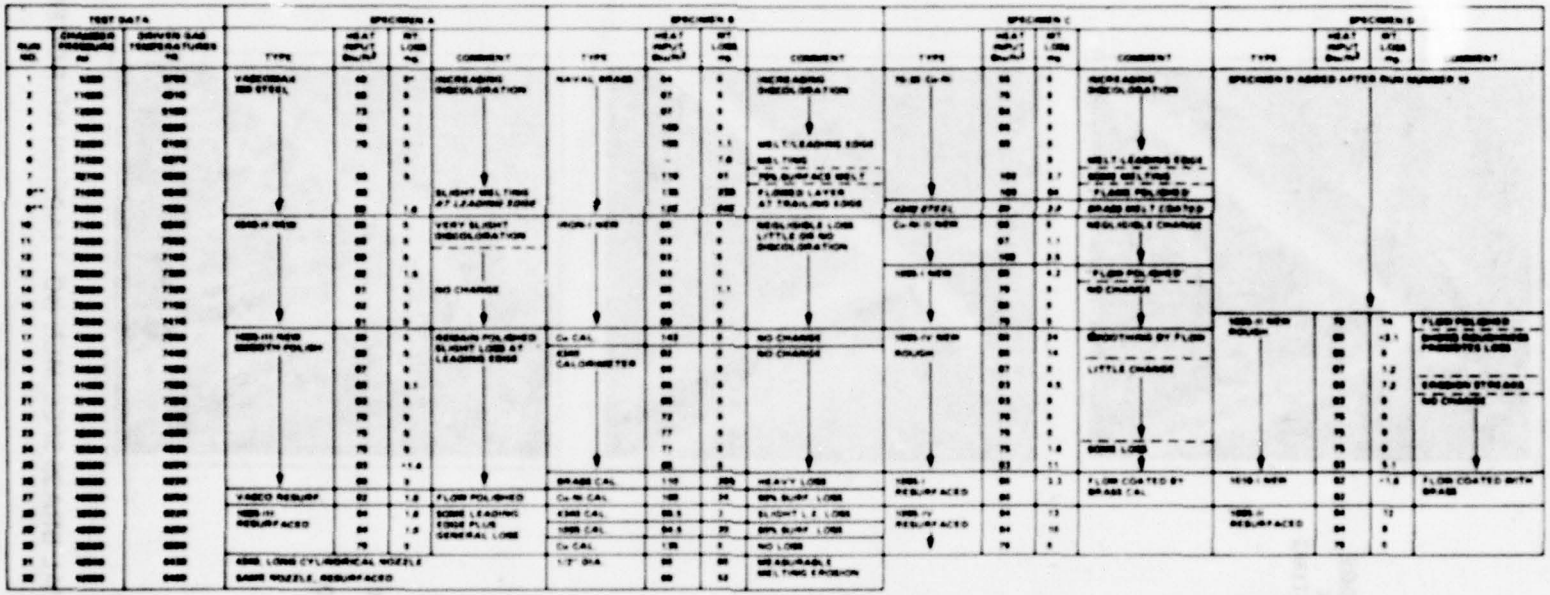

* INDICATED WEIGHT LOSSES LESS THAN ONE MILLIGRAM ARE LISTED AS ZERO.

**SPECIMEN WAS CHANGED TO NEW "STEPPED" ID AFTER RUNS 9 AND 10. SEE TEXT.

TRAILING EDGE INDEX MARK BEFORE TESTING (100X SEM)

RUN NO. 5
HEAT INPUT
105 Btu/ft^2
(100X SEM)

ONLY THIN PROJECTING "BURRS" LOST HERE AT TRAILING EDGE; THRESHOLD MELTING NEAR LEADING EDGE (NOT SHOWN)

RUN NO. 6
HEAT INPUT
115 Btu/ft^2
(ESTIMATED)
(100X SEM)

SHOWS THRESHOLD MELTING HERE AT TRAILING EDGE; DEFINITE MELTING NEAR LEADING EDGE (NOT SHOWN)

Figure 13 NAVAL BRASS SPECIMEN NO. I (ARGON-NITROGEN γ_m =1.5 MIXTURE)

TRAILING EDGE
INDEX MARK
BEFORE TESTING
(100X SEM)

RUN NO. 8
HEAT INPUT
135 Btu/ft^2
(100X SEM)

AREA COVERED
WITH FLOWED
METAL

RUN NO. 8
NEAR INDEX
MARK
(1000X SEM)

SHOWS "FROZEN
WAVES" OF MELT

Figure 14 NAVAL BRASS SPECIMEN NO. II (ARGON-NITROGEN γ_m = 1.5 MIXTURE)

LEADING EDGE
AFTER RUN NO. 9
HEAT INPUT
128 Btu/ft^2

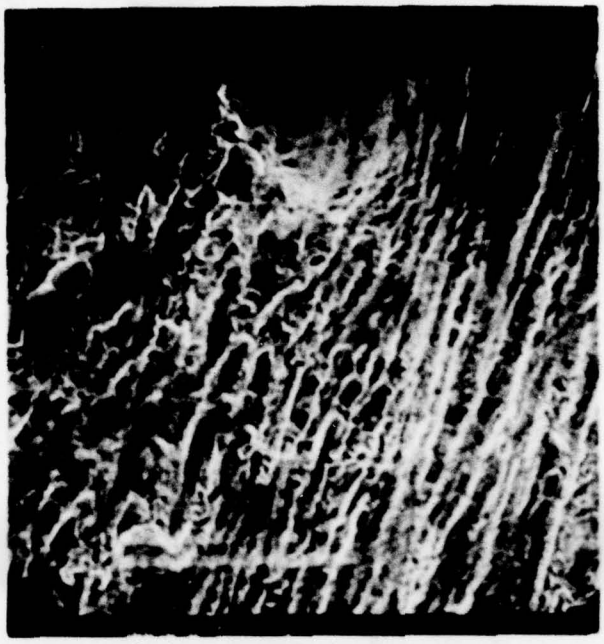

SHOWS "MASSIVE"
EROSION AT
LEADING EDGE,
SUBSTANTIAL
EROSION TOWARD
REAR

TRAILING EDGE
AFTER RUN
NO. 9

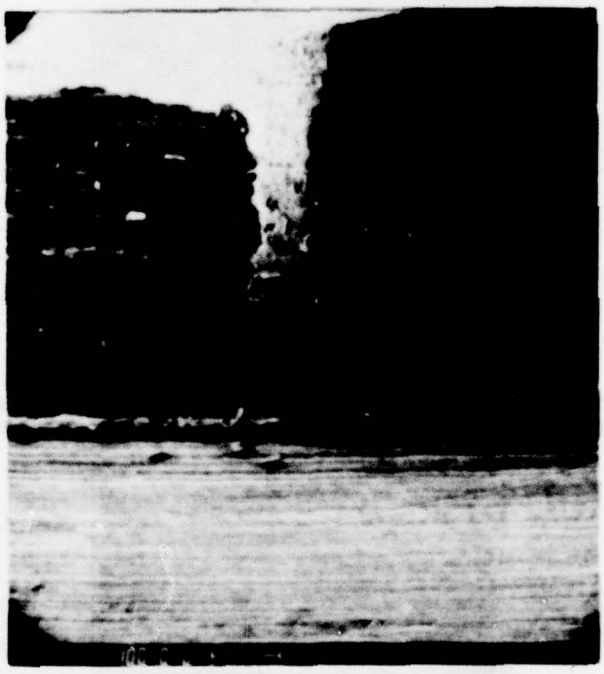

SHOWS FROZEN
MELT OVER
LAYER OF
DUCTILE BRASS

Figure 15 NAVAL BRASS SPECIMEN NO. II (ARGON-NITROGEN $\gamma_m = 1.5$ MIXTURE)

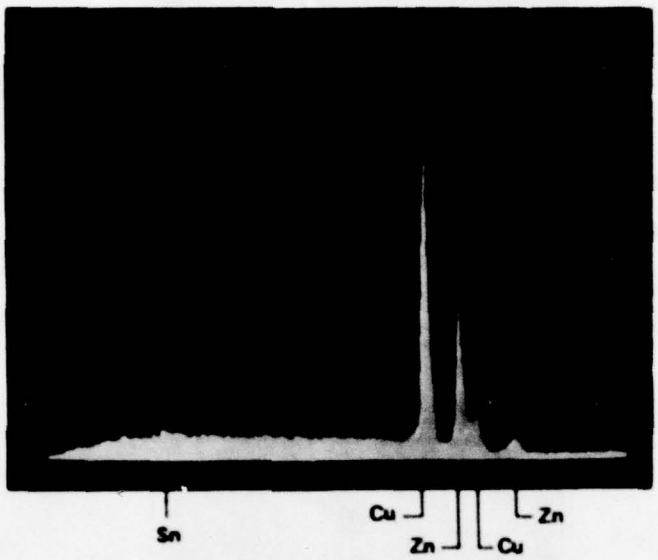

(a) Before Test

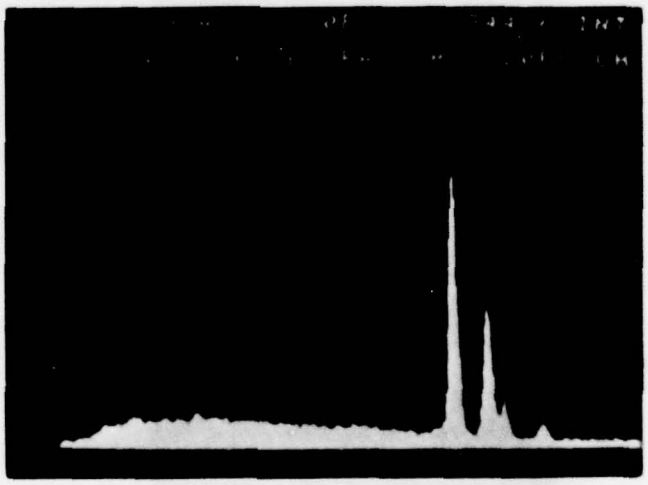

(b) Eroded Area after Test No. 6

Figure 16 NAVAL BRASS SPECIMEN SURFACE X-RAY SPECTRA (SEM)

TRAILING EDGE INDEX MARK AFTER RESURFACING (100X SEM)

RUN NO. 8 HEAT INPUT 103 Btu/ft^2 (100X SEM)

SHOWS SAME FLOW OVER INDEX MARK, SOME EROSION HERE AT TRAILING EDGE

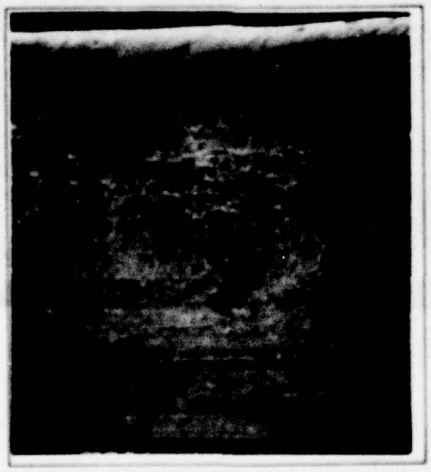

RUN NO. 8 LEADING EDGE (100X SEM)

SHOWS EROSION AT LEADING EDGE "STEP"

Figure 17 CUPRONICKEL ALLOY SPECIMEN NO. 1 (ARGON-NITROGEN γ_m = 1.5 MIXTURE)

TRAILING EDGE
INDEX MARK
BEFORE TESTING
(100X SEM)

RUN NO. 9
HEAT INPUT
90 Btu/ft^2
(100X SEM)

SHOWS NEGLIGIBLE
EROSION HERE AT
TRAINING EDGE

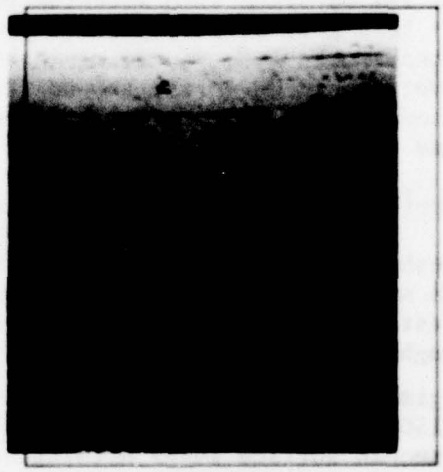

RUN NO. 9
LEADING EDGE
(100X SEM)

SHOWS THRESHOLD
EROSION HERE AT
LEADING EDGE
"STEP"

Figure 18 MARAGING STEEL (18% Ni) SPECIMEN NO. I (ARGON-NITROGEN γ_m = 1.5 MIXTURE)

In summary of the specimen response observations of the first nine runs, it was clear that a full melting condition was reached on the brass at a heat input slightly greater than 120 Btu/ft^2. The maraging steel at the 90 Btu/ft^2 level was showing just the beginning of leading edge melting on a stepped specimen where the actual heat input was no doubt greater than 90 Btu/ft^2 on the edge; the Cupronickel at 103 Btu/ft^2 lost 64 mg but mostly from the leading edge step where heat input was probably above 103 Btu/ft^2. It was thought that the stepped specimen configuration had served its purpose in runs eight and nine and all subsequent specimens had no leading edge step.

Runs 10 through 25 represent a portion of the program in which attempts were being made to increase heating and special calorimeter specimens were designed and employed to make certain that good heat input data were being obtained. Melting was not generally achieved in the 4340 steel, 1095 steel, ingot iron, or Cupronickel specimens employed as shown in Table 4. Important observations were made, however, on surface cracking (discussed later) and on the effect of surface roughness on erosion loss as discussed below.

It was noted in Run 13 that the new 1095 steel specimen (1095-I) lost about four milligrams; but in the next three runs under essentially identical heating conditions there was no additional loss. Suspecting that the smoothing effect of the first shot was responsible for the change to the "no loss" result in subsequent runs, much rougher 1095 steel specimens were introduced into a new "D" position in Run 16 and also into the "C" position in Run 17.

The rough 1095-II specimen is shown before and after firing in Figure 19. Loss was 14 mg which may be compared with the 4.2 mg loss cited above on a less rough specimen under the same heating conditions.

Specimen 1095-IV was machined with accentuated surface roughness in a way which (Figure 20) left more of the specimen projecting above a certain elevation so to speak. The loss was 24 mg in the first shot at the nominal 80 Btu/ft^2 level and 14 mg in the second (Runs 17 and 18). In the same two runs a polished 1095 steel specimen (Figure 21) lost no weight, i.e., less than one mg.

The above observations lead to the following statements:

1. As the threshold of complete melting is approached for high carbon steel (at nominally the 80 Btu/ft^2 level in these tests), a limited regime is reached in which surface roughness controls the amount of melt loss.

2. In this regime an extremely rough surface can lose more than 150 microinches in one shot while an extremely smooth surface loses nothing.

(a) BEFORE RUN 16 (NEW, ROUGH)

(b) AFTER RUN 16 (14 Mg LOSS)

Figure 19 SPECIMEN 1095-II AFTER ONE SHOT AT 79 Btu/ft^2 LEVEL

(a) BEFORE RUN 17 (NEW, ROUGH)

(b) AFTER RUN 17 (24 Mg LOSS)

Figure 20 SPECIMEN 1095-IV AFTER ONE SHOT AT 80 Btu/ft^2 LEVEL

(a) BEFORE RUN 17 (NEW, POLISHED)

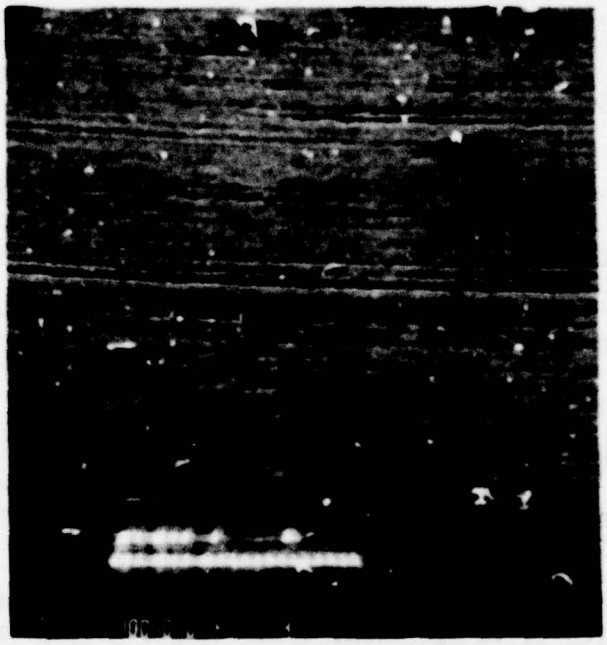

(b) AFTER RUN 17 (NEGLIGIBLE LOSS)

Figure 21 SPECIMEN 1095-III AFTER ONE RUN AT 80 Btu/ft^2 LEVEL

3. The loss from an initially rough surface will decrease with each succeeding shot in this regime.

One implication of the above is that it behooves the experimenter to finish each specimen similarly when testing in this regime. Along this line it can be noted that when losses greater than say 30-40 mg are obtained on the half-inch wide specimens, it can be concluded that the heat input has exceeded the level of the "roughness dominated regime" even for extremely rough specimens. For the bulk of the present study surface finish was held fairly constant at a roughness level in which roughness variations would account for no more than a very few milligrams loss variation on new specimens heated near threshold melting.

Specimen 1095-IV (shown in Figure 20) presents very interesting features at higher magnification in the SEM. These features can be associated with the iron-carbon equilibrium diagram, a portion of which is shown as Figure 22. In 1095 steel, the carbon content is 0.95 percent. Upon heating this composition to about 2450°F (1343°C), the phase boundary between solid austenite and the liquid + austenite region is encountered at the point circled in Figure 22. This temperature thus marks the appearance of the very first liquid. In real metals, however, impurities tend to reside in the grain boundaries such that the first liquid forms there at a temperature somewhat below the phase diagram equilibrium temperature. Taking the latter point into consideration but insisting also that several percent of liquid might be necessary to reduce the metal to a very soft mush (solid grains in a liquid matrix resembling wet cement), it is reasonable to take about 2450°F as the effective temperature at which material could be sheared from the surface of rapidly heated 1095 steel.

Figure 23 consists of "blow-ups" at 500X and 1000X of an area at the center left of Figure 20b. It seems unmistakable that the top of each ridge on the rough specimen has reached the mushy temperature and been carried away such that some material was entrained in the flow but some was blown down the side of the ridge where it resolidified. The mushy character of the material is even more clear at 2000X, Figure 24. These specific areas, therefore, indicate that at least the 2450°F level has been reached for this material.

For Test Runs 25-30, the STG facility was operated at present maximum conditions to evaluate material's comparative response. In these tests, conical calorimeter specimens were used. Surface appearance of specimens after test is shown in the photographs of Figures 25 through 28. It is clearly evident that at least local areas of each of the samples have reached their melting points. Figure 25 shows gross melting of the naval brass sample which is in agreement with the 269 milligrams lost on this sample. About eighty percent of the surfaces of the 1095 and Cupronickel samples are indicated to have reached melting. Typical melted areas are

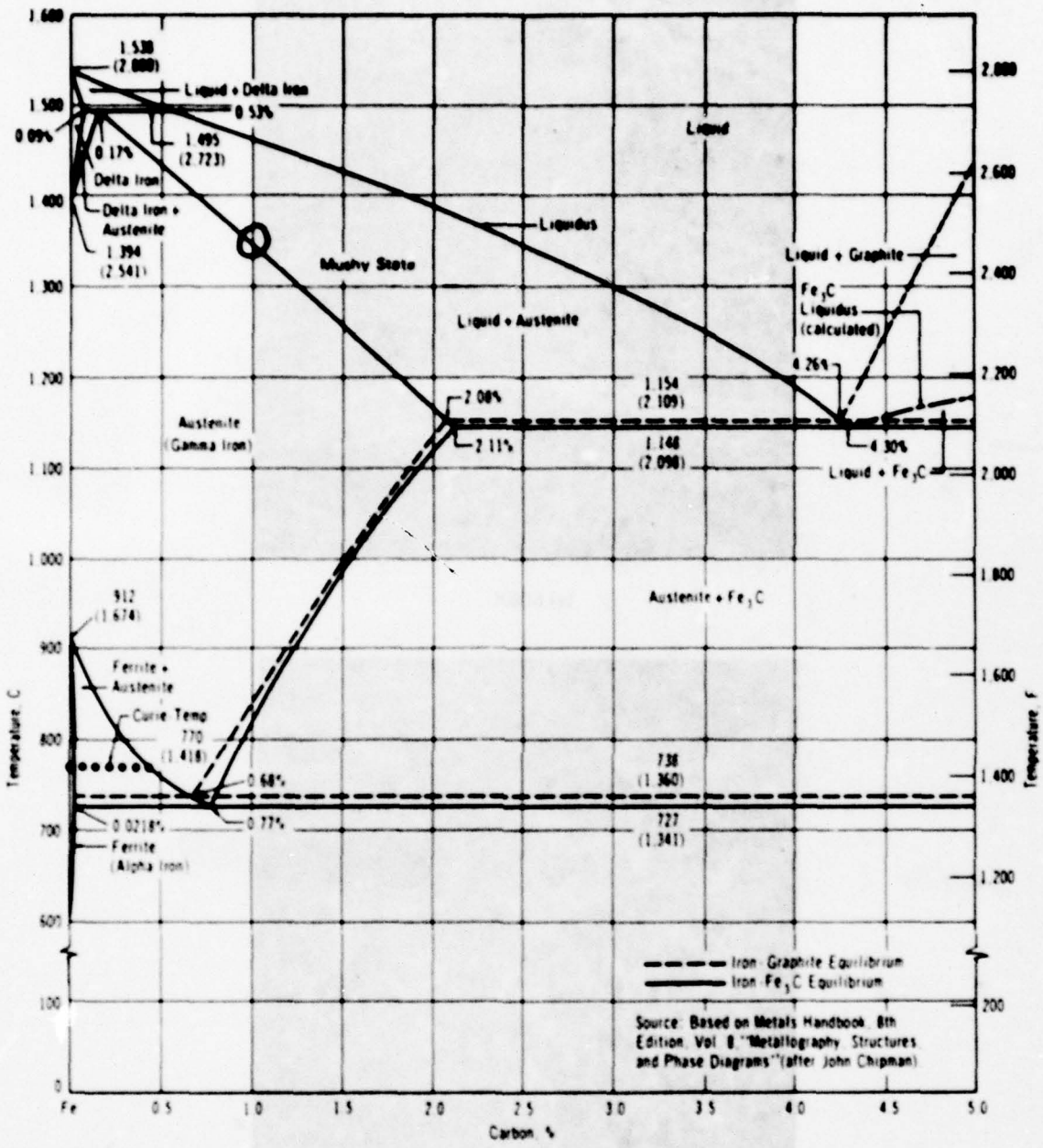

Figure 22 IRON-CARBON EQUILIBRIUM DIAGRAM

(a) 500X

(b) 1000X

Figure 23 SPECIMEN 1095-IV AFTER ONE SHOT

Figure 24 SPECIMEN 1095-IV, AREA NEAR TOP OF RIDGE (2000X)

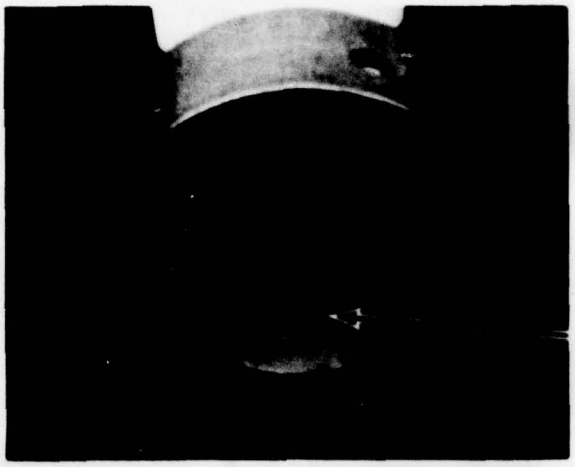

SHOWS
MASSIVE
SURFACE
MELTING

SHOWS FLOWED
MELT ON
SURFACE

(MAG. 100X)

Figure 25 SURFACE OF NAVAL BRASS CALORIMETER SAMPLE AFTER TEST NO. 26

shown in Figures 26 and 27. It is notable that at areas of the surface where no melting has taken place, the surface shows essentially no damage (see Figure 27). Very little total melting of the 4340 sample was produced. However, there is some indication of melting over about 10% of the surface and this is shown in Figure 28. Again, essentially no damage is evident where melting is absent. Thus, any material loss in these tests is attributable to melting alone in accordance with the goals of the study.

4. Surface Cracking

Calspan has noted in recent studies involving large caliber guns[3,4] that gun steel sensors and test rings invariably show prominent surface cracks after as few as two or three shots, if the heating is such as to drive the surface temperature to the range covering about 1900°F to perhaps 2500°F. Lower peak temperatures cause no apparent surface damage of any kind while higher ones result in erosion so rapid as to preclude crack development. Since gun steels contain about 0.4 percent carbon it has been thought in the past that crack initiation was simply attributable to the inevitable formation of a brittle hard martensite layer as the red-to white-hot bore surface layer was quenched by the cold underlying steel after the first shot.

Close examination of a 4340 steel test ring after seven STG "shots" in the current testing reveals that cracking has not been initiated despite the fact that heat inputs and resultant peak temperatures have been those known to cause rapid crack initiation and growth in the same steel when it is exposed to gun gases. It is clear, therefore, that some chemical effect of propellant gases not operative in the present STG Argon-Nitrogen mix causes crack initiation.

Figures 29-34 serve to document the above findings. Figure 29 shows the complete absence of cracks (even at 100X magnification) in a 4340 steel STG ring after seven tests, all of which yielded peak surface temperatures in the 1900°F to 2500°F range. The hard martensite layer would be at least as well formed as that of Figure 30b, and there was virtually no erosion of the ring surface, i.e., conditions would have been ideal for crack initiation if the hot surface had been exposed to propellant gases.

Very strong additional support for the above finding is found in the fact that the STG test section entrance throat of 4340 steel shows no

---

3. F.A. Vassallo, "An Evaluation of Heat Transfer and Erosion in the 155mm M185 Cannon," Calspan Technical Report No. VL-5337-D-1, July 1976.

4. F.A. Vassallo, W.R. Brown, "Heat Transfer and Erosion in the Ares 75mm High Velocity Cannon - Vol. II," Calspan Technical Report No. VL-5873-D-1 October 1977.

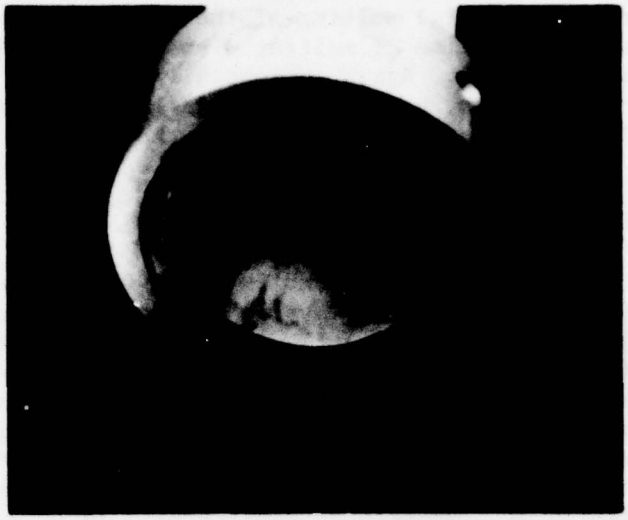

NO MELT HERE

SURFACE GENERALLY MELTED

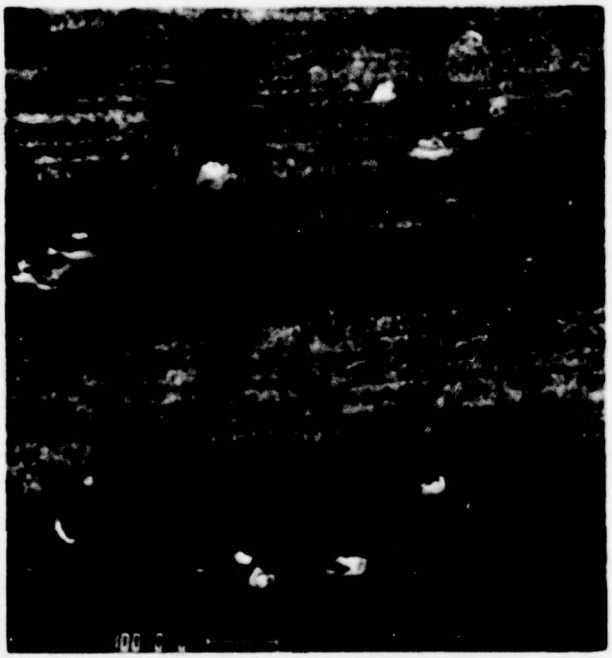

RELATIVELY UNIFORM MELTING IN THIS VIEW

(MAG. 100X)

Figure 28 SURFACE OF 1095 CALORIMETER SAMPLE AFTER TEST NO. 29

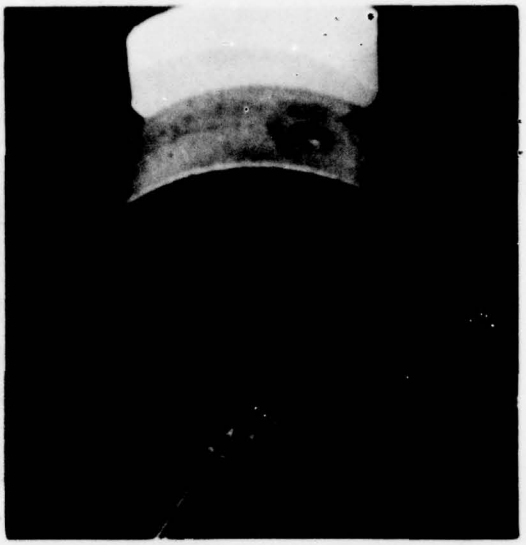

"DARK"
AREAS NOT
MELTED

MELTED
REGION

MELTED
AREA

ESSENTIALLY
UNDAMAGED AREA

(MAG. 100X)

Figure 27 SURFACE OF CUPRONICKEL CALORIMETER SAMPLE AFTER TEST NO. 27

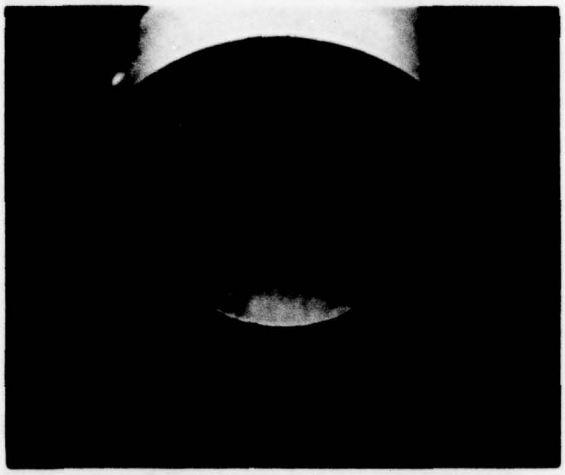

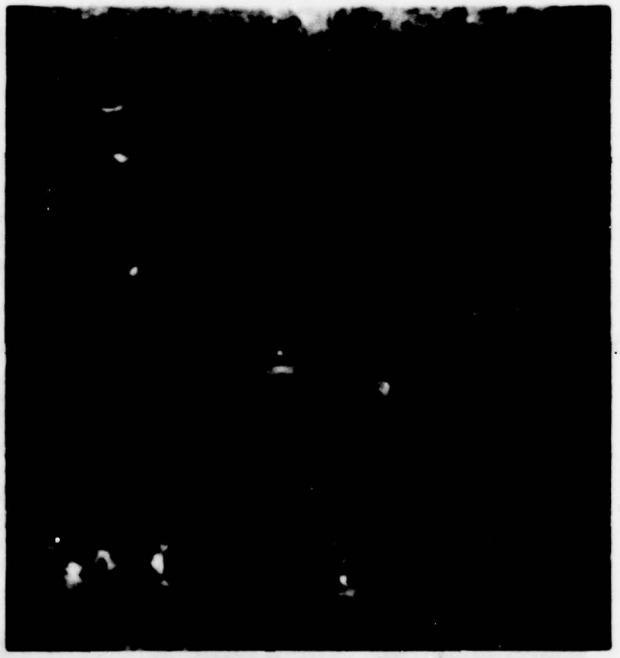

Figure 28 SURFACE OF 4340 CALORIMETER SAMPLE AFTER TEST NO. 28

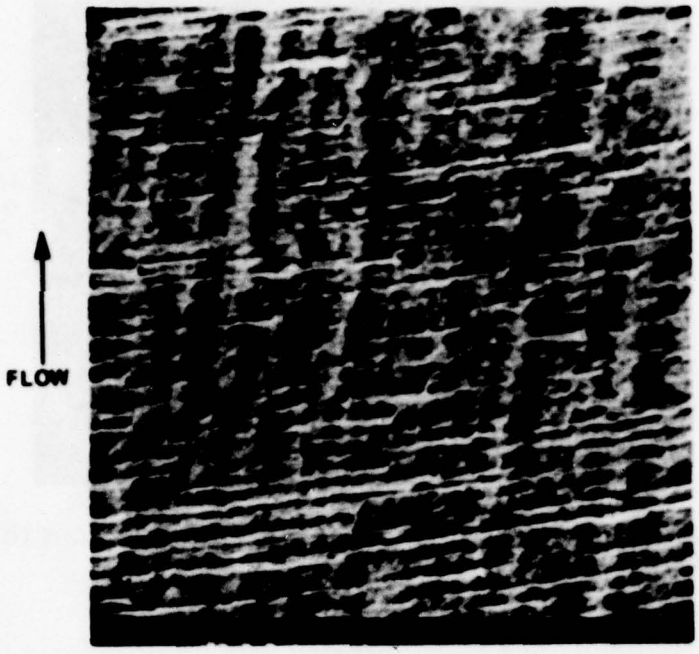

Figure 29 4340 STEEL RING SURFACE AFTER SEVEN STG TESTS IN ARGON-NITROGEN MIXTURE (100X, SEM)

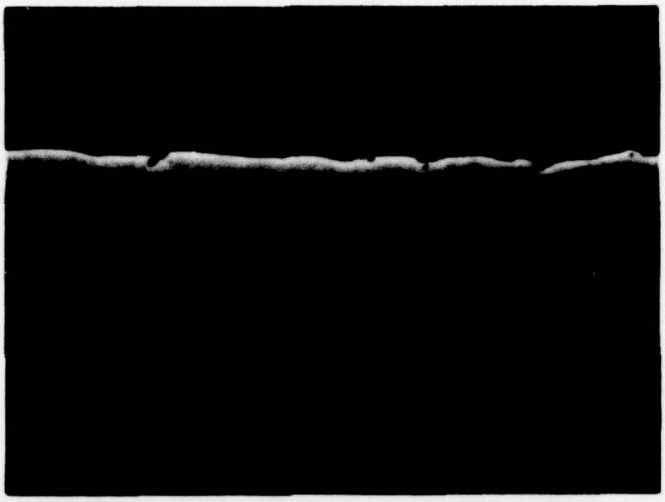

(a) 4340 STEEL SURFACE CROSS-SECTION AFTER SEVERAL EXCURSIONS TO 2200-2400°F IN PROPELLANT GASES (75MM GUN)

(b) 4340 STEEL SURFACE CROSS-SECTION AFTER ONE EXCURSION TO 2200-2400°F IN STG ARGON-NITROGEN

Figure 30 HARD MARTENSITE LAYERS IN 4340 STEEL RINGS SHOWN IN POLISHING RELIEF - NO ETCH (130X)

cracking after the entire test matrix. The straight portion of the throat received the same heating as do the test rings.

Crack development in 4340 rings and stud sensors fired in various guns is illustrated in Figures 31-34. The presence of non-axial cracks in rings and the presence of cracking in stud sensors (Figure 34) and sensor holders (not shown) proves that it is not the increase in bore surface "hoop" stress due to gas pressure that causes cracks to form in guns but not in the present STG testing. Studs experience no hoop stress. It is probable that stresses due to pressure do augment the formation of axial cracks, but it is clear that the basic cause of crack initiation is the surface tensile stress which develops as the white-hot surface layer cools from peak temperature. What the current STG results show is that the additional necessary condition for crack initiation is exposure to reactive propellant gases rather than to Argon-Nitrogen mixture.

It can be theorized that the operative chemical effect of propellant gases in crack initiation is the embrittlement of a very thin surface layer due to the diffusion into this layer of one or more chemical species. Taking reaction and diffusion rates into consideration, hydrogen, oxygen, nitrogen, and carbon are the possible candidates. Oxygen ions are too large to diffuse rapidly in steel, but it is conceivable that a surface oxide layer could provide microscopic-scale local stress concentrations and that microscopic cracks thus started could propagate into the "hot-short" hard martensite layer. Nitrogen is currently present in the STG gas mixture with no observed cracking. Hence, hydrogen and carbon are the most likely surface cracking initiators. Future testing in the STG using reactive gas mixtures will no doubt lead to a better understanding of surface crack phenomena, but it is clear from present results that bore heating alone is insufficient to produce bore surface cracking.

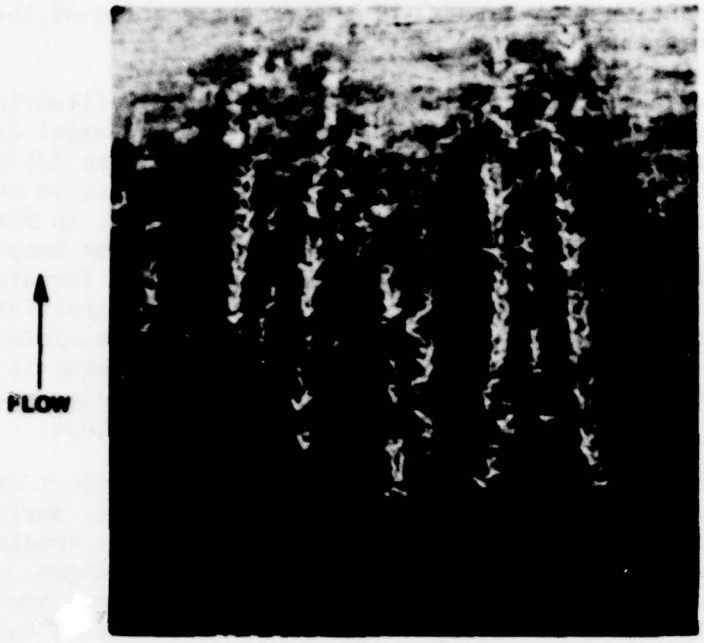

Figure 31 4340 RING SURFACE AFTER 19 SHOTS IN 75 MM GUN (20X, SEM)

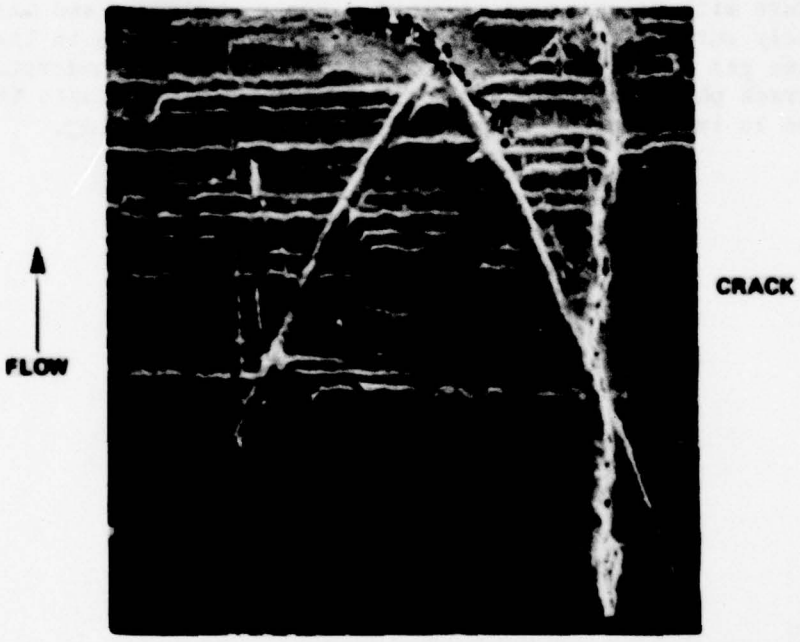

Figure 32 4340 RING SURFACE AFTER TEN SHOTS IN 60 MM GUN (REPLICA, 40X, SEM)

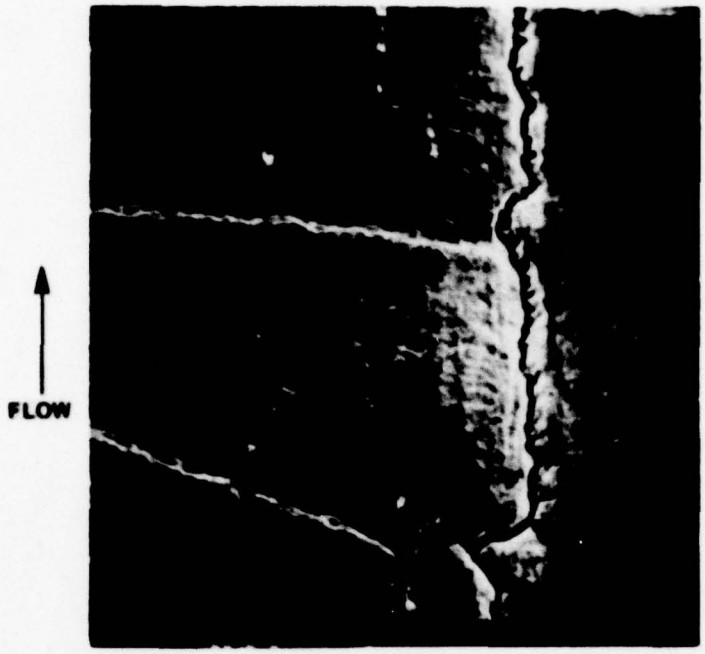

Figure 33 4340 RING SURFACE AFTER 24 SHOTS IN 60 MM GUN (100X, SEM)

Figure 34 Cv-Mo-V GUN STEEL STUD SENSOR SURFACE AFTER FIVE 155 MM, XM 201 E2 SHOTS (200X, SEM)

V. COMPUTER ANALYSIS AND TEMPERATURE/MELTING DETERMINATIONS

1. Convective Heating Code

Some effort in this study was devoted to the formulation and solution of working relationships which couple thermal data with specimen surface response observations such that a basis is formed for improved understanding of factors affecting melting erosion. A basic goal of the analysis was to establish a simple computational method and computer code by which the approximate surface temperature histories of test samples could be computed for measured heating and interior ballistic conditions. Demonstration of the ability of the computational method to predict melting conditions where melting is known to be present is necessary to establish the credibility to the method as a means of predicting bore surface temperature for given bore heating conditions. Additionally, correct order of magnitude estimation of the amount of melting expected under specific ballistic conditions would permit better understanding of the effects of changes in bore heating on tube erosion.

In any particular test in the Shock Tube Gun (or any other instrumented test gun), chamber pressure history, projectile muzzle velocity, and total heat input to the specimens or bore can be measured. Chamber pressure is obtained using piezoelectric pressure transducers recorded on tape, muzzle velocity is measured via velocity screens, and total heat input is computed from the output of thermocouples embedded in the specimens as discussed in Section III. Furthermore, projectile interior ballistics can readily be estimated from the known pressure history and muzzle velocity. Hence, the essential factors governing the bore heat transfer coefficient and bore heating rates are known with sufficient accuracy to permit their approximation.

Bore heating rate is determined by the relation

$$q(t) = h(t)[T_g(t) - T_w(t)] \tag{15}$$

in which $q(t)$ is the heating rate - $\frac{\text{Btu}}{\text{ft}^2 - \text{sec}}$

$h(t)$ is the heat transfer coefficient - $\frac{\text{Btu}}{\text{ft}^2 - \text{sec} \ ^\circ\text{F}}$

$T_g(t)$ is the gas temperature - °F

$T_w(t)$ is the bore surface temperature - °F

and t is the time

Note that q, h, T_g and T_w are all functions of time and these functions must be determined by analysis.

The total bore heat input is obtained by an integration of Equation 15 over entire heating time. Thus

$$Q_{IN} = \int_0^{t_f} h(t)[T_g(t) - T_w(t)]dt, \tag{16}$$

where t_f is the time at which $h(t) \approx 0$. Because the actual total heat is known from the measured data, Equation 16 provides one fundamental relationship for determination of h(t).

In the Shock Tube Gun, gas pressure is generated by adiabatic compression of a known test gas. Therefore, a direct relationship exists between gas pressure and temperature. This is

$$\frac{Tg(t)}{Tg_0} = \frac{Pg(t)}{Pg_0}^{\frac{\gamma-1}{\gamma}} \tag{17}$$

in which $Pg(t)$ is the measured chamber pressure - psi
Pg_0 is the initial pressure in the driven tube - psi
Tg_0 is the initial temperature in the driven tube - °R
γ is the ratio of specific heats for the test gas

Using Equation 17 and the recorded pressure history, the gas temperature history is directly established.*

Traditional analytical solutions for determination of convection coefficient in tube flow generally result in a non-dimensional relationship of the form[5]

$$Nu = B(Re)^n(Pr)^m \tag{18}$$

where the Nusselt number, Nu, is given by

$$Nu = \frac{hL}{K_g} \tag{19}$$

---

*For an actual gun the propellant gas temperature may be estimated by other methods. For example see that of Reference 2.

5. Max Jakob, "Heat Transfer," Vol. I, pp. 476-482, John Wiley & Sons, Inc., Fourth Printing, 1955.

and the Reynolds and Prandtl numbers given by

$$Re = \frac{V\rho_g L}{\mu_g}, \quad Pr = \frac{c_p \mu_g}{K_g} \tag{20}$$

with n and m fixed exponents. In these relations

K_g = thermal conductivity of the test gas
ρ_g = density of the test gas
μ_g = viscosity of the test gas
c_p = specific heat of the test gas
V = velocity of the test gas
L = a length dimension

In the interest of simplicity, the test gas density is given by

$$\rho_g = \frac{P_g(t)}{RT_g(t)} \tag{21}$$

in which R = the gas constant.

Combining Equations 18, 19, 20 and 21 we get:

$$h(t) = \beta\left(\frac{K_g}{L}\right)\left(\frac{L}{R\mu_L}\right)^n \left(\frac{c_p \mu_g}{K_g}\right)^m \left(\frac{V(t)Pg(t)}{Tg(t)}\right)^n . \tag{22}$$

Observe that the first four groups on the right of equation 22 involve essentially invariant terms. These may therefore be lumped into a single "constant" with the result

$$h(t) = \beta\left[\frac{V(t)Pg(t)}{Tg(t)}\right]^n \tag{23}$$

With values of gas velocity, V(t), pressure Pg(t), and temperature Tg(t) given for any test run in addition to a measured total input, the value of the constant, β, may be determined for any selected value of n. The computational method utilized in the convection code involves an initial selection of β based upon the given total heat input and the following relation derived by combining Equations 16 and 23

$$\beta_1 = \frac{Q_{IN}}{\int_0^{t_f} \left[\frac{Pg(t)V(t)}{Tg(t)}\right]^n [Tg(t) - 1500]dt} \quad (24)$$

Here, for convenience, $T_w(t)$ has been taken as 1500°R for this initial determination of β. As will be evident by the following discussion, almost any realistic value for T_w could have been chosen with little change in results. In the computer, the actual integration extends over the period for which pressure data are given and this should cover the entire pressure history if possible.

Once this initial value of β has been determined, the initial heat transfer coefficient history can be found by direct use of Equation 23. At this point, these values of hg and Tg now permit a computation of bore temperatures and heating using a conventional finite difference heat conduction subroutine. A basic result of the conduction subroutine is a computed value of total heat input for these initial values of hg and Tg as applied to the bore surface which is taken to have the same thermal properties as the material on which the total heat input was measured. The calculated total heat input, Q_{CAL}, should agree with that measured within some acceptable accuracy. If it does not, an adjusted value of β is determined from

$$\beta_2 = \beta_1 \frac{Q_{IN}}{Q_{CAL}} \quad (25)$$

This new value of β then results in a second heat transfer coefficient history from Equation 23 and the conduction calculation is repeated. This iteration continues until the calculated heat input, Q_{CAL}, agrees with the known, Q_{IN}, within a specified accuracy. Once the accuracy criterion is met, the corresponding values of Pg(t), hg(t), Tg(t), $T_w(t)$, q(t), and Q(t) are presented as both tabulated and plotted functions of time.

The computer code is further generalized in that it permits computation of temperature and bore heating histories for other selected bore materials subjected to the same heating parameters, hg(t) and Tg(t). These are also presented as both tabulated and plotted functions of time.

The computer code listing which consists of the MAIN, SLAB, and ARRAY subroutines is presented in Appendix I of this report.

2. Reactive Heating

The original convection code was further expanded to account for possible additional heating due to diffusion controlled surface

reactions and heat absorption due to melting. When diffusion controlled surface reactions are present there is an added heat input to the surface described in simplest terms by the relation

$$q_r = \dot{m}\, Q_r \tag{26}$$

where $\dot{m}$ is the rate of reactant flow to the surface and Q_r is the heat release per unit mass of reactant. In the case of simple mass diffusion to the surface, the rate of reactant flow, $\dot{m}$, is approximated by

$$\dot{m} = \frac{D}{\alpha} \frac{h_g(t)}{c_p} \frac{\Delta C_r}{w} \tag{27}$$

in which

D = the coefficient of mutual diffusivity
α = thermal diffusivity of the gas

The ratio D/α is termed the Lewis number and is available for many gas combinations. The factor $\Delta C/w$ is the mass fraction of the reactant in the gas mix. As before $h_g(t)$ is the heat transfer coefficient. Thus using equations 26 and 27 we may obtain a measure of the reaction heating. This is added to that of pure convection with the result

$$q_{tot} = q_{con} + q_r \tag{28}$$

As a general rule such diffusion controlled reactions occur once the surface is above some temperature threshold, say T_R. Above this temperature the materials natural resistance to reaction is overcome. Hence, we may say that below $T_w = T_R$, $q = q_{con}$ and above $T_w = T_R$,

$$q_{tot} = h_g \left\{ (T_g - T_w) + \left[\frac{D}{\alpha} \frac{Q_r}{c_p} \frac{\Delta C_r}{w} \right] \right\} \tag{29}$$

These relations are included within the convection code for possible later application to reactive gas conditions.

3. Surface Melting

Once the surface reaches its melting point (solidus temperature), there begins material loss controlled by the excess of surface heating over that of conduction. Therefore, above $T_w = T_m$

$$\left.\frac{dx}{dt}\right|_w = \frac{q_{tot} + K_m \left.\frac{dT}{dX}\right|_w}{\rho L_m} \qquad (30)$$

in which

$\left.\frac{dx}{dt}\right|_w$ is the material loss rate

and

$\left.\frac{dT}{dX}\right|_w$ is the thermal gradient at the bore surface.

In the computer, temperature response is determined using conventional finite difference methods. Consequently, the heated body is subdivided into a number of elements of finite thickness. Net heat transferred to each element is stored within the element and indicated in terms of its temperature rise. During melting, because no net temperature rise occurs, a portion, ΔX, of the element is removed in each time interval according to Equation 30 above. As material is removed, the conduction path lengths are shortened to more correctly represent the conduction effects. The program logic is complicated by the need to produce a temperature arrest in each element at the melting point and to maintain an accounting of all heat transfer within the body.

A listing of the entire melting code is given in Appendix II of this report. The listing consists of:

1. MAIN - Provides input/output instructions and logic.
2. SLAB - Determines heat transfer coefficients.
3. MELTED - Establishes amount of melt.
4. ARRAYS - Interpolates tabular values.
5. TMTEST - Establishes acceptable time interval.
6. GRAPH - Provides tabular output and normalizes computed data for the plotter.
7. VELOCT - Approximates projectile interior ballistics based upon pressure and muzzle velocity.

4. Bore Temperature Computations

As illustrations of the performance and operation of the two computer codes, the heating parameters $h_g(t)$ and $T_g(t)$ and corresponding sample temperatures were computed for several Shock Tube Gun tests.

The convective heating (no melt) code was exercised using data derived in STG Run Number 7. Based upon the measured pressure history and heating, Figures 35 through 37 illustrate the computed heating parameters and bore surface temperature histories for each specimen in that run. As may be observed, the naval brass is above its melting point at the surface which is in essential agreement with the observed melting on that sample. The Cupro-Nickel in the same test is computed to be close to melting at the surface which again agrees with evidence of observed local surface melting on that specimen. Finally, the surface temperature of the Vascomax is computed to be below its melting temperature which is consistent with the evidence which shows no surface melting of this specimen.

A second illustration of the applicability of the code to analysis of test data is given by reference to Table 7. Here, the computed surface temperature responses for all samples are compared for Test Runs 13, 26, 27, 28, 29 and 30 which were at essentially the same ballistic conditions. The computed maximum temperatures are further compared with the corresponding melting points and the actual observed surface effects. As shown, the convection code indicates a melting condition where melting was actually observed. Furthermore, the actual amount of melting observed is basically in agreement with the relative excess of computed bore surface temperature over that of the melting point.

In comparing the melting performance of the various materials listed in Table 7 with their orders of merit as given in Table 2 earlier, it is found that the low melting point brass is considerably out of proper order. A probable reason for this is the failure of the order-of-merit relation of Section III to properly account for change of heat rate with surface temperature rise. Hence, insufficient weight is given to the effect of melting temperature. A better order-of-merit relationship for the situation involving convective heating is

$$\text{MERIT} = \frac{\Delta T_m \sqrt{k c \rho}}{(T_{EFF} - T_m)} \tag{31}$$

where T_{EFF} is an effective temperature of the gas. This is unknown but for convenience may be taken as that temperature at which no net heat input to the wall occurs. This is

$$T_{EFF} = \frac{\int_0^\infty h_g T_g \, dt}{\int_0^\infty h_g \, dt} \tag{32}$$

For the conditions of the above test series T_{EFF} is computed as 5400°F. The new order of merit ranking based upon Equation 31 is shown in Table 8.

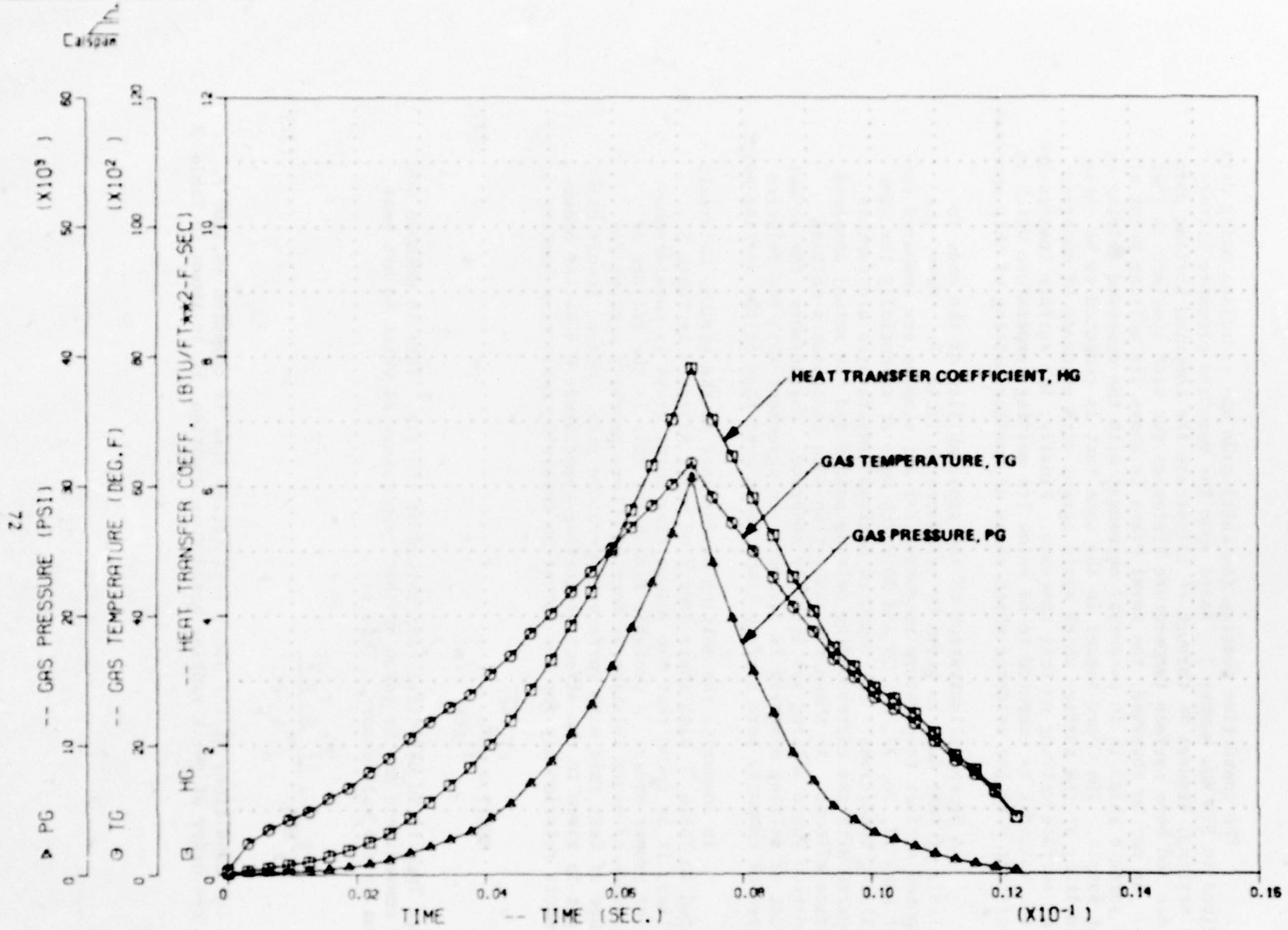

Figure 35 HG PG AND TG FOR SHOCK TUBE GUN STG NO. 7

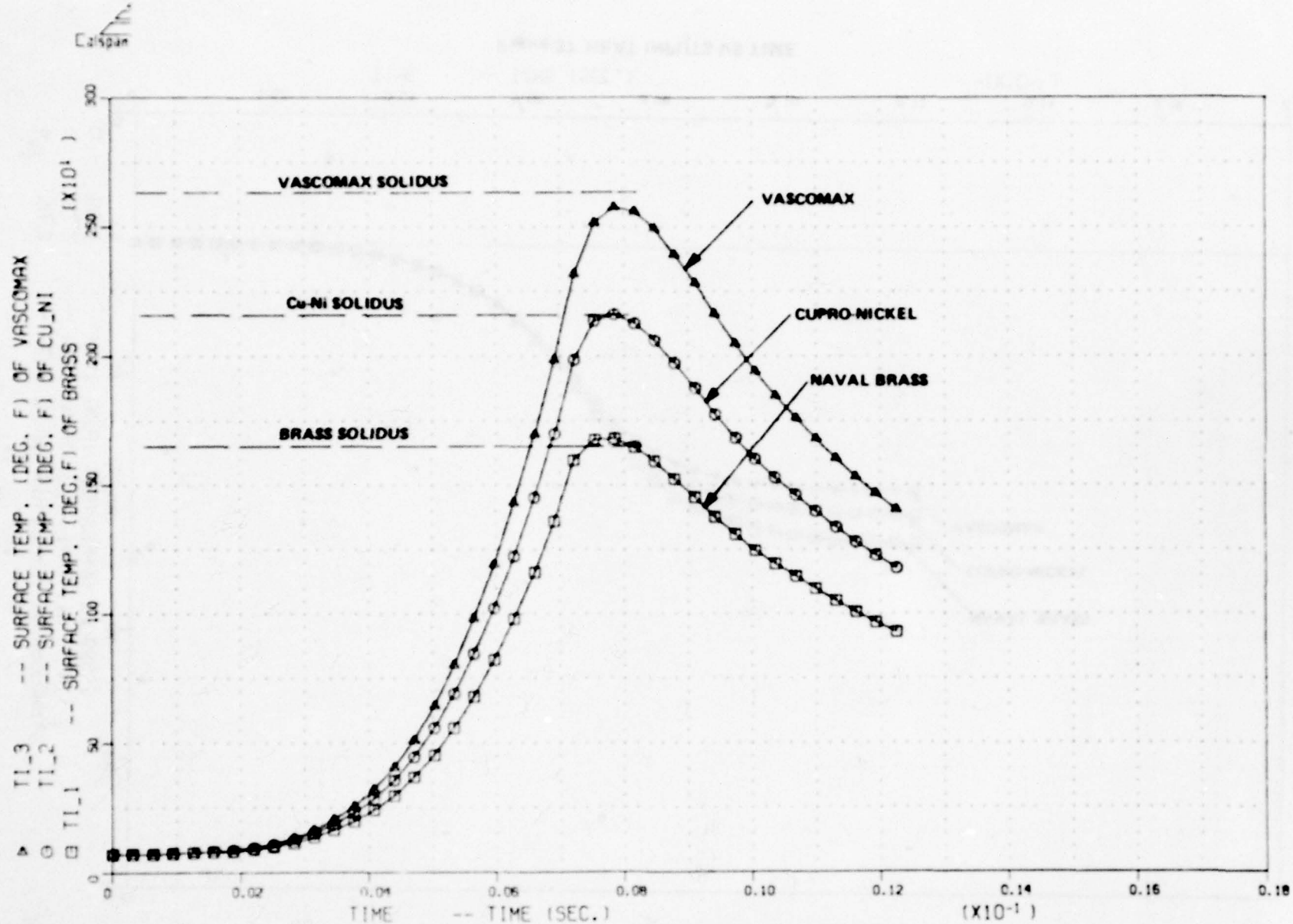

Figure 36 SURFACE TEMPERATURES OF MATERIALS VS TIME

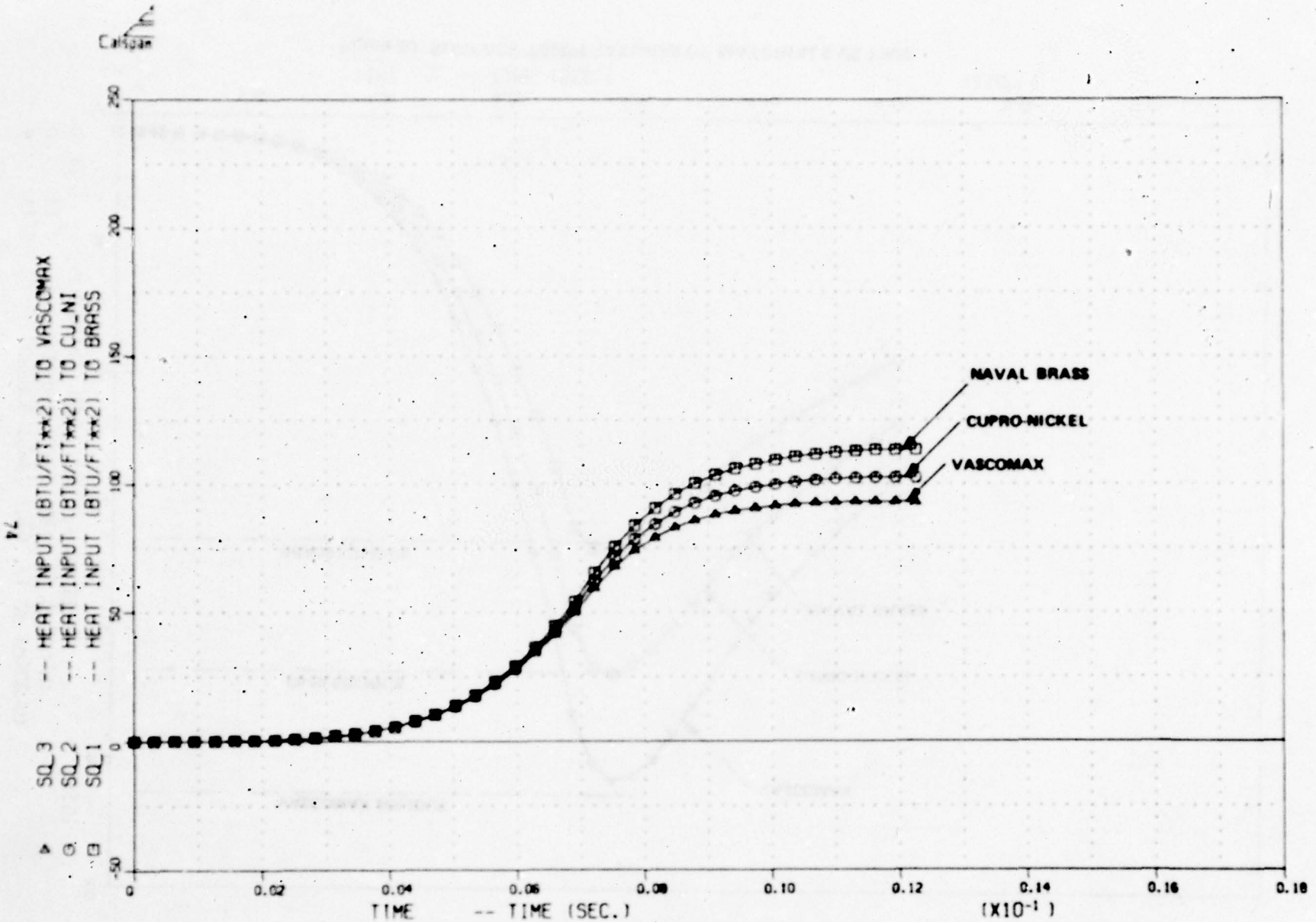

Figure 37 HEAT INPUTS VS TIME

TABLE 7. TEMPERATURE/MELTING COMPARISONS

Run No.	Specimen Type	Heat Input Btu/Ft^2	Computed Temperature °F	Melting Temperature °F	Above Melt?	Actual Test Results
13	Iron	93	2535	2780	No	No melting
26	Brass	110	1800	1630	Yes	100% of surface melted Large loss
27	Cupro Nickel	100	2375	2140	Yes	80% of surface melted
28	4340 Steel	86.5	2756	2640	Yes	10% of surface melted
29	1095 Steel	84.5	2960	2450	Yes	80% of surface melted
30	Copper	135	1450	1930	No	No melting

TABLE 8. ORDER-OF-MERIT FOR CONVECTION CONDITIONS

Material	Merit = $\frac{\Delta T_m \sqrt{kc\rho}}{(T_{EFF} - T_m)}$	Actual Ranking from Table 7
Copper	60	1
Iron	42	2
4340	34	3
Cu-Ni	29	4
Naval	27	6
1095	25	5

Using Equation 31 above we note from Table 8, naval brass is much more correctly placed than using the earlier relationship of Section III. Equation 31 is therefore recommended for use in selection of materials for service in severe convective heating environments where dimensional stability is a major consideration.

The above computer results were obtained using a value of the exponent, n, of 0.8 which corresponds to that usually taken for turbulent pipe flow. One might question the sensitivity of the temperature computations to selection of the exponent. Using the convection code, results show that computed maximum bore temperatures are very insensitive to the exponent, n. This is shown in Table 9 where a range of exponent from 0.6 to 1.0 produces only a 5 percent change in maximum bore temperature. Hence, where bore temperatures are concerned, great latitude in estimation of the exponent is allowed.

5. Heat Input Comparisons

When subjected to the same interior ballistic conditions, the bore surface temperature response of various materials has been shown above to be significantly different. The materials possessing the greater conductivities and heat capacities, of course, exhibit the lower bore surface temperatures. As a direct consequence of these differences in bore surface temperatures, there are inverse differences in absorbed heat. This is shown in Table 7 above where the copper sample is observed to have absorbed 60 percent more total heat than that of the 1095 steel sample when subjected to essentially the same conditions. In general, the amount of absorbed heat increases according to the value $\sqrt{kc\rho}$ for the material. Figure 38 demonstrates this for the several materials of the test program with heat input data obtained from Runs 13, 26, 27, 28, 29, and 30. Because these runs were at essentially the same ballistic conditions, convection coefficients should have been about the same. Therefore, a

TABLE 9. EFFECT OF EXPONENT FOR CONDITIONS OF STG RUN NO. 5

Q_{IN} = 105 Btu/Ft^2 (on Brass)

Exponent, n	Maximum Bore Temperatures	
	Naval Brass	Cu-Ni
	°F	°F
0.6	1320	1720
0.8	1338	1737
1.0	1385	1798

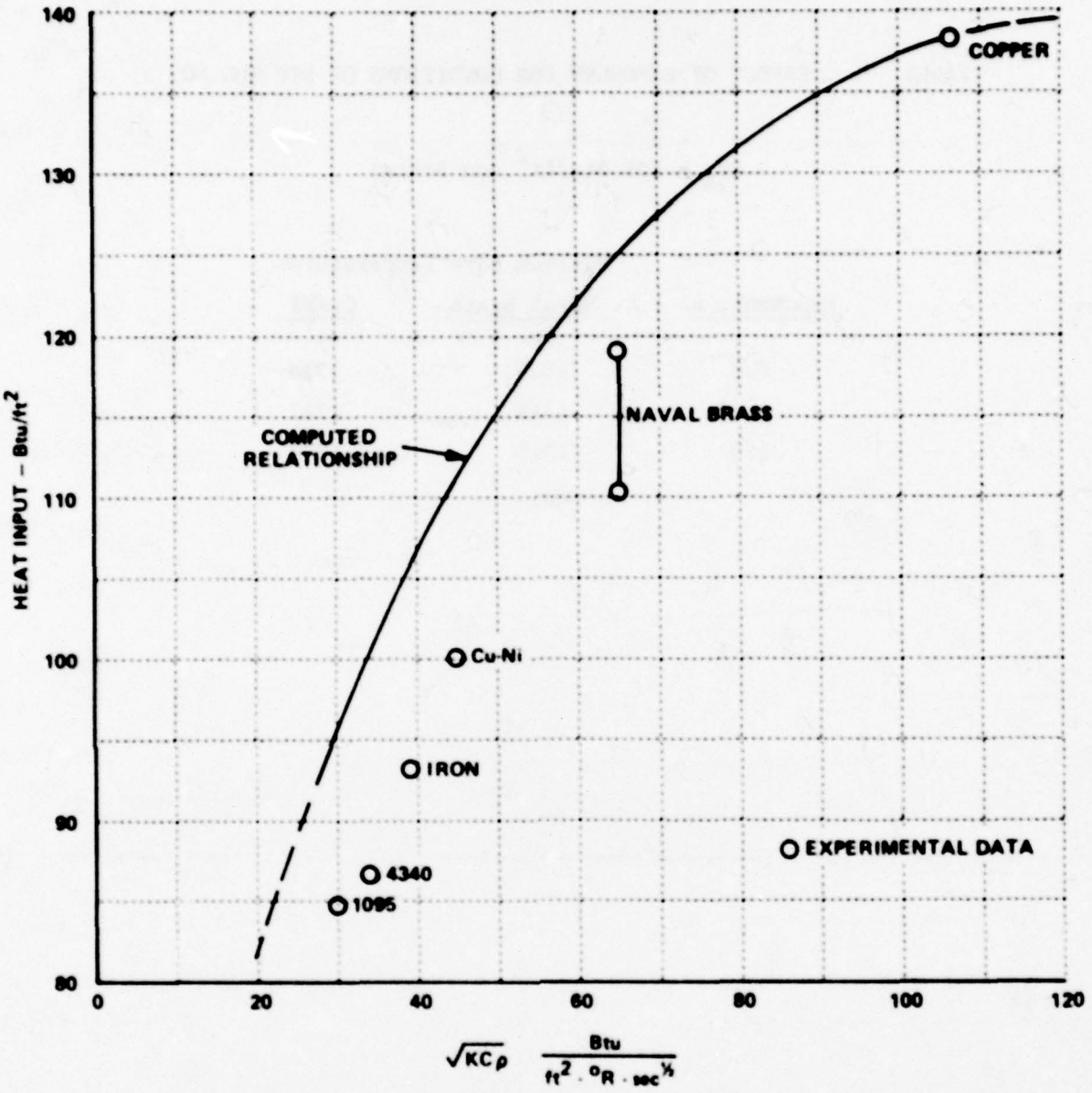

Figure 38 EFFECT OF THE PRODUCT $\sqrt{KC\rho}$ ON TOTAL HEAT INPUT AT CONSTANT BALLISTIC CONDITIONS

determination of convection coefficient for any one should be applicable to the others. A computed variation in heat input as a function of $\sqrt{\rho c}$ for the test samples is also shown in Figure 38. For this computation convection coefficients and gas temperatures were based upon the results of the copper test as a standard. One may observe from Figure 38 that the computed results show the proper trend; however, the heat input magnitudes are too great. At the present writing no clear reason for this discrepancy has been found, but the data suggest that the effective temperature of the gas is significantly below that computed for reversible adiabatic compression and used in the computations. The limited scope of the present study does not permit detailed examination of this temperature behavior. It is however, believed to be an important area for future work in that it has direct bearing on the ability of a gas stream to melt refractory metals such as chromium and tantalum.

For given total heating and ballistic conditions, it appears that the code adequately defines heat transfer coefficient histories and resulting bore surface temperature histories. As presently written, it therefore provides a basic tool for analysis of measured Shock Tube Gun data. With later refinement, it may provide a tool for determination of the severity of erosion conditions in actual guns for which similar test data are available.

6. Melting Comparisons

The melting code was used to determine the amount of melt expected for those samples which exhibited material loss by melting as described in Table 7 above. Computed amounts of loss are shown in Table 10 along with the losses actually measured. For this comparison, the weight losses in milligrams actually measured were converted to average radial enlargement in microinches.

The agreement between measured and computed losses, while appearing poor, is actually very good considering the simplicity of the code and the precision of the inputs. All computed losses of Table 10 were based upon full absorption of latent heat of fusion at the solidus temperature, although, all of the materials tested melt over a range in temperature through which the entire heat of fusion is absorbed.

It is beyond the scope of the present study to determine and model the entire fusion and melt removal process and this would need to be done to establish loss with precision. For example, if some partially melted material is removed prior to complete change of state, the effective latent heat is lowered and the amount of material loss is increased by an amount nearly proportionate with the relative effective latent heat. As a demonstration of this fact, the predicted melt for the brass specimen in Run No. 26 was recomputed using a latent heat value one-half of that for complete melting. The amount of loss was increased to 570 microinches, or nearly twice that of Table 10. At very high gas shear stress such as

TABLE 10. MATERIAL LOSS COMPARISONS

Run No.	Specimen Type	Heat Input Btu/Ft^2	Measured Radial Loss Microinches	Computed Radial Loss Microinches
26	Brass	110	1545	345
27	Cupro Nickel	100	130	160
28	4340 Steel	86.5	18	30
29	1095 Steel	84.5	120	500
31	4340 Cyl.	90	200	160

that present in the STG it is possible, indeed likely, that material is removed before complete melting and, therefore, greater loss is expected than that predicted by the computer code using full latent heat value.

A second and probably more important consideration is the precision of the heat input data. Small error in this value near the melting threshold can have large influence on the computed loss. For illustration, material loss for the brass sample was again recomputed using one-half the latent heat, but with a 5 percent increase in the heat input. The computed loss increased nearly threefold to 1433 microinches compared to the 570 microinches computed earlier.

Comparison of the losses for tests 28 and 31 further demonstrate the importance of heating. For these, the major difference was the input heat which increased by only 4 percent, but resulted in a fivefold increase in computed material loss.

When one considers the large changes in loss which accompany these rather minor changes in input, the agreement between the computed and measured losses is remarkably good. Thus, one has great confidence both in the accuracy of the measured heating data and in the ability of the computer code to predict loss for a given heat input.

7. Significance of Findings

With development and validation of the melting code, it is of interest to apply the code to a real large caliber gun situation in order to determine its degree of approach to bore surface melting. For this, ballistic conditions within the 155mm M185 cannon firing the XM201E2 charge were selected as these are known and have already been documented.

Consequently, bore surface temperature determinations were made for this cannon with increase in the bore surface heat input until bore surface melting was indicated. The resulting maximum bore temperatures are as shown in Figure 39. The results indicate melting to be achieved at a bore heat input level of about 160 Btu/ft^2. In actual fact, heat input measurements for this gun/charge combination were found to show less than 120 Btu/ft^2 (see pg. 19, Reference 3). At this heating level, relatively low maximum bore temperatures are predicted ($\leq$1900°F). There is, however, measurable erosion in the M185 cannon when firing the XM201E2 charge. Hence, some surface reaction effects are implied. The amount of type of reactions present must await the results of future Shock Tube Gun testing, but it appears that substantial chemical effect must be present in this cannon if the results of Figure 39 are correct.

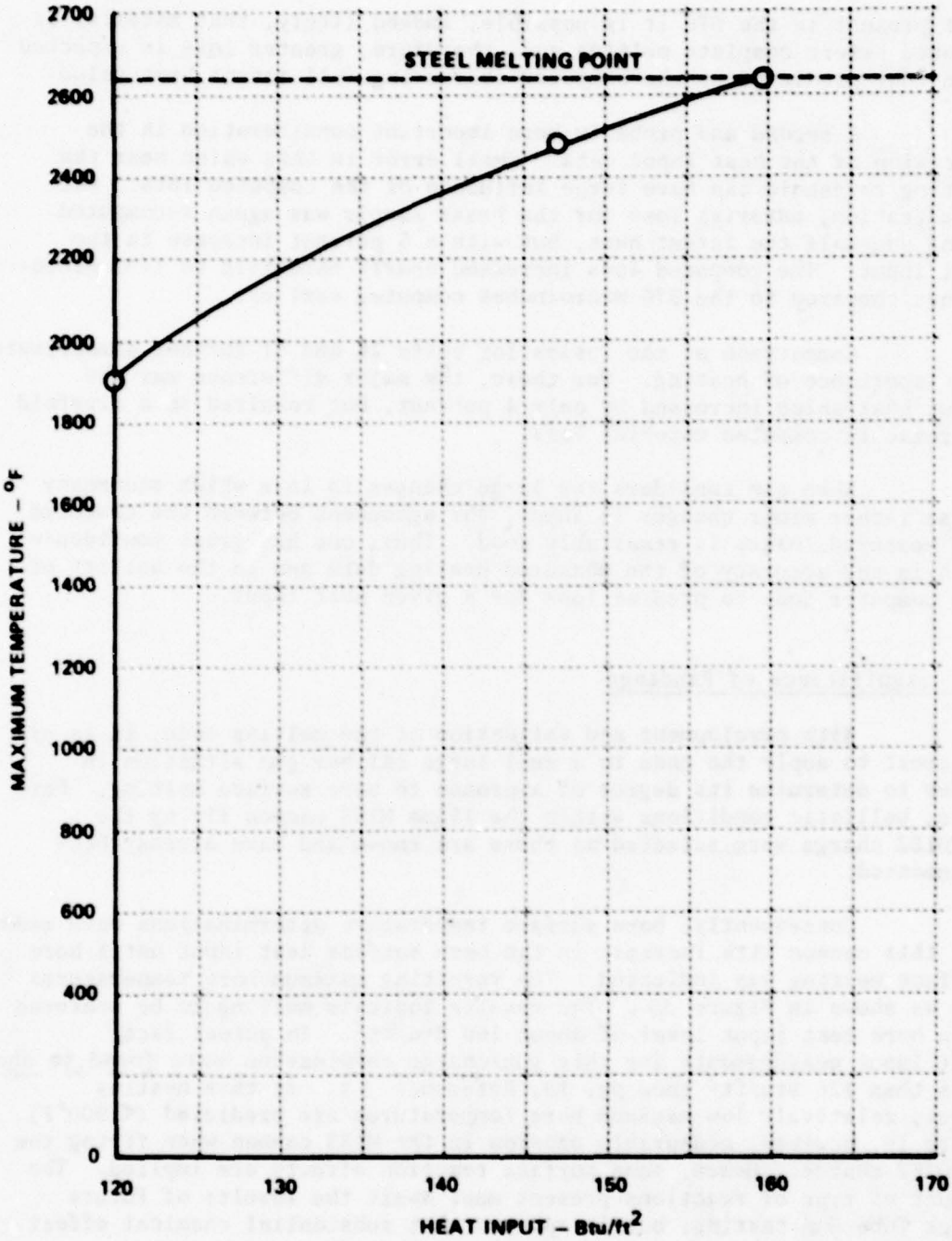

Figure 39 EFFECT OF HEAT INPUT ON COMPUTED MAXIMUM BORE TEMPERATURE IN 155 MM GUN (XM201 E2 BALLISTIC CONDITIONS)

VI. CONCLUSIONS

1. Shock Tube Gun heating conditions required to produce pure melting of steel have been determined.

2. Measurement techniques, for use with the Shock Tube Gun, which permit accurate determination of material loss and heating have been established.

3. A computer code by which ballistic and gross heating measurements may be normalized to find bore surface temperature histories and melting rates has been formulated, tested, and found to agree with measured observations.

4. Preliminary analysis through application of the computer code indicates chemical reactions to play a significant part in erosion of some large caliber guns.

5. The STG test results indicate that initiation of bore surface cracking requires exposure to a reactive gas rather than to an Argon-Nitrogen mixture. Heating alone appears insufficient to produce surface cracking.

Appendix I

CONVECTION CODE LISTING

MAIN

```
C ********************************************************************************
C                          LIST OF VARIABLES
C
C NT=NUMBER OF TEMPERATURES TO BE READ IN AS A TABLE.

C NV=NUMBER OF VELOCITY VALUES TO BE READ IN AS A TABLE.

C NP=NUMBER OF PRESSURE VALUES TO BE READ IN AS A TABLE.

C NH=NUMBER OF HTC VALUES TO BE READ IN AS A TABLE. IF HTC'S ARE TO
C BE CALCULATED FROM H(I)=A*(P(I)*V(I)/TG(I))**EXP, NH=1,HG(1)=0. AND TMH(1)=0.
C IF HTC VALUES ARE TO BE READ IN AS A TABLE,NV=1,VG(1)=0. AND TMV(1)=0.

C N=NUMBER OF GRID POINTS.

C INTRVL=PRINT INTERVAL OF OUTPUT (IE. IF OUTPUT IS EVERY TENTH
C CALCULATED VALUE INTRVL=10)

C TG(ARRAY)=GAS TEMPERATURES IN INPUT TABLE (DEGREES R). IF GAS TEMPS ARE
C NOT TO BE READ IN BUT CALCULATED FROM TG=TG0(P/P0)**(GAMA-1/GAMA),NT=1
C AND TG(1)=INITIAL GAS TEMP.

C TMG(ARRAY)=CORRESPONDING GAS TEMPERATURE TIMES (SEC). IF NT=1,TMG(1)=0.

C VG(ARRAY)=VELOCITIES IN INPUT TABLE (FT/SEC.).

C TMV(ARRAY)=CORRESPONDING VELOCITY TIMES (SEC.).

C PG(ARRAY)=PRESSURE VALUES IN INPUT TABLE (PSI).

C TMP(ARRAY)=CORRESPONDING PRESSURE TIMES (SEC.).

C HG(ARRAY)=HEAT TRANSFER COEFF. IN INPUT TABLES (BTU/FT**2-SEC-R).

C TMH(ARRAY)=CORRESPONDING HTC TIMES (SEC.).

C TIMEF=TOTAL TIME OF INTEREST (SEC.).

C TSO=INITIAL SURFACE TEMP.(R).

C PO=INITIAL GAS PRESSURE (PSI).

C GAMA=RATIO OF SPECIFIC HEATS

C ERROR=CONVERGENCE ERROR. READ IN AS A DECIMAL (IE. IF CONVERGENCE ERROR IS TO
C BE LESS THAN 5 PERCENT, ERROR=.05).

C QIN=TOTAL HEAT FLUX INPUT (BTU/FT**2).

C XYZ=COMMENT CARD. INPUT IS ALPHAMERIC (IE. ANYTHING CAN BE WRITTEN AND
C WILL BE PRINTED AS SUCH) AND IS CONSTRAINED TO ONLY ONE CARD PER DATA
C SET (80 CHARACTERS OR LESS).

C K=THERMAL CONDUCTIVITY OF MATERIAL (BTU/FT.-HR-R).

C C=HEAT CAPACITY OF MATERIAL (BTU/LB).

C ROH=DENSITY OF MATERIAL (LB/FT.**3).

C DEPTH=TOTAL DEPTH OF INTEREST (FT.).

C EXP=EXPONENT
C
```

```
C ********************************************************************************
      DIMENSION TI(50),TEMPI(200,50),PRESS(200),TEMPG(200),VEL(200)
     *,H(200),TIME(200),PVTEXP(200),TG(50),VG(50),PG(50),TMG(50),TMV(50)
     *,TMP(50),SIGMAQ(200),XYZ(20),HG(50),TMH(50)
      REAL K
      COMMON/SHKTUB/TI,TEMPI,PRESS,TEMPG,VEL,H,TIME,PVTEXP,TG,VG,PG,
     *TMG,TMV,TMP,NT,NV,NP,XYZ,SIGMAQ,THC,HG,NH,TMH
      COMMON/BARREL/TIMEF,C,ROH,DEPTH,N,K,EXP,TSO,PO,DEL,GAMA,INTRVL
     *,QIN,QCAL,ERROR,TMAX,I,DT,A,NRUN
      ARG=1.
      NRUN=0
C
      NAMELIST/NUM/NT,NV,NP,NH,N,INTRVL
      READ(5,NUM)
      READ(5,101) (TG(J),J=1,NT),(TMG(J),J=1,NT)
      READ(5,101) (VG(J),J=1,NV),(TMV(J),J=1,NV)
      READ(5,101) (PG(J),J=1,NP),(TMP(J),J=1,NP)
      READ(5,101) (HG(J),J=1,NH),(TMH(J),J=1,NH)
C
      WRITE(6,NUM)
      DO 1 L=1,NP
1     PG(L)=PG(L)*144.
C
      NAMELIST/BARL/TIMEF,TSO,PO,GAMA,ERROR,QIN,DEPTH,EXP
      READ(5,BARL)
C
      WRITE(6,BARL)
      PO=PO*144.
C
2     READ(5,100,END=3) XYZ
      READ(5,101,END=3) K,C,ROH
C
      K=K/3600.
      CALL SLAB(ARG)
      ARG=2.
      GO TO 2
3     WRITE(6,199)
      DO 7 J=1,1000
      IF(J.GT.NT) GO TO 6
      WRITE(6,200) TG(J),TMG(J)
6     IF(J.GT.NV) GO TO 4
      WRITE(6,201) VG(J),TMV(J)
4     IF(J.GT.NP) GO TO 5
      PG(J)=PG(J)/144.
      WRITE(6,202) PG(J),TMP(J)
7     WRITE(6,203)
5     CONTINUE
      WRITE(6,204)
      DO 8 J=1,NH
8     WRITE(6,205) HG(J),TMH(J)
100   FORMAT(20A4)
101   FORMAT(8F10.0)
199   FORMAT(1H1,T40,12HINPUT TABLES/1H0,19HGAS TEMPERATURE (R),T22,10HT
     *IME (SEC),T42,21HGAS VELOCITY (FT/SEC),T66,10HTIME (SEC),T86,18HGA
     *S PRESSURE (PSI),T107,10HTIME (SEC)/1H0)
200   FORMAT(1H ,T5,F9.2,T24,E11.4)
201   FORMAT(1H ,T46,F9.2,T66,E11.4)
202   FORMAT(1H ,T91,F9.2,T107,E11.4)
203   FORMAT(1H )
204   FORMAT(1H0,25HGAS HTC (BTU/FT**2-SEC-R),T30,10HTIME (SEC))
205   FORMAT(1H ,T7,F9.2,T30,E11.4)
      STOP
      END
```

```
      SUBROUTINE SLAB(ARG)
      DIMENSION TI(50),TEMPI(200,50),PRESS(200),TEMPG(200),VEL(200)
     *,H(200),TIME(200),PVTEXP(200),TG(50),VG(50),PG(50),TMG(50),TMV(50)
     *,TMP(50),SIGMAQ(200),XVZ(20),HG(50),TMH(50)
      REAL K,X(6)
      COMMON/SHKTUB/TI,TEMPI,PRESS,TEMPG,VEL,H,TIME,PVTEXP,TG,VG,PG,
     *TMG,TMV,TMP,NT,NV,NP,XVZ,SIGMAQ,THC,HG,NH,TMH
      COMMON/BARREL/TIMEF,C,ROH,DEPTH,N,K,EXP,TSO,PO,DEL,GAMA,INTRVL
     *,QIN,QCAL,ERROR,TMAX,I,DT,A,NRUN
      IF(ARG.EQ.2.) GO TO 5
      DEL=DEPTH/(N-1)
      DO 7 J=1,5
    7 X(J)=(J-1.)*DEL
      X(6)=9.*DEL
      DEL2=DEL**2
      DT1=TIMEF/100.
      DT2=C*ROH*DEL2/(8.*K)
      DT=DT1
      IF(DT2.LE.DT1) DT=DT2
      I=(TIMEF/DT)+1
      DT=TIMEF/(I-1)
      BIG=1
      WRITE(6,500) BIG,DT
      IF(I.GT.200) I=200
      DT=TIMEF/(I-1)
      IF(I.EQ.200) WRITE(6,600) DT
      DDT=DT/10.
      CALL ARRAYS
      T=DT
      DO 6  M=1,I
      IF((HG(1).EQ.0.).AND.(NH.EQ.1))      PVTEXP(M)=(PRESS(M)*VEL(M)/TEM
     *PG(M))**EXP
      T=T+DT
    6 TIME(M)=T
      IF((HG(1).NE.0.).AND.(NH.NE.1)) GO TO 5
      SUM=0.
      DO 2 M=1,I
    2 SUM=SUM+PVTEXP(M)*(TEMPG(M)-1500.)*DT
      A=QIN/SUM
    5 TMAX=TSO
      QCAL=0.
      DO 1 M=1,50
      TEMPI(1,M)=TSO
    1 TI(M)=TSO
      IAVE=0
      DO 4 M=1,I
      IF((HG(1).EQ.0.).AND.(NH.EQ.1))      H(M)=A*PVTEXP(M)
      HAVE=A/2.*(PVTEXP(M-IAVE)+PVTEXP(M))
      IAVE=1
      TEMPI(M,1)=(2.*DT/(C*ROH*DEL))*(HAVE*(TEMPG(M)-TI(1))-(K/DEL)*
     *(TI(1)-TI(2)))+TI(1)
      TI(1)=TEMPI(M,1)
      QCAL=QCAL+HAVE*(TEMPG(M)-TI(1))*DT
      SIGMAQ(M)=QCAL
      IF(TMAX.LE.TI(1)) TMAX=TI(1)
      J=N-1
      DO 4 MA=1,10
      DO 3 NA=2,J
```

```
      TEMPI(M,NA)=(K*DDT/(C*ROH*DEL2))*(TI(NA-1)+TI(NA+1)
     *-2.*TI(NA))+TI(NA)
3     TI(NA)=TEMPI(M,NA)
      TEMPI(M,N)=(2.*K*DDT/(C*ROH*DEL2))*(TI(NA)-TI(N))+TI(N)
4     TI(N)=TEMPI(M,N)
      IF(ARG.EQ.2.) GO TO 20
      IF (.NOT.((NH.EQ.1).AND.(HG(1).EQ.0.))) GO TO 20
      E=ABS((QIN-QCAL)/QIN)
      IF(E.LE.ERROR) GO TO 20
      A=A*QIN/QCAL
      GO TO 5
20    WRITE(6,700) XYZ
      THC=K*3600.
      WRITE(6,800) THC,C,ROH
      WRITE(6,101) (X(J),J=1,6),DEPTH
      WRITE(6,100) N
      WRITE(6,200)
      NRUN=NRUN+1
      DO 21 J=1,I,INTRVL
21    WRITE(7,1000) NRUN,TIME(J),TEMPI(J,1), H(J),TEMPG(J),PRESS(J)
     *,SIGMAQ(J)
      DO 22 J=1,I,INTRVL
22    WRITE(6,300) TIME(J),H(J),TEMPG(J),TEMPI(J,1),TEMPI(J,2),
     *TEMPI(J,3),TEMPI(J,4),TEMPI(J,5),TEMPI(J,10),TEMPI(J,N),SIGMAQ(J)
      IF(J.NE.I) WRITE(6,300) TIME(I),H(I),TEMPG(I),TEMPI(I,1),
     *TEMPI(I,2),TEMPI(I,3),TEMPI(I,4),TEMPI(I,5),TEMPI(I,10),TEMPI(I,N)
     *,SIGMAQ(I)
      WRITE(6,400) A,QCAL,TMAX
100   FORMAT(1HO,T3,4HTIME,T20,2HHG,T32,12HTEMP. OF GAS,T48,2HT1,T57,2HT
     *2,T66,2HT3,T75,2HT4,T84,2HT5,T93,3HT10,T102,1HT,I2,T115,6HSIGMAQ)
101   FORMAT(1HO,T66,12HDEPTH (FEET)/1HO,T46,7(F8.5,1X))
200   FORMAT(1H,T2,6H(SEC.),T12,18H(BTU/FT**2-R-SEC.),T36,3H(R),9X,7(3H(
     *R),6X),T112,11H(BTU/FT**2)/1HO)
300   FORMAT(1HO,E11.4,T16,E11.4,T32,F9.2,T46,F7.2,6(2X,F7.2),T115,F7.2)
400   FORMAT(1HO,12HCONSTANT, A=,E11.4/1H ,20HTOTAL HEAT INPUT, Q=,F9.2,
     *11H(BTU/FT**2)/1H ,34HMAXIMUM SURFACE TEMPERATURE, TMAX=,F9.2,3H(R
     *))
500   FORMAT(1HO,64HTHE NUMBER OF DATA PTS.REQ.'D USING THE SMALLEST VAL
     *UE OF DT IS ,E12.5,23H THE VALUE OF DT BEING ,E12.5)
600   FORMAT(1HO,116HTHE MAXIMUM PERMISSABLE NUMBER OF DATA PTS. ALLOWED
     * BY THIS PROGRAM'S DIMENSIONAL ARRAYS ARE 200. THEREFORE 200 WILL/
     *1H ,58HBE THE REQ.'D NUMBER OF DATA PTS. THE VALUE OF DT WILL BE .
     *E12.5,12H BY DEFAULT.)
700   FORMAT(1H1,20A4)
800   FORMAT(1HO,32HINTRINSIC PROPERTIES OF MATERIAL/1H ,2HK=,F7.2,12H B
     *TU/FT-HR-R/1H ,2HC=,F7.2,7H BTU/LB/1H ,4HROH=,F7.2,9H LB/FT**3)
1000  FORMAT(I5,5E15.8,/,E15.8)
      RETURN
      END
```

```
      SUBROUTINE ARRAYS
C ***********************************************************************
C
C     SUBROUTINE ARRAYS WILL EITHER GENERATE VALUES OF TEMP.,PRESS.,VELOCITY
C AND HG BY LINEAR INTERPOLATION FROM TABULAR INPUT DATA OR BY
C                  TG=TG0*(P/P0)**(GAMA-1/GAMA).
C
C ***********************************************************************
      DIMENSION TI(50),TEMPI(200,50),PRESS(200),TEMPG(200),VEL(200)
     *,H(200),TIME(200),PVTEXP(200),TG(50),VG(50),PG(50),TMG(50),TMV(50)
     *,TMP(50),SIGMAQ(200),XYZ(20),HG(50),TMH(50)
      REAL K
      COMMON/SHKTUB/TI,TEMPI,PRESS,TEMPG,VEL,H,TIME,PVTEXP,TG,VG,PG,
     *TMG,TMV,TMP,NT,NV,NP,XYZ,SIGMAQ,THC,HG,NH,TMH
      COMMON/BARREL/TIMEF,C,ROE,DEPTH,N,K,EXP,TSO,PO,DEL,GAMA,INTRVL
     *,QIN,QCAL,ERROR,TMAX,I,DT,A,NRUN
      IF((HG(1).EQ.0.).AND.(NH.EQ.1)) GO TO 9
      J=2
      ACUTME=-DT
      DO 7 M=1,I
      ACUTME=ACUTME+DT
      IF(ACUTME.GT.TMH(J)) J=J+1
7     H(M)=HG(J-1)+((HG(J)-HG(J-1))/(TMH(J)-TMH(J-1)))*
     *(ACUTME-TMH(J-1))
9     CONTINUE
      IF((HG(1).NE.0.).AND.(NH.NE.1)) GO TO 8
      J=2
      ACUTME=-DT
      DO 1 M=1,I
      ACUTME=ACUTME+DT
      IF(ACUTME.GT.TMV(J)) J=J+1
1     VEL(M)=VG(J-1)+((VG(J)-VG(J-1))/(TMV(J)-TMV(J-1)))*
     *(ACUTME-TMV(J-1))
      J=2
      ACUTME=-DT
      DO 2 M=1,I
      ACUTME=ACUTME+DT
      IF(ACUTME.GT.TMP(J)) J=J+1
2     PRESS(M)=PG(J-1)+((PG(J)-PG(J-1))/(TMP(J)-TMP(J-1)))*
     *(ACUTME-TMP(J-1))
      IF(NT.EQ.1) GO TO 4
8     J=2
      ACUTME=-DT
      DO 3 M=1,I
      ACUTME=ACUTME+DT
      IF(ACUTME.GT.TMG(J)) J=J+1
3     TEMPG(M)=TG(J-1)+((TG(J)-TG(J-1))/(TMG(J)-TMG(J-1)))*
     *(ACUTME-TMG(J-1))
      GO TO 5
4     CPCV=(GAMA-1.)/GAMA
      DO 6 M=1,I
6     TEMPG(M)=TG(1)*(PRESS(M)/PO)**CPCV
5     RETURN
      END
```

INPUT

```
&NUM
NT=          1,NV=          10,NP=          21,NH=          1,N=          30,INTRVL=          5
&END
&BARL
TIMEF=  .124999993E-01,TSO=  530.000000     ,PO=  14.4300003     ,GAMA=  1.50000000     ,ERROR=  .500000007E-01,QIN=  117.000000     ,
DEPTH=  .124999993E-01,EXP=  .800000012
&END
```


THE NUMBER OF DATA PTS.REQ.'D USING THE SMALLEST VALUE OF DT IS 0.24600E+03 THE VALUE OF DT BEING 0.51020E-04

THE MAXIMUM PERMISSABLE NUMBER OF DATA PTS. ALLOWED BY THIS PROGRAM'S DIMENSIONAL ARRAYS ARE 200. THEREFORE 200 WILL BE THE REQ.'D NUMBER OF DATA PTS. THE VALUE OF DT WILL BE 0.62814E-04 BY DEFAULT.

HTC AND TEMPS. FOR BRASS STG NO.7

INTRINSIC PROPERTIES OF MATERIAL
K= 84.00 BTU/FT-HR-R
C= 0.10 BTU/LB
ROH= 512.00 LB/FT**3

			DEPTH (FEET)							
			0.0	0.00043	0.00086	0.00129	0.00172	0.00388	0.01250	
TIME (SEC.)	HG (BTU/FT**2-R-SEC.)	TEMP. OF GAS (R)	T1 (R)	T2 (R)	T3 (R)	T4 (R)	T5 (R)	T10 (R)	T30 (R)	SIGMAD (BTU/FT**2)
0.0	0.1714E-01	528.40	530.00	530.00	530.00	530.00	530.00	530.00	530.00	-0.00
0.3141E-03	0.5998E-01	943.12	530.26	530.06	530.01	530.00	530.00	530.00	530.00	0.00
0.6281E-03	0.1041E+00	1152.36	530.98	530.32	530.08	530.02	530.00	530.00	530.00	0.02
0.9422E-03	0.1519E+00	1304.83	532.20	530.86	530.29	530.08	530.02	530.00	530.00	0.05
0.1256E-02	0.2036E+00	1430.42	533.93	531.73	530.68	530.24	530.07	530.00	530.00	0.09
0.1570E-02	0.2832E+00	1627.19	536.79	533.10	531.30	530.52	530.19	530.00	530.00	0.17
0.1884E-02	0.3669E+00	1789.61	540.91	535.22	532.32	530.98	530.39	530.00	530.00	0.29
0.2198E-02	0.4974E+00	2040.50	547.56	538.49	533.88	531.72	530.73	530.00	530.00	0.48
0.2513E-02	0.6332E+00	2248.70	556.91	543.41	536.31	532.89	531.28	530.00	530.00	0.77
0.2827E-02	0.8747E+00	2566.18	572.32	550.97	539.97	534.67	532.14	530.02	530.00	1.22
0.3141E-02	0.1122E+01	2820.07	594.18	562.44	545.63	537.41	533.46	530.04	530.00	1.89
0.3455E-02	0.1377E+01	3035.02	621.60	577.91	553.77	541.53	535.49	530.08	530.00	2.81
0.3769E-02	0.1646E+01	3233.80	654.46	597.39	564.62	547.30	538.46	530.16	530.00	4.00
0.4083E-02	0.2010E+01	3553.59	699.16	622.69	578.71	555.03	542.58	530.27	530.00	5.58
0.4397E-02	0.2375E+01	3833.11	754.73	655.44	597.19	565.26	548.14	530.46	530.00	7.64
0.4711E-02	0.2846E+01	4177.51	826.80	697.33	621.00	578.64	555.54	530.74	530.00	10.31
0.5025E-02	0.3314E+01	4480.27	913.42	749.86	651.48	595.97	565.25	531.15	530.00	13.67
0.5339E-02	0.3838E+01	4820.93	1017.78	813.88	689.43	618.01	577.80	531.73	530.00	17.85
0.5653E-02	0.4360E+01	5128.71	1136.80	889.83	735.75	645.49	593.76	532.53	530.00	22.89
0.5967E-02	0.4994E+01	5488.26	1278.84	979.57	791.13	679.03	613.65	533.63	530.00	28.96
0.6281E-02	0.5620E+01	5811.46	1439.32	1084.37	856.98	719.49	638.03	535.10	530.00	36.14
0.6595E-02	0.6308E+01	6146.46	1620.39	1204.20	933.78	767.59	667.53	537.03	530.00	44.52
0.6909E-02	0.7021E+01	6470.26	1818.41	1338.82	1022.01	823.92	702.68	539.53	530.00	54.12
0.7224E-02	0.7815E+01	6814.68	2055.30	1494.74	1123.21	889.10	744.00	542.72	530.00	65.34

0.7538E-02	0.7021E+01	6282.02	2135.86	1623.01	1229.80	962.90	792.00	546.73	530.00	76.54
0.7852E-02	0.6452E+01	5883.68	2138.88	1694.12	1316.96	1036.23	844.57	551.69	530.00	83.82
0.8166E-02	0.5803E+01	5438.77	2104.57	1728.17	1380.73	1101.04	897.12	557.75	530.00	90.55
0.8480E-02	0.5231E+01	5035.88	2052.84	1736.28	1423.50	1154.40	946.05	565.03	530.00	95.98
0.8794E-02	0.4580E+01	4580.18	1983.24	1725.07	1448.95	1196.05	989.34	573.54	530.00	100.22
0.9109E-02	0.4057E+01	4197.71	1911.61	1700.69	1459.99	1226.63	1026.09	583.22	530.00	103.51
0.9422E-02	0.3487E+01	3768.15	1834.16	1667.29	1460.05	1247.46	1056.15	593.92	530.00	105.95
0.9736E-02	0.3205E+01	3488.42	1767.99	1630.41	1451.86	1259.95	1079.80	605.42	530.00	107.86
0.1005E-01	0.2874E+01	3183.96	1706.18	1593.50	1438.91	1265.99	1097.70	617.47	530.00	109.35
0.1036E-01	0.2694E+01	2990.57	1663.66	1557.95	1423.01	1267.19	1110.73	629.85	530.00	110.58
0.1068E-01	0.2463E+01	2768.32	1605.51	1524.53	1405.81	1264.95	1119.75	642.31	530.00	111.58
0.1099E-01	0.2166E+01	2503.39	1557.81	1491.65	1387.66	1260.21	1125.56	654.66	530.00	112.34
0.1131E-01	0.1819E+01	2200.66	1509.38	1458.22	1368.36	1253.40	1128.73	666.75	530.00	112.83
0.1162E-01	0.1597E+01	1991.15	1466.11	1425.55	1348.07	1244.76	1129.62	678.43	530.00	113.15
0.1193E-01	0.1302E+01	1724.71	1425.65	1394.39	1327.54	1234.73	1128.57	689.63	530.00	113.33
0.1225E-01	0.8692E+00	1332.03	1386.41	1364.10	1306.94	1223.67	1125.91	700.27	530.00	113.37
0.1250E-01	0.2012E+00	531.26	1356.90	1340.50	1290.41	1214.24	1122.81	708.35	530.00	113.32

CONSTANT, A= 0.1450E-03
TOTAL HEAT INPUT, Q= 113.32(BTU/FT**2)
MAXIMUM SURFACE TEMPERATURE, TMAX= 2142.17(R)

HTC AND TEMPS. FOR CU-NI STG NO. 7

INTRINSIC PROPERTIES OF MATERIAL
K= 32.00 BTU/FT-HR-R
C= 0.12 BTU/LB
ROH= 540.00 LB/FT**3

			DEPTH (FEET)							
			0.0	0.00043	0.00086	0.00129	0.00172	0.00388	0.01250	
TIME (SEC.)	HG (BTU/FT**2-R-SEC.)	TEMP. OF GAS (R)	T1 (R)	T2 (R)	T3 (R)	T4 (R)	T5 (R)	T10 (R)	T30 (R)	SIGMAQ (BTU/FT**2)
0.0	0.1714E-01	528.40	530.00	530.00	530.00	530.00	530.00	530.00	530.00	-0.00
0.3141E-03	0.5998E-01	943.12	530.25	530.02	530.00	530.00	530.00	530.00	530.00	0.00
0.6281E-03	0.1041E+00	1152.36	531.05	530.14	530.01	530.00	530.00	530.00	530.00	0.02
0.9422E-03	0.1519E+00	1304.83	532.50	530.45	530.05	530.00	530.00	530.00	530.00	0.05
0.1256E-02	0.2036E+00	1430.42	534.66	531.01	530.17	530.02	530.00	530.00	530.00	0.09
0.1570E-02	0.2832E+00	1627.19	538.12	531.93	530.38	530.06	530.00	530.00	530.00	0.17
0.1884E-02	0.3669E+00	1789.61	543.27	533.41	530.75	530.14	530.01	530.00	530.00	0.29
0.2198E-02	0.4974E+00	2040.50	551.38	535.71	531.36	530.29	530.04	530.00	530.00	0.48
0.2513E-02	0.6332E+00	2248.70	563.12	539.25	532.33	530.53	530.10	530.00	530.00	0.77
0.2827E-02	0.8747E+00	2566.18	581.76	544.62	533.83	530.93	530.20	530.00	530.00	1.21
0.3141E-02	0.1122E+01	2820.07	609.08	552.86	536.15	531.57	530.36	530.00	530.00	1.88
0.3455E-02	0.1377E+01	3035.02	644.29	564.60	539.64	532.55	530.63	530.00	530.00	2.79
0.3769E-02	0.1646E+01	3233.80	687.03	580.22	544.64	534.03	531.04	530.00	530.00	3.97
0.4083E-02	0.2010E+01	3553.59	743.36	600.57	551.49	536.17	531.67	530.00	530.00	5.53
0.4397E-02	0.2375E+01	3833.11	814.51	627.13	560.67	539.16	532.58	530.00	530.00	7.55
0.4711E-02	0.2846E+01	4177.51	905.47	661.25	572.79	543.25	533.88	530.00	530.00	10.16
0.5025E-02	0.3314E+01	4480.27	1016.29	704.64	588.57	548.72	535.68	530.00	530.00	13.44
0.5339E-02	0.3839E+01	4820.93	1149.06	758.40	608.79	555.93	538.13	530.00	530.00	17.48
0.5653E-02	0.4360E+01	5128.71	1301.60	823.54	634.18	565.27	541.39	530.00	530.00	22.32
0.5967E-02	0.4994E+01	5488.26	1480.40	901.09	665.47	577.16	545.67	530.01	530.00	28.12
0.6281E-02	0.5620E+01	5811.46	1683.30	992.50	703.47	592.03	551.19	530.02	530.00	34.92
0.6595E-02	0.6308E+01	6146.46	1910.19	1098.25	748.90	610.36	558.19	530.05	530.00	42.79
0.6909E-02	0.7021E+01	6470.26	2157.49	1218.58	802.39	632.61	566.93	530.08	530.00	51.72
0.7224E-02	0.7815E+01	6814.68	2445.65	1355.74	864.58	659.23	577.68	530.13	530.00	62.08

0.7538E-02	0.7021E+01	6282.02	2594.38	1494.61	935.32	690.65	590.74	530.21	530.00	71.27
0.7852E-02	0.6452E+01	5883.68	2620.43	1606.65	1009.31	726.66	606.34	530.31	530.00	78.54
0.8166E-02	0.5803E+01	5438.77	2585.68	1687.87	1080.51	765.99	624.51	530.45	530.00	84.34
0.8480E-02	0.5231E+01	5035.88	2519.96	1740.92	1144.66	806.90	644.98	530.63	530.00	88.95
0.8794E-02	0.4580E+01	4580.18	2431.62	1770.41	1200.28	847.66	667.28	530.87	530.00	92.49
0.9108E-02	0.4057E+01	4197.71	2336.30	1780.74	1245.97	886.85	690.81	531.18	530.00	95.18
0.9422E-02	0.3487E+01	3768.15	2235.46	1776.42	1282.07	923.42	714.91	531.58	530.00	97.14
0.9736E-02	0.3205E+01	3488.42	2143.71	1761.57	1309.25	956.66	739.01	532.07	530.00	98.65
0.1005E-01	0.2874E+01	3183.96	2059.75	1740.49	1328.70	986.21	762.59	532.68	530.00	99.80
0.1036E-01	0.2694E+01	2990.57	1986.45	1715.77	1341.70	1012.00	785.23	533.42	530.00	100.72
0.1068E-01	0.2463E+01	2768.32	1920.79	1689.50	1349.52	1034.16	806.65	534.31	530.00	101.46
0.1099E-01	0.2166E+01	2503.39	1857.80	1662.19	1353.21	1052.94	826.65	535.35	530.00	102.00
0.1131E-01	0.1819E+01	2200.66	1795.20	1633.71	1353.52	1068.64	845.13	536.56	530.00	102.31
0.1162E-01	0.1597E+01	1991.15	1737.65	1604.48	1350.96	1081.53	862.05	537.94	530.00	102.48
0.1193E-01	0.1302E+01	1724.71	1684.53	1575.26	1346.06	1091.90	877.41	539.49	530.00	102.54
0.1225E-01	0.8692E+00	1332.03	1634.25	1546.28	1339.26	1100.00	891.24	541.22	530.00	102.49
0.1250E-01	0.2012E+00	531.26	1597.15	1523.40	1332.72	1105.02	901.25	542.74	530.00	102.40

CONSTANT, A= 0.1450E-03
TOTAL HEAT INPUT, Q= 102.40(BTU/FT**2)
MAXIMUM SURFACE TEMPERATURE, TMAX= 2620.76(R)

HTC AND TEMPS. FOR VASCOMAX MARAGING STEEL STG NO. 7

INTRINSIC PROPERTIES OF MATERIAL
K= 17.00 BTU/FT-HR-R
C= 0.14 BTU/LB
ROH= 490.00 LB/FT**3

			DEPTH (FEET)							
			0.0	0.00043	0.00086	0.00129	0.00172	0.00388	0.01250	
TIME (SEC.)	HG (BTU/FT**2-R-SEC.)	TEMP. OF GAS (R)	T1 (R)	T2 (R)	T3 (R)	T4 (R)	T5 (R)	T10 (R)	T30 (R)	SIGMAQ (BTU/FT**2)
0.0	0.1714E-01	528.40	530.00	530.00	530.00	530.00	530.00	530.00	530.00	-0.00
0.3141E-03	0.5998E-01	943.12	530.25	530.01	530.00	530.00	530.00	530.00	530.00	0.00
0.6281E-03	0.1041E+00	1152.36	531.09	530.08	530.00	530.00	530.00	530.00	530.00	0.02
0.9422E-03	0.1519E+00	1304.83	532.69	530.26	530.01	530.00	530.00	530.00	530.00	0.05
0.1256E-02	0.2036E+00	1430.42	535.14	530.64	530.05	530.00	530.00	530.00	530.00	0.09
0.1570E-02	0.2832E+00	1627.19	539.09	531.28	530.13	530.00	530.00	530.00	530.00	0.17
0.1884E-02	0.3669E+00	1789.61	545.02	532.34	530.29	530.02	530.00	530.00	530.00	0.29
0.2198E-02	0.4974E+00	2040.50	554.31	534.02	530.56	530.05	530.00	530.00	530.00	0.48
0.2513E-02	0.6332E+00	2248.70	567.89	536.62	531.00	530.12	530.00	530.00	530.00	0.77
0.2827E-02	0.8747E+00	2566.18	589.22	540.61	531.70	530.23	530.01	530.00	530.00	1.21
0.3141E-02	0.1127E+01	2820.07	620.74	546.73	532.79	530.41	530.04	530.00	530.00	1.87
0.3455E-02	0.1377E+01	3035.02	662.11	555.64	534.47	530.70	530.08	530.00	530.00	2.78
0.3769E-02	0.1645E+01	3233.80	713.06	567.83	536.94	531.16	530.16	530.00	530.00	3.95
0.4083E-02	0.2010E+01	3553.59	779.60	584.03	540.43	531.84	530.28	530.00	530.00	5.49
0.4397E-02	0.2375E+01	3833.11	863.85	605.36	545.25	532.82	530.46	530.00	530.00	7.48
0.4711E-02	0.2846E+01	4177.51	971.02	633.00	551.74	534.22	530.73	530.00	530.00	10.04
0.5025E-02	0.3314E+01	4480.27	1102.09	668.40	560.35	536.15	531.13	530.00	530.00	13.24
0.5339E-02	0.3838E+01	4820.93	1259.11	712.73	571.56	538.76	531.69	530.00	530.00	17.17
0.5653E-02	0.4360E+01	5128.71	1440.13	767.08	585.92	542.23	532.46	530.00	530.00	21.85
0.5967E-02	0.4991E+01	5488.26	1650.83	832.46	603.95	546.76	533.51	530.00	530.00	27.42
0.6281E-02	0.5620E+01	5811.46	1889.53	910.13	626.24	552.59	534.91	530.00	530.00	33.90
0.6595E-02	0.6308E+01	6146.46	2155.28	1000.76	653.37	559.95	536.75	530.00	530.00	41.34
0.6909E-02	0.7021E+01	6470.26	2443.90	1104.79	685.88	569.11	539.12	530.00	530.00	49.71
0.7224E-02	0.7815E+01	6814.68	2774.22	1223.52	724.30	580.35	542.12	530.00	530.00	59.33

0.7538E-02	0.7021E+01	6282.02	2973.98	1349.73	768.94	593.94	545.89	530.00	530.00	67.68
0.7852E-02	0.6452E+01	5883.68	3035.68	1465.60	818.50	610.08	550.54	530.00	530.00	74.10
0.8166E-02	0.5803E+01	5438.77	3016.89	1563.70	870.67	628.71	556.18	530.00	530.00	79.09
0.8480E-02	0.5231E+01	5035.88	2951.33	1641.63	923.14	649.58	562.90	530.00	530.00	82.95
0.8794E-02	0.4580E+01	4580.18	2853.45	1699.77	973.98	672.24	570.71	530.00	530.00	86.82
0.9108E-02	0.4057E+01	4197.71	2741.66	1739.71	1021.69	696.18	579.60	530.01	530.00	87.96
0.9422E-02	0.3487E+01	3768.15	2621.26	1763.90	1065.27	720.87	589.49	530.02	530.00	89.45
0.9736E-02	0.3205E+01	3488.42	2507.17	1775.07	1104.15	745.77	600.27	530.03	530.00	90.56
0.1005E-01	0.2874E+01	3183.96	2400.97	1776.39	1138.11	770.43	611.82	530.06	530.00	91.38
0.1036E-01	0.2694E+01	2990.57	2306.16	1770.34	1167.25	794.46	623.97	530.08	530.00	92.02
0.1068E-01	0.2463E+01	2788.32	2220.90	1759.14	1191.86	817.56	636.57	530.12	530.00	92.51
0.1099E-01	0.2166E+01	2503.39	2140.68	1744.08	1212.30	839.50	649.46	530.17	530.00	92.83
0.1131E-01	0.1819E+01	2200.66	2062.87	1725.90	1228.96	860.15	662.49	530.24	530.00	92.97
0.1162E-01	0.1597E+01	1991.15	1991.06	1705.31	1242.20	879.40	675.54	530.32	530.00	93.00
0.1193E-01	0.1302E+01	1724.71	1924.93	1683.12	1252.37	897.20	688.48	530.41	530.00	92.95
0.1225E-01	0.8692E+00	1332.03	1863.36	1659.88	1259.83	913.54	701.22	530.53	530.00	92.82
0.1250E-01	0.2012E+00	531.26	1818.87	1640.86	1264.07	925.57	711.20	530.64	530.00	92.70

CONSTANT, A= 0.1450E-03
TOTAL HEAT INPUT, Q= 92.70(BTU/FT**2)
MAXIMUM SURFACE TEMPERATURE, TMAX= 3037.56(R)

INPUT TABLES

GAS TEMPERATURE (R)	TIME (SEC)
530.00	0.0

GAS VELOCITY (FT/SEC)	TIME (SEC)
100.00	0.0
300.00	0.1250E-02
500.00	0.2500E-02
800.00	0.3750E-02
1000.00	0.5000E-02
1300.00	0.7500E-02
1500.00	0.9375E-02
1800.00	0.1063E-01
2100.00	0.1187E-01
2200.00	0.1312E-01

GAS PRESSURE (PSI)	TIME (SEC)
14.30	0.0
281.00	0.1250E-02
547.50	0.1875E-02
1080.70	0.2500E-02
2147.00	0.3125E-02
3213.50	0.3750E-02
5346.30	0.4375E-02
8545.50	0.5000E-02
12811.00	0.5625E-02
18676.30	0.6250E-02
25608.00	0.6875E-02
31473.00	0.7188E-02
24542.00	0.7500E-02
16010.00	0.8125E-02
9612.00	0.8750E-02
5346.00	0.9375E-02
3214.00	0.1000E-01
2147.00	0.1063E-01
1081.00	0.1125E-01
548.00	0.1187E-01
14.30	0.1250E-01

GAS HTC (BTU/FT**2-SEC-R)	TIME (SEC)
0.0	0.0

APPENDIX II

MELTING CODE LISTING

```
      MAIN
C                          LIST OF INPUT VARIABLES

C NT=NUMBER OF TEMPERATURES TO BE READ IN AS A TABLE.
C NV=NUMBER OF VELOCITY VALUES TO BE READ IN AS A TABLE.
C NP=NUMBER OF PRESSURE VALUES TO BE READ IN AS A TABLE.
C NH=NUMBER OF HTC VALUES TO BE READ IN AS A TABLE. IF HTC'S ARE TO
C BE CALCULATED FROM H(I)=A*(P(I)*V(I)/TG(I))**EXP, NH=1,HG(1)=0. AND TMH(1)=0.
C IF HTC VALUES ARE TO BE READ IN AS A TABLE,NV=1,VG(1)=0. AND TMV(1)=0.
C N=NUMBER OF GRID POINTS.
C INTRVL=PRINT INTERVAL OF OUTPUT (IE. IF OUTPUT IS EVERY TENTH
C CALCULATED VALUE INTRVL=10)

C VM = MUZZLE VELOCITY
C AREA = BASE AREA OF PROJECTILE
C PMASS = MASS OF PROJECTILE
C ST = TUBE LENGTH

C TG(ARRAY)=GAS TEMPERATURES IN INPUT TABLE (DEGREES R). IF GAS TEMPS ARE
C NOT TO BE READ IN BUT CALCULATED FROM TG=TG0(P/P0)**(GAMA-1/GAMA),NT=1
C AND TG(1)=INITIAL GAS TEMP. CORRECTED FOR BOUNDARY LAYER EFFECTS.
C TMG(ARRAY)=CORRESPONDING GAS TEMPERATURE TIMES (SEC). IF NT=1,TMG(1)=0.

C VG(ARRAY)=VELOCITIES IN INPUT TABLE (FT/SEC.).
C TMV(ARRAY)=CORRESPONDING VELOCITY TIMES (SEC.).

C PG(ARRAY)=PRESSURE VALUES IN INPUT TABLE (PSI).

C TMP(ARRAY)=CORRESPONDING PRESSURE TIMES (SEC.).

C HG(ARRAY)=HEAT TRANSFER COEFF. IN INPUT TABLES (BTU/FT**2-SEC-R).
C TMH(ARRAY)=CORRESPONDING HTC TIMES (SEC.).

C TIMEF=TOTAL TIME OF INTEREST (SEC.).
C TSO=INITIAL SURFACE TEMP.(R).
C PO=INITIAL GAS PRESSURE (PSI).
C GAMA=RATIO OF SPECIFIC HEATS
C ERROR=CONVERGENCE ERROR. READ IN AS A DECIMAL (IE. IF CONVERGENCE ERROR IS TO
C BE LESS THAN 5 PERCENT, ERROR=.05).
C QIN=TOTAL HEAT FLUX INPUT (BTU/FT**2).
C DEPTH=TOTAL DEPTH OF INTEREST (FT.).
C EXP=EXPONENT

C XYZ=COMMENT CARD. INPUT IS ALPHAMERIC (IE. ANYTHING CAN BE WRITTEN AND
C WILL BE PRINTED AS SUCH) AND IS CONSTRAINED TO ONLY ONE CARD PER DATA
C SET (80 CHARACTERS OR LESS).

C K=THERMAL CONDUCTIVITY OF MATERIAL (BTU/FT.-HR-R).
C C=HEAT CAPACITY OF MATERIAL (BTU/LB).
C ROH=DENSITY OF MATERIAL (LB/FT.**3).
C L=HEAT OF FUSION OF MATERIAL (BTU/LB). IF MELTING IS NOT TO BE
C CONSIDERED, LEAVE FORMAT FIELD BLANK.
C TM= SOLIDUS TEMPERATURE OF MATERIAL (R). IF MELTING IS NOT TO BE
C CONSIDERED, LEAVE FORMAT FIELD BLANK.
C TR=REACTION TEMPERATURE OF MATERIAL (R). IF MELTING IS NOT TO BE
C CONSIDERED, LEAVE FORMAT FIELD BLANK.
C CHD=HEAT AND MASS REACTION COEFFICIENT FOR MATERIAL (1/R).
C IF MELTING IS NOT TO BE CONSIDERED, LEAVE FORMAT FIELD BLANK.
```

```
                    MAIN

      DIMENSION TI(50),TEMPI(500,50),PRESS(500),TEMPG(500),VEL(500)
     *,H(500),TIME(500),PVTEXP(500),TG(50),VG(50),PG(50),TMG(50),TMV(50)
     *,TMP(50),SIGMAQ(500),XYZ(20),HG(50),TMH(50),SUMX(500)
     *,TT(50,4),N9(4),CPR(20),CKRT(20,7),ZYX(20,20),SEI(7)
      REAL K,L
      COMMON/BARREL/TIMEF,DEPTH,N,EXP,TSO,PO,DEL,GAMA,INTRVL,QIN,QCAL,
     *ERROR,TMAX,I,DT,A,NRUN,TEMPI,TI,PRESS,TEMPG,VEL,H,TIME,PVTEXP,TG,
     *VG,PG,XYZ,SIGMAQ,THC,HG,TMV,TMG,TMP,TMH,NV,NT,NP,NH,K,C,ROH,TM,L,
     *CHD,TR
      COMMON/PROJ/VM,AREA,PMASS,ST
      EQUIVALENCE (TT(1,1),TMV(1)),(N9(1),NV),(SEI(1),K)
      DATA CPR/20*10.0E+06/
      ARG=1.
      NRUN=0
      NAMELIST/NUM/NT,NV,NP,NH,N,INTRVL
      READ(5,NUM)
      IF(NV.EQ.1)  READ(5,101) VM,AREA,PMASS,ST
      READ(5,101) (TG(J),J=1,NT),(TMG(J),J=1,NT)
      READ(5,101) (VG(J),J=1,NV),(TMV(J),J=1,NV)
      READ(5,101) (PG(J),J=1,NP),(TMP(J),J=1,NP)
      READ(5,101) (HG(J),J=1,NH),(TMH(J),J=1,NH)
      WRITE(6,99)
      WRITE(6,NUM)
      DO 1 I=1,NP
1     PG(I)=PG(I)*144.
      NAMELIST/BARL/TIMEF,TSO,PO,GAMA,ERROR,QIN,DEPTH,EXP
      READ(5,BARL)
      WRITE(6,BARL)
      PO=PO*144.
      IF=0
      DO 9 I=1,20
      READ(5,100,END=2) XYZ
      READ(5,101,END=2) K,C,ROH,TM,L,CHD,TR
      IF=IF+1
      K=K/3600.
      DO 12 J=1,7
12    CKRT(I,J)=SEI(J)
      DO 10 J=1,20
10    ZYX(I,J)=XYZ(J)
      CPR(I)=C*ROH/K
9     CONTINUE
2     Y=R4MIN(CPR,20)
      INV=NV
      CALL TMTEST(TT,N9,DT,ARG,TIMEF,N,DEPTH,Y,DEL,I)
      IF(ARG.EQ.3.) GO TO 3
      DO 13 M=1,IF
      DO 14 J=1,20
14    XYZ(J)=ZYX(M,J)
      DO 11 J=1,7
11    SEI(J)=CKRT(M,J)
13    CALL SLAB(ARG)
3     WRITE(6,199)
      N9(1)=INV
      ID=I4MAX(N9,4)
      DO 5 J=1,ID
      IF(J.GT.NT) GO TO 6
      WRITE(6,200) TG(J),TMG(J)
6     IF(J.GT.INV) GO TO 4
```

AD-A076 219 CALSPAN CORP BUFFALO N Y F/G 19/6
SHOCK TUBE GUN MELTING EROSION STUDY.(U)
AUG 79 F A VASSALLO , W R BROWN DAAK11-77-C-0018
UNCLASSIFIED CALSPAN-VQ-6123-D-1 ARBRL-CR-00406 NL

2 OF 2
AD-
A076219

END
DATE
FILMED
11-79
DDC

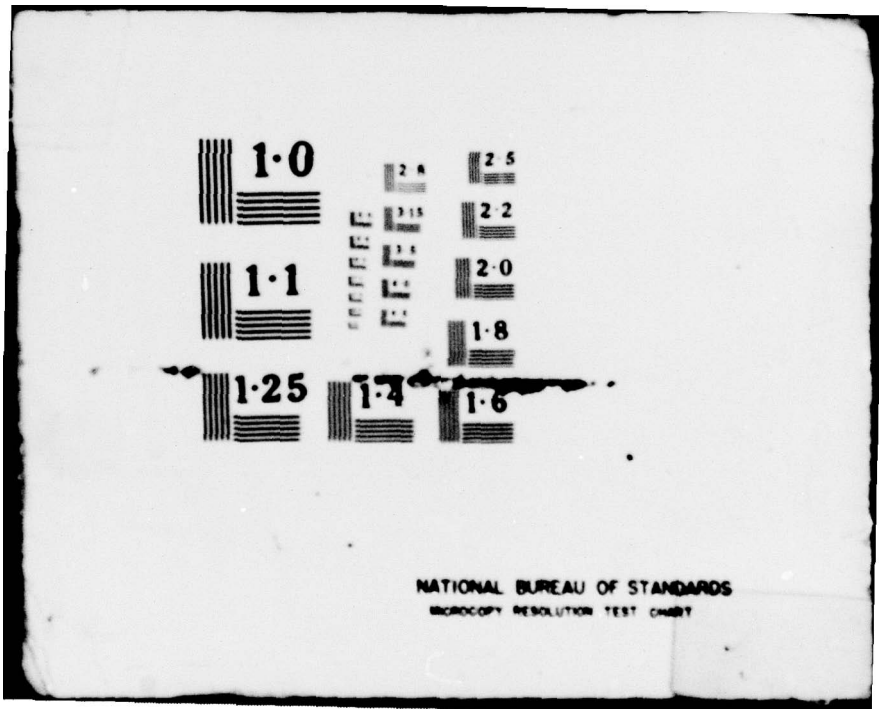
1·0
1·1
1·25
1·4
1·6
1·8
2·0
2·2
2·5
NATIONAL BUREAU OF STANDARDS
MICROCOPY RESOLUTION TEST CHART

```
      WRITE(6,201) VG(J),TMV(J)
4     IF(J.GT.NP) GO TO 5
      PG(J)=PG(J)/144.
      WRITE(6,202) PG(J),TMP(J)
5     WRITE(6,203)
      WRITE(6,204)
      DO 8 J=1,NH
8     WRITE(6,205) HG(J),TMH(J)
99    FORMAT(1H1)
100   FORMAT(20A4)
101   FORMAT(8F10.0)
199   FORMAT(1H1,T40,12HINPUT TABLES/1H0,19HGAS TEMPERATURE (R),T22,10HT
     •IME (SEC),T42,21HGAS VELOCITY (FT/SEC),T66,10HTIME (SEC),T86,18HGA
     •S PRESSURE (PSI),T107,10HTIME (SEC)/1H0)
200   FORMAT(1H•,T5,F9.2,T24,E11.4)
201   FORMAT(1H•,T46,F9.2,T66,E11.4)
202   FORMAT(1H•,T91,F9.2,T107,E11.4)
203   FORMAT(1H )
204   FORMAT(1H0,25HGAS HTC (BTU/FT**2-SEC-R),T30,10HTIME (SEC))
205   FORMAT(1H ,T7,F9.2,T30,E11.4)
      STOP
      END
```

```
      SUBROUTINE SLAB(ARG)
      DIMENSION TI(50),TEMPI(500,50),PRESS(500),TEMPG(500),VEL(500)
     *,H(500),TIME(500),PVTEXP(500),TG(50),VG(50),PG(50),TMG(50),TMV(50)
     *,TMP(50),SIGMAQ(500),XYZ(20),HG(50),TMH(50),SUMX(500)
      REAL K,X(7),L
      LOGICAL ZEB1
      COMMON/BARREL/TIMEF,DEPTH,N,EXP,TSO,PO,DEL,GAMA,INTRVL,QIN,QCAL,
     *ERROR,TMAX,I,DT,A,NRUN,TEMPI,TI,PRESS,TEMPG,VEL,H,TIME,PVTEXP,TG,
     *VG,PG,XYZ,SIGMAQ,THC,HG,TMV,TMG,TMP,TMH,NV,NT,NP,NH,K,C,ROH,TM,L,
     *CHD,TR
      ZEB1=.TRUE.
      IF(((TM.EQ.TR).AND.(CHD.EQ.L)).AND.(CHD.EQ.TR)) ZEB1=.FALSE.
      IF(ARG.EQ.2.) GO TO 5
      DO 7 J=1,5
7     X(J)=(J-1.)*DEL*12.
      X(6)=9.*DEL*12.
      X(7)=DEPTH*12.
      DEL2=DEL**2
      DDT=DT/10.
      T=-DT
      DO 6  M=1,I
      T=T+DT
6     TIME(M)=T
      CALL ARRAYS
      IF((HG(1).NE.0.).AND.(NH.NE.1)) GO TO 5
      SUM=0.
      DO 2 M=1,I
      PVTEXP(M)=(PRESS(M)*VEL(M)/TEMPG(M))**EXP
2     SUM=SUM+PVTEXP(M)*(TEMPG(M)-1500.)*DT
      A=QIN/SUM
5     TMAX=TSO
      QCAL=0.
      DO 1 M=1,N
      TEMPI(1,M)=TSO
1     TI(M)=TSO
      IAVE=0
      ZEB2=0.
      IQ=1
      QNET=0.
      DX=DEL/2.
      DO 4 M=1,I
      IF((HG(1).EQ.0.).AND.(NH.EQ.1))      H(M)=A*PVTEXP(M)
      HAVE=A/2.*(PVTEXP(M-IAVE)+PVTEXP(M))
      IAVE=1
      IF(IQ.EQ.(N-1)) GO TO 20
      HREAC=0.
      IF((TI(IQ).GT.TR).AND.ZEB1) HREAC=CHD
      QG=HAVE*DT*(TEMPG(M)-TI(IQ)+HREAC)
9     HEAT=QG+QNET
      TEMPI(M,IQ)=(HEAT-K*DT/(DEL-DX*ZEB2)*(TI(IQ)-TI(IQ+1)))/(C*ROH*(
     *DEL-DX))+TI(IQ)
      IG=IQ
      IF((TEMPI(M,IQ).GT.TM).AND.ZEB1) CALL MELTED(IQ,DX,M,HEAT
     *,QNET,ZEB2)
      TI(IG)=TEMPI(M,IG)
      IF(TMAX.LE.TI(IG)) TMAX=TI(IG)
      TI(IQ)=TEMPI(M,IQ)
      IF(IG.LT.IQ) GO TO 9
```

```
      QNET=0.
      QCAL=QCAL+QG
      SIGMAQ(M)=QCAL
      SUMX(M)=((IQ-1.5)*DEL+DX)*12.
      IF(IQ.EQ.N-1) GO TO 20
      J=N-1
      DO 4 MA=1,10
      TEMPI(M,IQ+1)=K*DDT/(C*ROH*DEL)*((TI(IQ)-TI(IQ+1))/(DEL-ZERO*DX)-(
     *TI(IQ+1)-TI(IQ+2))/DEL)+TI(IQ+1)
      TI(IQ+1)=TEMPI(M,IQ+1)
      IF(IQ+1.EQ.J) GO TO 8
      IB=IQ+2
      DO 3 NA=IB,J
      TEMPI(M,NA)=(K*DDT/(C*ROH*DEL2))*(TI(NA-1)+TI(NA+1)
     *-2.*TI(NA))+TI(NA)
3     TI(NA)=TEMPI(M,NA)
8     TEMPI(M,N)=(2.*K*DDT/(C*ROH*DEL2))*(TI(NA)-TI(N))+TI(N)
4     TI(N)=TEMPI(M,N)
      IF(ARG.EQ.2.) GO TO 20
      IF (.NOT.((NH.EQ.1).AND.(HG(1).EQ.0.))) GO TO 20
      E=ABS((QIN-QCAL)/QIN)
      IF(E.LE.ERROR) GO TO 20
      A=A*QIN/QCAL
      GO TO 5
20    WRITE(6,700) XYZ
      THC=K*3600.
      WRITE(6,800) THC,C,ROH,TM,TR,CHD,L
      WRITE(6,101) X
      WRITE(6,100) N
      WRITE(6,200)
      NRUN=NRUN+1
      IZ=0
      IN=0
      DO 22 J=1,M
      IN=IN+1
      IF((J.EQ.1).OR.(J.EQ.M).OR.(IN.EQ.INTRVL).OR.(SUMX(J).GT.SUMX(J-IZ
     *))) WRITE(6,300) TIME(J),H(J),TEMPG(J),TEMPI(J,1),TEMPI(J,2),
     *TEMPI(J,3),TEMPI(J,4),TEMPI(J,5),TEMPI(J,10),TEMPI(J,N),SIGMAQ(J)
     *,SUMX(J)
      IZ=1
22    IF(IN.EQ.INTRVL) IN=0
      WRITE(6,400) A,QCAL,TMAX
      CALL GRAPH(X,SUMX,M)
      ARG=2.
100   FORMAT(1H0,T3,4HTIME,T20,2HHG,T32,12HTEMP. OF GAS,T48,2HT1,T57,2HT
     *2,T66,2HT3,T75,2HT4,T84,2HT5,T93,3HT10,T102,1HT,I2,T113,6HSIGMAQ,T
     *123,6HSUM DX)
101   FORMAT(1H0,T66,12HDEPTH (INCH)/1H0,T46,7(F8.5,1X))
200   FORMAT(1H,T2,6H(SEC.),T12,18H(BTU/FT**2-R-SEC.),T36,3H(R),9X,7(3H(
     *R),6X),T110,11H(BTU/FT**2),T123,6H(INCH))
300   FORMAT(1H0,E11.4,T16,E11.4,T32,F9.2,T46,F7.2,6(2X,F7.2),T113,F7.2,
     *T124,F7.6)
400   FORMAT(1H0,12HCONSTANT, A=,E11.4/1H ,20HTOTAL HEAT INPUT, Q=,F9.2,
     *11H(BTU/FT**2)/1H ,34HMAXIMUM SURFACE TEMPERATURE, TMAX=,F9.2,3H(R
     *))
700   FORMAT(1H1,20A4)
800   FORMAT(1H0,32HINTRINSIC PROPERTIES OF MATERIAL/1H ,2HK=,F7.2,12H B
     *TU/FT-HR-R/1H ,2HC=,F7.2,7H BTU/LB/1H ,4HROH=,F7.2,9H LB/FT**3,/1H
     * ,21HSOLIDUS TEMPERATURE= ,F7.2,2H R/1H ,21HREACTION TEMPERATURE=,
     *F7.2,2H R/1H ,4HCHD=,F8.5,4H 1/R/1H ,15HHEAT OF FUSION=,F7.2,7H BT
     *U/LB)
      RETURN
      END
```

MELTED

```
      SUBROUTINE MELTED(IQ,DX,M,HEAT,QNET,ZEB2)
      DIMENSION TI(50),TEMPI(500,50),PRESS(500),TEMPG(500),VEL(500)
     *,H(500),TIME(500),PVTEXP(500),TG(50),VG(50),PG(50),TMG(50),TMV(50)
     *,TMP(50),SIGMAQ(500),XYZ(20),HG(50),TMH(50),SUMX(500)
      REAL K,L
      COMMON/BARREL/TIMEF,DEPTH,N,EXP,TSO,PO,DEL,GAMA,INTRVL,QIN,QCAL,
     *ERROR,TMAX,I,DT,A,NRUN,TEMPI,TI,PRESS,TEMPG,VEL,H,TIME,PVTEXP,TG,
     *VG,PG,XYZ,SIGMAQ,THC,HG,TMV,TMG,TMP,TMH,NV,NT,NP,NH,K,C,ROH,TM,L,
     *CHD,TR
      DDX=DX
      DX=DX+(HEAT-C*ROH*(DEL-DX)*(TM-TI(IQ))-K*DT*(TI(IQ)-TI(IQ+1))
     */(DEL-ZEB2*DX))/(ROH*L)
      TEMPI(M,IQ)=TM
      IF((DX.GT.DEL/2.).AND.(DX.LT.DEL)) GO TO 1
      IF(DX.GT.DEL) GO TO 2
      GO TO 3
1     ZEB2=.5
      GO TO 3
2     QNET=ROH*L*(DDX-DEL)
      IQ=IQ+1
      DX=0.
      ZEB2=0.
      DO 4 J=M,1
4     TEMPI(J,IQ-1)=TM
3     RETURN
      END
```

```
      SUBROUTINE ARRAYS
C ***********************************************************************
C
C     SUBROUTINE ARRAYS WILL EITHER GENERATE VALUES OF TEMP.,PRESS.,VELOCITY
C AND HG BY LINEAR INTERPOLATION FROM TABULAR INPUT DATA OR BY
C                  TG=TG0*(P/P0)**(GAMA-1/GAMA).
C
C ***********************************************************************
      DIMENSION TI(50),TEMPI(500,50),PRESS(500),TEMPG(500),VEL(500)
     *,H(500),TIME(500),PVTEXP(500),TG(50),VG(50),PG(50),TMG(50),TMV(50)
     *,TMP(50),SIGMAQ(500),XYZ(20),HG(50),TMH(50),SUMX(500)
      REAL K
      COMMON/BARREL/TIMEF,DEPTH,N,EXP,TSO,PO,DEL,GAMA,INTRVL,QIN,QCAL,
     *ERROR,TMAX,I,DT,A,NRUN,TEMPI,TI,PRESS,TEMPG,VEL,H,TIME,PVTEXP,TG,
     *VG,PG,XYZ,SIGMAQ,THC,HG,TMV,TMG,TMP,TMH,NV,NT,NP,NH,K,C,ROH,TM,L,
     *CHD,TR
      IF((HG(1).EQ.0.).AND.(NH.EQ.1)) GO TO 9
      J=2
      ACUTME=-DT
      DO 7 M=1,I
      ACUTME=ACUTME+DT
      IF((ACUTME.GT.TMH(J)).AND.((J+1).LE.NH)) J=J+1
7     H(M)=HG(J-1)+((HG(J)-HG(J-1))/(TMH(J)-TMH(J-1)))*
     *(ACUTME-TMH(J-1))
9     CONTINUE
      IF((HG(1).NE.0.).AND.(NH.NE.1)) GO TO 8
      J=2
      ACUTME=-DT
      DO 2 M=1,I
      ACUTME=ACUTME+DT
      IF((ACUTME.GT.TMP(J)).AND.((J+1).LE.NP)) J=J+1
2     PRESS(M)=PG(J-1)+((PG(J)-PG(J-1))/(TMP(J)-TMP(J-1)))*
     *(ACUTME-TMP(J-1))
      IF(NV.EQ.1) CALL VELOCT
      J=2
      ACUTME=-DT
      DO 1 M=1,I
      ACUTME=ACUTME+DT
      IF((ACUTME.GT.TMV(J)).AND.((J+1).LE.NV)) J=J+1
1     VEL(M)=VG(J-1)+((VG(J)-VG(J-1))/(TMV(J)-TMV(J-1)))*
     *(ACUTME-TMV(J-1))
      IF(NT.EQ.1) GO TO 4
8     J=2
      ACUTME=-DT
      DO 3 M=1,I
      ACUTME=ACUTME+DT
      IF((ACUTME.GT.TMG(J)).AND.((J+1).LE.NT)) J=J+1
3     TEMPG(M)=TG(J-1)+((TG(J)-TG(J-1))/(TMG(J)-TMG(J-1)))*
     *(ACUTME-TMG(J-1))
      GO TO 5
4     CPCV=(GAMA-1.)/GAMA
      DO 6 M=1,I
6     TEMPG(M)=1.0*TG(1)*(PRESS(M)/PO)**CPCV
5     RETURN
      END
```

```
      SUBROUTINE TMTEST(TM,N,DT,BOMB,TIMEF,L,DEPTH,V,DEL,I)
      DIMENSION TM(50,4),N(4),DUMP(4)
      DATA DUMP/4H VG ,4H TG ,4H PG ,4H HG /
      DEL=DEPTH/(L-1)
      DT1=TIMEF/100.
      DT2=V*DEL*DEL/8.
      DT=DT1
      IF(DT2.LE.DT1) DT=DT2
      I=(TIMEF/DT)+1
      DT=TIMEF/(I-1)
      BIG=I
      WRITE(6,500) BIG,DT
      IF(I.GT.500) I=500
      DT=TIMEF/(I-1)
      IF(I.EQ.500) WRITE(6,600) DT
500   FORMAT(1H0,64HTHE NUMBER OF DATA PTS.REQ.'D USING THE SMALLEST VAL
     +UE OF DT IS ,E12.5,23H THE VALUE OF DT BEING ,E12.5)
600   FORMAT(1H0,116HTHE MAXIMUM PERMISSABLE NUMBER OF DATA PTS. ALLOWED
     + BY THIS PROGRAM'S DIMENSIONAL ARRAYS ARE 500, THEREFORE 500 WILL/
     +1H ,58HBE THE REQ.'D NUMBER OF DATA PTS. THE VALUE OF DT WILL BE ,
     +E12.5,12H BY DEFAULT.)
      DO 1 IN=1,4
      IA=N(IN)-1
      IF(IA.EQ.0) GO TO 1
      DO 2 IM=1,IA
      II=IM+1
      IF((TM(IM+1,IN)-TM(IM,IN)).GE.DT) GO TO 2
      WRITE(6,100) DUMP(IN),II,IM
      BOMB=3.
2     CONTINUE
1     CONTINUE
100   FORMAT(1H0,24HTIME STEP IN INPUT TABLE,A4,15HBETWEEN VALUES ,I2,5H
     + AND ,I2,17H IS LESS THAN DT.)
      RETURN
      END
```

GRAPH

```
      SUBROUTINE GRAPH(X,SUMX,M)
      DIMENSION TI(50),TEMPI(500,50),PRESS(500),TEMPG(500),VEL(500)
     *,H(500),TIME(500),PVTEXP(500),TG(50),VG(50),PG(50),TMG(50),TMV(50)
     *,TMP(50),SIGMAQ(500),XYZ(20),HG(50),TMH(50),SUMX(500)
      REAL K,X(7),L
      COMMON/BARREL/TIMEF,DEPTH,N,EXP,TSO,PO,DEL,GAMA,INTRVL,QIN,QCAL,
     *ERROR,TMAX,I,DT,A,NRUN,TEMPI,TI,PRESS,TEMPG,VEL,H,TIME,PVTEXP,TG,
     *VG,PG,XYZ,SIGMAQ,THC,HG,TMV,TMG,TMP,TMH,NV,NT,NP,NH,K,C,ROH,TM,L,
     *CHD,TR
      D=X(2)/2.
      IZ=0
      IN=0
      IT=1
      DO 21 J=1,M
      IN=IN+1
      IF(SUMX(J).GT.(IT*X(2)-D)) IT=IT+1
      IF((J.EQ.1).OR.(J.EQ.M).OR.(IN.EQ.INTRVL).OR.(SUMX(J).GT.SUMX(J-IZ
     *))) WRITE(7,99) NRUN,TIME(J),TEMPI(J,IT),H(J),TEMPG(J)
     *,PRESS(J),VEL(J),SIGMAQ(J),SUMX(J)
      IF(IN.EQ.INTRVL) IN=0
21    IZ=1
99    FORMAT(I5,5E15.8,/,3E15.8)
      RETURN
      END
```

```
      SUBROUTINE VELOCT
      DIMENSION TI(50),TEMPI(500,50),PRESS(500),TEMPG(500),VEL(500)
     *,H(500),TIME(500),PVTEXP(500),TG(50),VG(50),PG(50),TMG(50),TMV(50)
     *,TMP(50),SIGMAQ(500),XYZ(20),HG(50),TMH(50),SUMX(500),S(500)
      COMMON/BARREL/TIMEF,DEPTH,N,EXP,TSO,PO,DEL,GAMA,INTRVL,QIN,QCAL,
     *ERROR,TMAX,I,DT,A,NRUN,TEMPI,TI,PRESS,TEMPG,VEL,H,TIME,PVTEXP,TG,
     *VG,PG,XYZ,SIGMAQ,THC,HG,TMV,TMG,TMP,TMH,NV,NT,NP,NH,K,C,ROH,TM,L,
     *CHD,TR
      COMMON/PROJ/VM,AREA,PMASS,ST
      IN=0
      F=1.
3     J=1
      S(1)=0.
      IN=IN+1
      DO 1 M=11,I,10
      J=J+1
      VG(J)=F*AREA*(PRESS(M)+PRESS(M-10))*DT*161./PMASS+VG(J-1)
      S(J)=S(J-1)+(VG(J)+VG(J-1))*DT*5.
      TMV(J)=TIME(M)
      IF(S(J).GE.ST) GO TO 5
1     CONTINUE
5     Z=ABS((VG(J)-VM)/VM)
      IF((Z.LE.0.1).OR.(IN.EQ.5)) GO TO 2
      F=F*VM/VG(J)
      GO TO 3
2     IF(J.EQ.I/10) GO TO 7
      VG(J+1)=VG(J)
      S(J+1)=(TIMEF-TIME(M))*VG(J)+S(J)
      TMV(J+1)=TIMEF
7     WRITE(6,99) VM,AREA,PMASS,ST,F
      DO 4 J1=1,J
4     WRITE(6,100) TMV(J1),S(J1),VG(J1)
      NV=J
99    FORMAT(1H1,T30,37HCALCULATED VELOCITY VALUES (FT./SEC.)/1H0,17H MU
     *ZZLE VELOCITY=,F8.2,11H (FT./SEC.)/1H ,25H BASE AREA OF PROJECTILE
     *=,F8.5,9H (FT.**2)/1H ,20H MASS OF PROJECTILE=,F8.5,6H (LB.)/1H ,1
     *3H TUBE LENGTH=,F8.5,6H (FT.)/1H0,30H          PRESSURE FACTOR, *F*
     *=,F8.2,6H       /1H0,T25,11HTIME (SEC.),T41,14HDISTANCE (FT.),T60,1
     *9HVELOCITY (FT./SEC.)/1H0)
100   FORMAT(1H ,T25,E11.4,T45,F8.5,T65,F8.2)
      RETURN
      END
```

INPUT

```
 &NUM
 NT=          1,NV=          1,NP=         24,NH=          1,N=         30,INTRVL=          5
 &END
 &BARL
 TIMEF= .124999993E-01,TSO=  530.000000    ,PO=  14.4300003    ,GAMA=  1.52999973    ,ERROR=  .199999996E-01,QIN=  86.5000000
 DEPTH= .124999993E-01,EXP=  .800000012
 &END

 THE NUMBER OF DATA PTS.REQ.'D USING THE SMALLEST VALUE OF DT IS  0.10100E+03 THE VALUE OF DT BEING  0.12500E-03
```

CALCULATED VELOCITY VALUES (FT./SEC.)

MUZZLE VELOCITY= 2800.00 (FT./SEC.)
BASE AREA OF PROJECTILE= 0.00360 (FT.**2)
MASS OF PROJECTILE= 0.25000 (LB.)
TUBE LENGTH=15.00000 (FT.)

PRESSURE FACTOR, "F" = 0.34

TIME (SEC.)	DISTANCE (FT.)	VELOCITY (FT./SEC.)
0.0	0.0	0.0
0.1250E-02	0.00739	11.82
0.2500E-02	0.05276	60.78
0.3750E-02	0.21766	203.06
0.5000E-02	0.70469	576.18
0.6250E-02	1.94228	1403.97
0.7500E-02	4.19276	2196.81
0.8750E-02	7.12826	2500.00
0.1000E-01	10.31159	2593.32
0.1125E-01	13.57370	2626.06
0.1250E-01	16.86226	2635.64

HTC AND TEMPS. FOR 4340 STG NO. 30

INTRINSIC PROPERTIES OF MATERIAL
K= 19.60 BTU/FT-HR-R
C= 0.12 BTU/LB
ROH= 490.00 LB/FT**3
SOLIDUS TEMPERATURE= 3100.00 R
REACTION TEMPERATURE= 0.0 R
CHD= 0.0 1/R
HEAT OF FUSION= 100.00 BTU/LB

			DEPTH (INCH)								
			0.0	0.00517	0.01034	0.01552	0.02069	0.04655	0.16000		
TIME (SEC.)	HG (BTU/FT**2-R-SEC.)	TEMP. OF GAS (R)	T1 (R)	T2 (R)	T3 (R)	T4 (R)	T5 (R)	T10 (R)	T30 (R)	SIGMAQ (BTU/FT**2)	SUM DX (INCH)
0.0	0.0	533.41	530.00	530.00	530.00	530.00	530.00	530.00	530.00	0.0	.0
0.5000E-03	0.3001E-02	1161.41	530.03	530.00	530.00	530.00	530.00	530.00	530.00	0.00	.0
0.1125E-02	0.1335E-01	2031.54	530.43	530.05	530.00	530.00	530.00	530.00	530.00	0.01	.0
0.1750E-02	0.4740E-01	2649.20	532.55	530.39	530.04	530.00	530.00	530.00	530.00	0.04	.0
0.2375E-02	0.9749E-01	3147.36	538.78	531.69	530.26	530.03	530.00	530.00	530.00	0.15	.0
0.3000E-02	0.2430E+00	3884.39	556.17	536.32	530.95	530.15	530.01	530.00	530.00	0.46	.0
0.3625E-02	0.4452E+00	4515.03	598.80	545.34	532.97	530.53	530.08	530.00	530.00	1.26	.0
0.4250E-02	0.9214E+00	5252.89	692.13	568.00	538.01	531.59	530.29	530.00	530.00	3.04	.0
0.4875E-02	0.1672E+01	6222.46	901.76	620.29	549.88	534.20	530.84	530.00	530.00	7.10	.0
0.5500E-02	0.3450E+01	7629.94	1385.65	737.24	576.76	540.30	532.19	530.00	530.00	16.37	.0
0.6125E-02	0.5203E+01	8208.07	2210.01	981.11	636.85	554.26	535.35	530.00	530.00	33.81	.0
0.6750E-02	0.6091E+01	7919.99	2919.57	1313.06	743.95	583.00	542.36	530.00	530.00	53.93	.0
0.7125E-02	0.5821E+01	7175.98	3100.00	1537.20	827.98	609.42	549.53	530.00	530.00	64.02	.000030
0.7375E-02	0.5331E+01	6495.67	2995.99	1679.58	892.61	631.23	555.88	530.00	530.00	69.06	.000030
0.8000E-02	0.4258E+01	5335.40	2732.11	1862.40	1050.59	698.28	578.07	530.02	530.00	77.53	.000030
0.8625E-02	0.3212E+01	4280.39	2492.42	1909.87	1174.95	773.09	608.77	530.06	530.00	82.43	.000030
0.9250E-02	0.2338E+01	3418.81	2261.50	1884.40	1259.20	844.69	645.26	530.15	530.00	84.74	.000030
0.9875E-02	0.1810E+01	2858.20	2079.53	1827.30	1309.07	906.75	684.06	530.34	530.00	85.85	.000030
0.1050E-01	0.1403E+01	2403.51	1939.58	1762.49	1334.15	957.09	722.23	530.66	530.00	86.42	.000030
0.1112E-01	0.1125E+01	2069.24	1826.90	1698.57	1342.75	996.13	757.79	531.17	530.00	86.65	.000030
0.1175E-01	0.6045E+00	1369.05	1727.66	1637.95	1340.75	1025.34	789.69	531.93	530.00	86.60	.000030
0.1237E-01	0.2643E+00	790.67	1647.37	1581.38	1331.77	1046.43	817.54	532.99	530.00	86.43	.000030
0.1250E-01	0.1461E+00	533.77	1633.95	1570.85	1329.40	1049.82	822.62	533.24	530.00	86.40	.000030

INPUT TABLES

GAS TEMPERATURE (R)	TIME (SEC)
530.00	0.0

GAS VELOCITY (FT/SEC)	TIME (SEC)
0.0	0.0

GAS PRESSURE (PSI)	TIME (SEC)
14.70	0.0
170.00	0.6250E-03
830.00	0.1250E-02
1670.00	0.1875E-02
2670.00	0.2500E-02
5000.00	0.3125E-02
7500.00	0.3750E-02
11670.00	0.4375E-02
19170.00	0.5000E-02
35000.00	0.5625E-02
37500.00	0.5800E-02
40000.00	0.6250E-02
38000.00	0.6600E-02
33330.00	0.6875E-02
16670.00	0.7500E-02
10000.00	0.8125E-02
5000.00	0.8750E-02
2670.00	0.9375E-02
1670.00	0.1000E-01
1000.00	0.1063E-01
670.00	0.1125E-01
330.00	0.1150E-01
170.00	0.1187E-01
14.70	0.1250E-01

CONSTANT, A= 0.8885E-04
TOTAL HEAT INPUT, Q= 86.40(BTU/FT**2)
MAXIMUM SURFACE TEMPERATURE, TMAX= 3100.00(R)

GAS HTC (BTU/FT**2-SEC-R)	TIME (SEC)
0.0	0.0

MELTING EROSION STUDY

OBS	NRUN	TIME	HG	TG	PG	VG	SIGQ	SDX	TI_1	FLUX_1	SQ_1	SX_1	TI_2	FLUX_2	SQ_2	SX_2
1	1	0.0000000	0.00000	73.41	14.7	0.00	0.0000	0.0000000000	70.00	0.0	0.0000	.	.	.	.	.
2	1	0.0005000	0.00300	701.41	138.9	4.73	0.0004	0.0000000000	70.03	1.9	0.0004	.	.	.	.	.
3	1	0.0011250	0.01335	1571.54	698.0	10.64	0.0063	0.0000000000	70.43	20.0	0.0063	.	.	.	.	.
4	1	0.0017500	0.04740	2189.20	1502.0	31.40	0.0402	0.0000000000	72.55	100.3	0.0402	.	.	.	.	.
5	1	0.0023750	0.09749	2687.36	2470.0	55.89	0.1496	0.0000000000	78.78	254.3	0.1496	.	.	.	.	.
6	1	0.0030000	0.24303	3424.39	4534.0	117.69	0.4580	0.0000000000	96.17	808.9	0.4580	.	.	.	.	.
7	1	0.0036250	0.44519	4055.03	7000.0	188.83	1.2538	0.0000000000	138.80	1743.5	1.2538	.	.	.	.	.
8	1	0.0042500	0.92139	4792.89	10835.9	352.31	3.0367	0.0000000000	232.13	4202.2	3.0367	.	.	.	.	.
9	1	0.0048750	1.67159	5762.46	17669.8	538.86	7.0998	0.0000000000	441.76	8894.0	7.0998	.	.	.	.	.
10	1	0.0055000	3.44999	7169.94	31833.4	907.29	16.3730	0.0000000000	925.65	21542.8	16.3730	.	.	.	.	.
11	1	0.0061250	5.20321	7748.07	39305.4	1321.19	33.8051	0.0000000000	1750.01	31209.2	33.8051	.	.	.	.	.
12	1	0.0067500	6.09149	7459.99	35453.5	1721.10	53.9293	0.0000000000	2459.57	30460.0	53.9293	.	.	.	.	.
13	1	0.0071250	5.82141	6715.98	26667.3	1958.95	64.0216	0.0000303165	2640.00	23728.0	64.0216	.	.	.	.	.
14	1	0.0073749	5.33061	6035.67	20003.4	2117.52	69.0554	0.0000303165	2535.99	18655.4	69.0554	.	.	.	.	.
15	1	0.0079999	4.25821	4875.40	11334.6	2318.08	77.5334	0.0000303165	2272.11	11085.3	77.5334	.	.	.	.	.
16	1	0.0086249	3.21224	3820.39	6000.5	2469.68	82.4313	0.0000303165	2032.42	5743.4	82.4313	.	.	.	.	.
17	1	0.0092499	2.33810	2958.81	3136.3	2537.33	84.7378	0.0000303165	1801.50	2705.9	84.7378	.	.	.	.	.
18	1	0.0098749	1.81045	2398.20	1870.1	2583.99	85.8506	0.0000303165	1619.53	1409.7	85.8506	.	.	.	.	.
19	1	0.0104999	1.40349	1943.51	1134.1	2606.42	86.4173	0.0000303165	1479.58	651.1	86.4173	.	.	.	.	.
20	1	0.0111249	1.12517	1609.24	736.1	2622.79	86.6505	0.0000303165	1366.90	272.7	86.6505	.	.	.	.	.
21	1	0.0117499	0.60448	909.05	223.4	2629.90	86.5963	0.0000303165	1267.66	-216.8	86.5963	.	.	.	.	.
22	1	0.0123749	0.26432	330.67	45.8	2634.69	86.4253	0.0000303165	1187.37	-226.4	86.4253	.	.	.	.	.
23	1	0.0124999	0.14611	73.77	14.7	2635.64	86.3967	0.0000303165	1173.95	-160.7	86.3967	.	.	.	.	.

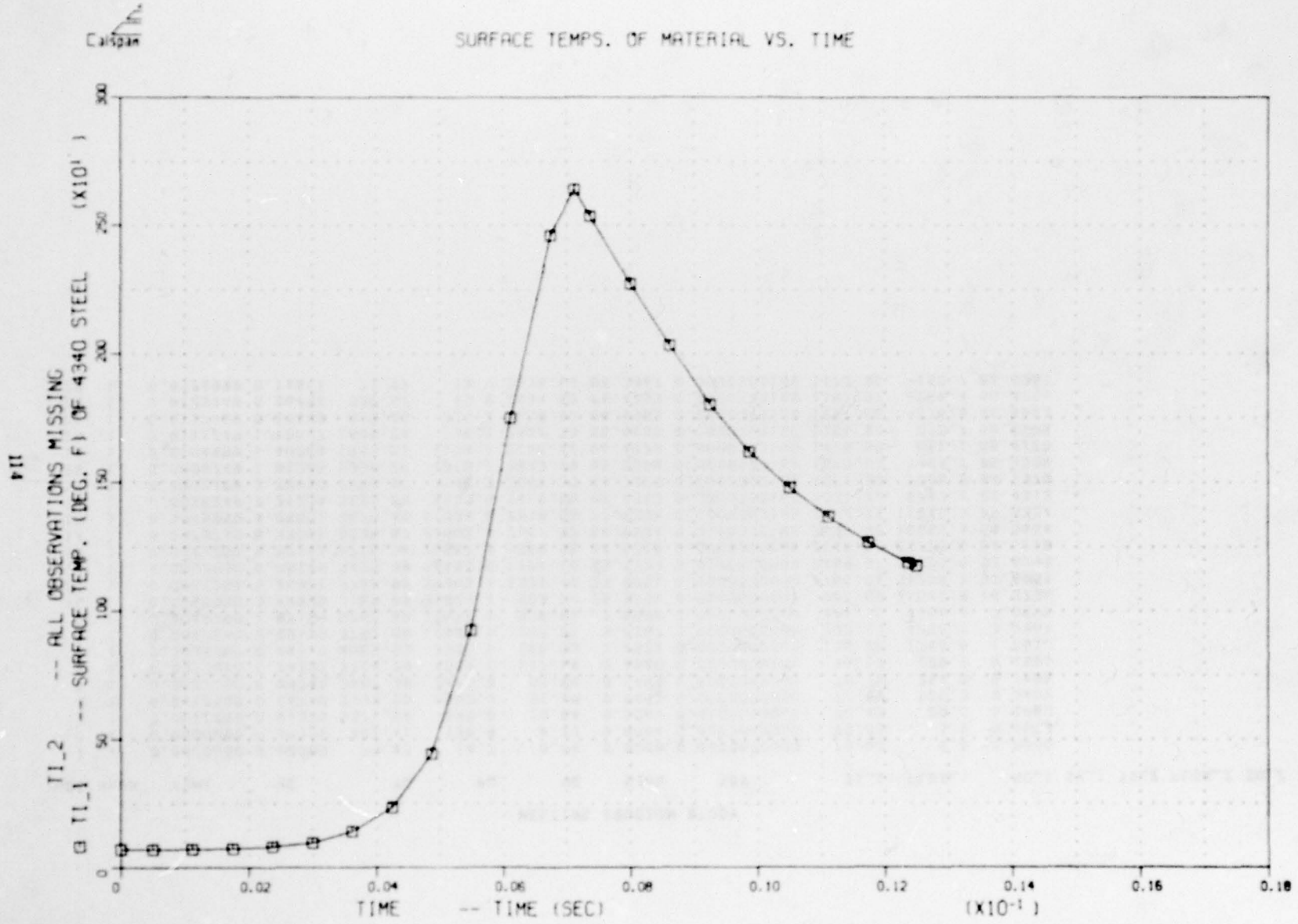
SURFACE TEMPS. OF MATERIAL VS. TIME
TI_2 -- ALL OBSERVATIONS MISSING
TI_1 -- SURFACE TEMP. (DEG. F) OF 4340 STEEL
(X10¹)
0
50
100
150
200
250
300
0
0.02
0.04
0.06
0.08
0.10
0.12
0.14
0.16
0.18
TIME -- TIME (SEC)
(X10⁻¹)

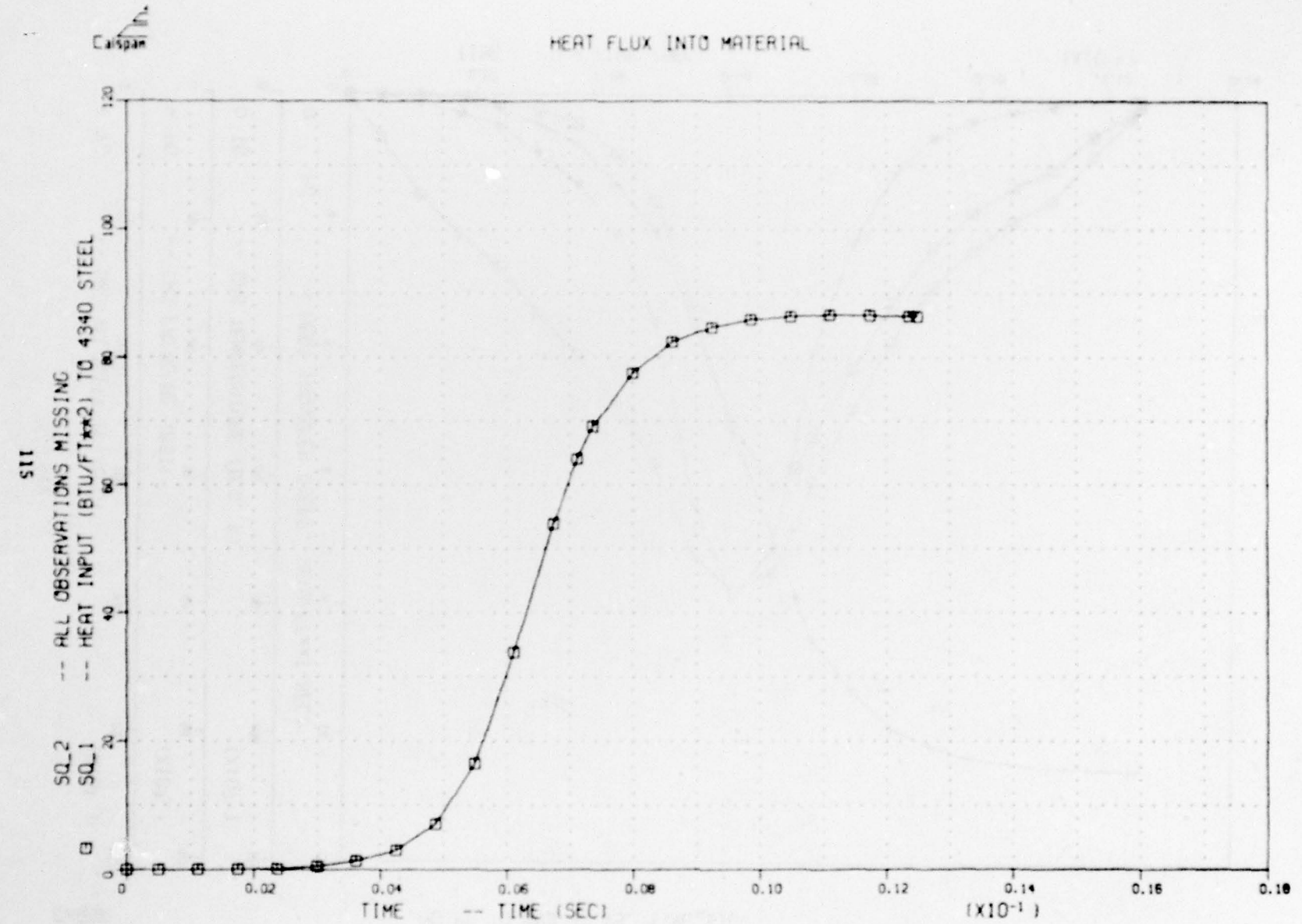
Calspan
HEAT FLUX INTO MATERIAL
SII
SQ_2 -- ALL OBSERVATIONS MISSING
SQ_1 -- HEAT INPUT (BTU/FT**2) TO 4340 STEEL
0
20
40
60
80
100
120
0
0.02
0.04
0.06
0.08
0.10
0.12
0.14
0.16
0.18
TIME -- TIME (SEC)
(X10-1)

HG PG TG AND VG VS. TIME_STG
TIME -- TIME (SEC)
(X10⁻¹)
0.14
0.12
0.10
0.08
0.06
0.04
0.02
0
□ HG -- HEAT TRANSFER COEFF. (BTU/FT**2-SEC)
0
2
4
6
8
10
12
G TG -- GAS TEMPERATURE (DEC. F)
(X10²)
0
20
40
60
80
100
120
▷ PG -- GAS PRESSURE (PSI)
(X10³)
0
10
20
30
40
50
60
+ VG -- GAS VELOCITY (FT/SEC)
(X10¹)
0
50
100
150
200
250
300
Calspan

DISTRIBUTION LIST

No. of Copies	Organization
12	Commander Defense Documentation Center ATTN: DDC-DDA Cameron Station Alexandria, VA 22314
1	Director of Defense Research and Engineering ATTN: R. Thorkildsen The Pentagon Arlington, VA 20301
1	Defense Advanced Research Projects Agency Director, Materials Division 1400 Wilson Boulevard Arlington, VA 22209
1	Commander US Army Materiel Development and Readiness Command ATTN: DRCDMD-ST 5001 Eisenhower Avenue Alexandria, VA 22333
1	Commander US Army Aviation Research & Development Command ATTN: DRSAV-E P.O. Box 209 St. Louis, MO 63166
1	Director US Army Air Mobility Research and Development Laboratory Ames Research Center Moffett Field, CA 94035
1	Commander US Army Research & Technology Laboratories ATTN: R.A. Langsworthy Ft. Eustis, VA 23604
1	Commander US Army Electronics Research & Development Command Technical Support Activity ATTN: DELSD-L Ft. Monmouth, NJ 07703
1	Commander US Army Communications Rsch and Development Command ATTN: DRDCO-PPA-SA Ft. Monmouth, NJ 07703
2	Commander US Army Missile Research & Development Command ATTN: DRDMI-R DRDMI-YDL Redstone Arsenal, AL 35809
1	Commander US Army Tank Automotive Rsch and Development Command ATTN: DRDTA-UL Warren, MI 48090
2	Commander US Army Armament Research & Development Command ATTN: DRDAR-TSS Dover, NJ 07801
1	Commander US Army Armament Materiel Readiness Command ATTN: DRSAR-LEP-L, Tech Lib Rock Island, IL 61299
5	Commander US Army Armament Research & Development Command ATTN: FC & SCWSL, D. Gyorog H. Kahn B. Brodman S. Cytron T. Hung Dover, NJ 07801

DISTRIBUTION LIST

No. of Copies	Organization
6	Commander US Army Armament Research & Development Command ATTN: DRDAR-LC, J. Frasier H. Fair J. Lannon C. Lenchitz A. Moss R. Walker Dover, NJ 07801
6	Commander US Army Armament Research & Development Command ATTN: DRDAR-LC, J. Picard D. Costa E. Barrieres R. Corn K. Rubin J. Houle Dover, NJ 07801
5	Commander US Army Armament Research & Development Command ATTN: DRDAR-LC, D. Katz E. Wurzel K. Russell D. Downs R.L. Trask Dover, NJ 07801
1	Commander US Army Armament Research & Development Command ATTN: DRDAR-QA, J. Rutkowski Dover, NJ 07801
4	Commander US Army Armament Research & Development Command Benet Laboratory ATTN: I. Ahmad T. Davidson J. Zweig G. Friar Watervliet, NY 12189
5	Commander US Army Armament Research & Development Command Benet Laboratory ATTN: J. Busuttil W. Austin R. Montgomery R. Billington J. Santini Watervliet, NY 12189
1	Project Manager, M60 Tanks US Army Tank & Automotive Cmd 28150 Dequindre Road Warren, MI 48090
4	Project Manager Cannon Artillery Weapons Systems ATTN: DRCPM-CAWS US Army Armament Research & Development Command Dover, NJ 07801
2	Project Manager - M110E2 ATTN: J. Turkeltaub S. Smith Rock Island, IL 61299
1	Project Manager - XM1 Tank US Army Tank Automotive Development Command 28150 Dequindre Road Warren, MI 48090
1	Project Manager - XM1 Tank Main Armament Dev Div Dover, NJ 07801
1	Project Manager - ARGADS Dover, NJ 07801
2	Director US Army Materials & Mechanics Research Center ATTN: J.W. Johnson R. Katz Watertown, MA 02172

DISTRIBUTION LIST

No. of Copies	Organization
1	Director US Army TRADOC Systems Analysis Activity ATTN: ATAA-SL, Tech Lib White Sands Missile Range, NM 88002
1	Commander US Army Air Defense Center ATTN: ATSA-SM-L Ft. Bliss, TX 79916
1	Commander US Army Armor Center ATTN: ATZK-XM1 Ft. Knox, KY 40121
1	President US Army Maintenance Mgmt Ctr Lexington, KY 40507
1	President US Army Armor & Engineer Bd Ft. Knox, KY 40121
1	Commander US Army Field Artillery School ATTN: J. Porter Ft. Sill, OK 73503
3	HDQA (DAMA-ARZ, DAMA-CSM, DAMA-WSW) Washington, DC 20301
2	Director US Army Research Office ATTN: P. Parrish E. Saibel P.O. Box 12211 Rsch Triangle Park, NC 27709
5	Commander US Naval Surface Wpns Center ATTN: M. Shamblen J. O'Brasky C. Smith L. Russell T.W. Smith Dahlgren, VA 22448
2	Commander US Naval Ordnance Station ATTN: L. Dickinson S. Mitchell Indian Head, MD 20640
1	Commander US Naval Ordnance Station, Louisville ATTN: F. Blume Louisville, KY 40202
2	AFATL (D. Uhrig, O. Heiney) Eglin AFB, FL 32542
1	National Bureau of Standards Materials Division ATTN: A.W. Ruff Washington, DC 20234
1	National Science Foundation Materials Division Washington, DC 20550
1	Battelle Columbus Laboratory ATTN: G. Wolken Columbus, OH 43201
1	Lawrence Livermore Laboratory ATTN: J. Kury Livermore, CA 94550

DISTRIBUTION LIST

No. of Copies	Organization
10	Calspan Corporation ATTN: G. Sterbutzel F. Vassallo E. Fisher D. Adams C. Morphy C. Treanor J. Weibel A. Ashby P. Wukovits T. Maj P.O. Box 235 Buffalo, NY 14221
1	Director Chemical Propulsion Info Agency Johns Hopkins University ATTN: T. Christian Johns Hopkins Road Laurel, MD 20810
2	Princeton University Forrestal Campus Library ATTN: L. Caveny Tech Lib P.O. Box 710 Princeton, NJ 08540
1	Purdue University School of Mechanical Engineering ATTN: J.R. Osborn W. Lafayette, IN 47909
1	SRI International Materials Research Center Menlo Park, CA 94025
1	University of Illinois Dept of Aeronautics and Aerospace Engineering ATTN: H. Krier Urbana, IL 61803

Aberdeen Proving Ground

Dir, USAMTD
ATTN: H. Graves, Bldg. 400
C. Lavery, Bldg. 400
L. Barnhardt, Bldg. 400
K. Jones, Bldg. 400
R. Moody, Bldg. 525

Cdr, TECOM
ATTN: DRSTE-FA
DRSTE-AR
DRSTE-AD
DRSTE-TO-F

Dir, USAMSAA
ATTN: Dr. J. Sperrazza
DRXSY-MP, H. Cohen
D. Barnhardt, RAM Div
G. Alexander, RAM Div
Air Warfare Div
Ground Warfare Div
RAM Division

Dir, Wpns Sys Concepts Team
Bldg. E3516, EA
ATTN: DRDAR-ACW

USER EVALUATION OF REPORT

Please take a few minutes to answer the questions below; tear out this sheet and return it to Director, US Army Ballistic Research Laboratory, ARRADCOM, ATTN: DRDAR-TSB, Aberdeen Proving Ground, Maryland 21005. Your comments will provide us with information for improving future reports.

1. BRL Report Number _____

2. Does this report satisfy a need? (Comment on purpose, related project, or other area of interest for which report will be used.)

_____

_____

_____

3. How, specifically, is the report being used? (Information source, design data or procedure, management procedure, source of ideas, etc.) _____

_____

_____

4. Has the information in this report led to any quantitative savings as far as man-hours/contract dollars saved, operating costs avoided, efficiencies achieved, etc.? If so, please elaborate.

_____

_____

5. General Comments (Indicate what you think should be changed to make this report and future reports of this type more responsive to your needs, more usable, improve readability, etc.) _____

_____

_____

_____

6. If you would like to be contacted by the personnel who prepared this report to raise specific questions or discuss the topic, please fill in the following information.

Name: _____

Telephone Number: _____

Organization Address: _____

_____

_____